Development of Nano Structured Photo-catalytic Textile Materials

A Thesis

by

Asena Cerhan

Submitted to the

Graduate School of Sciences and Engineering
In Partial Fulfillment of the Requirements for
the Degree of

Master of Science

in the
Department of Mechanical Engineering

Özyeğin University
July 2017

Development of Nano Structured Photocatalytic Textile Materials

Approved by:

Assoc. Prof. Dr. G. Bahar Başım, Advisor,

Department of Mechanical Engineering

Özyeğin University

Professor Dr. Taylan Akdoğan,

Department of Physics

Boğaziçi University

Professor Dr. Güray Erkol,

Department of Physics

Özyeğin University

Date Approved: 24 July 2017

To My Family

ABSTRACT

This study focuses on assisting problems which have delayed the commercialization of the photocatalytic textile applications by the following innovative technological developments related to photocatalytic compounds; (i) extension of light absorption in the visible light range through addition of composite dopants and novel branched particles, (ii) developing techniques to avoid the photo-deterioration of the textile materials and (iii) introducing technologies to uniformly deposit the photo-catalysts on the textiles at an optimized concentration to obtain an improved photocatalytic efficiency.

Utilization of novel nanoparticles such as branched silica is a newly explored area proposed in this thesis which is a potential breakthrough promoting photocatalytic activity visible light conditions while spontaneously enhancing particle attachment to the textile surface. Moreover, by doping TiO_2 with branched silica, it is possible to induce a synergy by (i) extending the TiO_2 band gap to the visible range, (ii) consequently decreasing the energy required for performing oxidation reactions, (iii) improving the photo-reaction speed and making an effective use of the solar and visible radiation and (iv) furthermore enhancing the water repelling activity on textiles.

The major accomplishments of this study can be summarized by starting by the synthesis of uniformly sized branched silica particles. Both crystalline and amorphous titania (TiO_2) particles were tested and found to improve in efficiency when they were mixed with branched silica in terms of extended absorption in the visible light range and deposition of photocatalytic compounds. Accordingly, an optimized dip coating process (via ultrasonic chemical bath deposition) was developed for textile manufacturing, which also helped improve hydrophobic performance and the surface attachment. This thesis

also provides a systematic methodology to enable production of self-cleaning textiles to

be able to produce them with a commercialization potential.

ÖZET

Bu çalışma, teknolojideki yenilikçi gelişmelerle fotokatalitik bileşiklerle ilgili olarak dallandırılmış silika parçacıkları kullanılarak ve kompozit katkılarla görülebilen ışık emiliminin uzatılması, nano tozlar ile tekstil malzemelerinin foto-bozulmasını önleme tekniklerini ve geliştirilmiş bir fotokatalitik etkinlik elde etmek için optimize edilmiş bir konsantrasyonda tekstiller üzerine yerleştirilmiş foto-katalizörler gibi fotokatalitik tekstil materyalinin ticari hale gelmesini geciktiren problemlerin çözümüne yardımcı olarak ileri sürülmektedir.

Dallandırılmış silika kullanımı yeni keşfedilen bir alandır. Lekeleri yok etmek için görünür ışık koşullarında aktif olan tekstiller üzerindeki yüksek etkiyi gösteren potansiyel bir gelişmedir. Dahası, TiO_2 yasak enerji aralığını görünür aralığa uzatmak ve böylece oksidasyon reaksiyonları gerçekleştirmek, foto-reaksiyon hızını arttırmak ve güneş ve görünür radyasyonu etkili bir şekilde kullanmak için gereken enerjiyi azaltmak, TiO_2'a dallandırılmış silika katkılanması suretiyle mümkün olmaktadır.

Bu çalışmanın sonuçları, düzgün boyutlandırılmış dallandırılmış silika parçacıklarının sentezi, görünür ışık aralığında uzatılmış absorpsiyon için TiO_2 ile dallı silikanın dekorasyonu ve optimize edilmiş dip kaplama tekniği ile tekstil yüzeyine fotokatalitik bileşiklerin depolanması ve bunun yanı sıra, partiküllerin ultrasonik kimyasal banyo birikimi kaplamasıyla geliştirilmiş hidrofobik tekstil performansı saglaması şeklinde özetlenebilir.

ACKNOWLEDGEMENTS

TABLE OF CONTENTS

LIST OF FIGURES

xv

xvi

LIST OF TABLES

CHAPTER 1

INTRODUCTION

1.1. Background

Increasing environmental pollution and the heavy consumption of raw materials force humanity to make smart use of resources, including textiles. Particularly, the excessive environmental cost of the conventional cleaning methods implemented on textiles challenges the market to introduce new and more technological products. The apprehension of the severity of the problem, starting with the embargo of Organization of Arab Petroleum Exporting Countries (OAPEC) in 1970s, brought about the search for alternative energy sources in order to rid these countries of their petroleum dependence (Cor., 2013).

Photo-catalysis, which became popular in the 1970's is one of the conservation techniques among the textile cleaning methods. The photo-catalytic materials have also started to appear as an efficient treatment for water pollution over the last five decades. The use of photo-catalytic materials has been diversified based on a deeper understanding of photo-catalysis. Advances in this field have come from very different disciplines such as photochemistry and semiconductor physics (Cor., 2013). Scientific studies conducted on the textiles are linked to the desire of producing eco-friendly photo-catalysis over the last few decades. Although many of these studies have brought potential solutions, in order to widen the diversity of photo-catalytic materials, these solutions will still take a lot of time to be perfected, due to the variation in the demand (Kiw., 2016).

This thesis contains new findings on both the synthesis and combination of photocatalytic particles as well as manufacturing process of the photocatalytic textiles. In particular, the textiles described have been optimized for photocatalytic activity under natural visible

light rather than UV light, in addition to processing hydrophobic and anti-stain properties. These textiles were prepared and characterized in detail at laboratory scale as well as at a pilot scale production at the Kıvanç Tekstil facilities.

1.2. Literature Review

Beginning in 1970's, the self-cleaning textiles have been examined by several researchers, often with an interest in improving the photocatalytic process to replace the traditional cleaning techniques. These studies have made progress towards understanding and overcoming the deficiencies of self-cleaning.

The authors of more recent studies have reported on coating of self-cleaning particles of self-cleaning textiles, typically wool-polyamide and polyester materials (synthetic textile) with colloidal TiO_2 suspension at ambient temperatures. The preparation of TiO_2 suspensions with Degussa P-25 formulation, as one of the titanium oxide forms in a colloids solution, include titanium tetra-isopropoxide and titanium tetrachloride. Synthetic textiles exposed to pretreatments such as Radio Frequency (RF)-plasma, Microwave (MW)-plasma, Vacuum-UV were coated with a TiO_2 suspension in colloid solutions by Chemical Bath Deposition (CBD) for testing. After being stained with wine and coffee, these textiles were exposed to three different types of light sources, each with a different light intensity and wavelength. The authors characterized the coated textiles using X-Ray Diffractometer (XRD), and Transmission Electron Microscopy (TEM) and reported that the TiO_2 particles remained in significant concentrations after exposure to the UV radiation. It was found that applying the colloids were useful in cleaning the wine and coffee stains when irradiated with an artificial light source designed to emulate normal daylight (the remainder of the solar light received on the surface of the earth) (Boz., 2005).

Meilert et. Al. examined TiO_2 deposited onto cotton via chemical spacers in terms of elemental analysis of the TiO_2 loading. Non-toxic reagents and Degussa P-25 were used with a CBD-based coating procedure. The Attenuated Total Reflection Infra-Red (ATR-IR) spectroscopy, Atomic Absorption Spectrometry (AAS) and TEM techniques were utilized to characterize the samples. The ATR-IR spectroscopy analyses revealed that the presence of esters between the chemical spacers and the cotton surface. The samples were irradiated with a solar light simulator (90 mW/cm^2) which was operated continuously for a total of 24 hours. Cotton textiles irradiated with light and processed with only a minimal amount of chemical treatment showed to possess better self-cleaning properties, with respect to certain stains than heavily treated counterparts. However, this feasibility study did not include any specific empirical optimization of the various process parameters (Meilert, Laub, and Kiwi 2005).

Uddin et. al. synthesized Au/TiO_2 films and used them to coat cotton textile fibers. Au/TiO_2 cotton nanocomposite textile was prepared at low temperature (100℃) by a sol-gel and photo-deposition process. The Au/TiO_2 fibers were stained with methylene blue solution and exposed to the solar-light (50mW/cm^2) to test the photo-catalytic activity of the samples. Characterization of the synthesized Au/TiO_2 fibers was performed with a Scanning Electron Microscope (SEM), an Energy Dispersive Spectrometer (EDS), a TEM and a Raman and a UV spectrometer. The stained Au/TiO_2 fibers displayed color change under the sunlight from blue to purple. Also, surface morphology of the coated fibers suggested a good stability (Udd., 2008).

Yuranova et. al. synthesized colloidal TiO_2 from titanium tetra isopropoxide. Using the CBD method, cotton fabrics were coated with 1:1 mixture of TiO_2 and SiO_2 colloids. Samples were tested under solar light simulator with a power flux density of 90 mW/cm^2. The textiles coated with the freshly synthesized TiO_2 were also characterized by using

3

XRD, ATR-IR, EDS, and TEM. Stain discoloration were observed after 24 hours of continuous irradiation with the solar light simulator. However, the cotton textile surface was considered to be too rough and non-uniform (Yur., 2006).

Considering the available literature data, we can reasonably surmise that for optimal photocatalytic activity, it is necessary to examine through systematic experiments within the following two areas; (i) the optimum photocatalytic coating, (in terms of compounds used and their chemical modification) for the textile in most common use and with the widest applicability i.e. cotton/elastin blends and, (ii) the best process by which the coating is made and applied to the cotton/elastin blend in terms of e.g. simplicity, cost and environmental by-products. These two main research areas identified are of greatest pertinence if clothes with an effective and convenient self-cleaning property are to become a reality. Reflecting on the potential benefits of self-cleaning textile technology, (what has been achieved so far by various researchers and on what still needs to be achieved and investigated), it can be concluded that the topic requires an additional research effort.

1.3. Functional Textiles

Functional textiles are categorized based on their protective, medical, antibacterial and anti-wettable properties or by their application such as sportswear, vanity clothing, cross-functional clothing assemblies in addition to clothing for special needs. Various textiles have protective functionality and possess this property in relation to the environmental, chemical, biological and radiation hazards as well as injury protection. As an example, medical protective textiles cover therapeutic and rehabilitative as well as bio-sensing clothing. Another example of vanity clothing is used for compressing or supporting certain body parts to create a 'perfectly' shaped body and cross–functional

clothing is expected to simultaneously possess cross-functionality for use as, for example, military clothing and space suits (Gup., 2011).

Advanced textiles have been developed by the evolution of fiber encompassing conventional fibers, highly functional fibers and high-performance fibers. These new fibers are often blended with conventional textile fibers such as wool and cotton. The classification of sportswear is typically done according to the area in which its particular functionality is most relevant. Thus, performance wear, outdoor wear and sport-inspired wear all belong to the sportswear classification. The crossover between sportswear and leisure apparel is also growing in importance. Indeed, the increase in the use of functional textile fibers and fabrics in sportswear has to a large extent been driven from the intense interest of humankind in the active indoor and outdoor sports as well as outdoor leisure pursuits (Qiu., 2012).

In order to meet consumer demands in the new developed functional textiles, applications, progress has taken place regarding intelligent textiles and interactive materials and there is still great market potential for further developments in functional outwear applications. Materials used for these intelligent textiles are chosen according to the intended area of application and can be further specified as self-cleaning textiles, hydrophobic textiles and anti-bacterial textiles within the interest of this thesis.

1.3.1. Self-cleaning textiles

Self-cleaning textiles possess the property such that the textile surface cleans itself without resort to laundry action. This attribute provides significant benefits with respect to the prevention of environment pollution and the advantage of clean uniforms and fresh garments for the people who has to work in uniforms.

Some self-cleaning materials utilize photo-catalysis. Standard photocatalytic activity requires sunlight (natural UV), air and water vapor in order to produce highly oxidative radicals that are able to break down contamination. Photocatalytic additives can also endow textiles with hydrophobicity and protection against the bacteria, viruses and fungus besides self-cleaning (Kiw., 2016)(Qiu., 2012).

A self-cleaning textile production process for the treatment at industrial scale includes the following two steps; (i) development of photo-catalytic additives and (ii) the coating processes. The assessment of self-cleaning textiles as a product with photo-catalytic activity in textile applications has demonstrated that self-cleaning textiles are generally best made from either cotton or elastin type fibers (Kiw., 2016).

1.3.2. Hydrophobic textiles

Hydrophobicity is one of the physical properties of a substance that is non-polar in nature. The hydrophobic molecules do not dissolve in water and repel the water molecules, which help render the surfaces not water liking.

Likewise, textiles coated with hydrophobic materials demonstrate resistance to becoming wet. On hydrophobic textiles the water tends not to be absorbed and, instead, droplets stay on the surface of the textiles with a beaded up structure, which has a high contact angle value. This property of hydrophobic textiles is particularly desirable for use in protective clothing, which under, in difficult weather conditions, help to maintain comfortable and safe conditions for the body as well as providing durability for synthetic fabrics. In addition, the hydrophobic textiles have stain resistant properties which help in their cleaning as well (Zim., 2008).

1.3.3. Antibacterial textiles

Textile and clothing materials provide a suitable environment for the breeding of microorganisms such as bacteria and fungi. studies indicate that microorganisms could survive on fabric materials for more than 90 days. Such a high survival rate of pathogens on medically used textiles have caused concerns about contaminated clothing contributing to the transmission of contagious diseases (Qia., 2005).

Antibacterial textiles usually go through a finishing process. Gradually, however, this finishing process is being replaced by the use of photo-catalytic materials, which can self-clean organic and inorganic pollution. Therefore, antibacterial textiles are becoming more useful in not only hospital environments but also wherever a sterile and hygienic environment is important such as in schools, the army as well as for everyday casual usage (G. Fou., 2012).

1.4. Photo-catalysis

Based on the review in sections 1.3.1 through 1.3.3, the use of photocatalytic materials in textiles to perform the self-cleaning, hydrophobicity and anti-bacterial functions should be thoroughly investigated and this in turn means it is vital to understand the background of photo-catalysis.

A catalyst is a substance which can accelerate a reaction without consumption by reactants and is a compound which can be used to lower the free activation enthalpy of the reaction (Wub., 1983). Therefore, photo-catalysis can be defined as a process of reaction actualized to photoreaction by the presence of a catalyst. In this process, chemical alteration occurs in one molecular entity as a result of the initial absorption of radiation by another molecular entity called the photosensitizer. Yet, it dismisses the photo-

acceleration of stoichiometric thermal reaction regardless of whether it emerges in a homogenous solution or at the surface of a lighted-up electrode. The catalyst might speed up the photoreaction by interaction with the substrate in its ground state or with a primer photoproduct (Cas., 2011).

As the light is absorbed by the catalyst D, a sensitized reaction may occur in two different ways as represented by Equations 1.1 and 1.2. Equation 1.1 explains the sensitized photoreaction via energy transfer by forming an activated state of reactant of interest, "B". Thus, oxidation occurs more easily as compared to the non-sensitized reaction;

$$D \xrightarrow{h\nu} {}^*D$$
$${}^*D + B \rightarrow {}^*B + D \qquad \qquad [1]$$
$${}^*B \rightarrow P$$

$$D \xrightarrow{h\nu} {}^*D$$
$${}^*D + B \rightarrow B^- + D^+$$
$$B^- \rightarrow P^- \qquad \qquad [2]$$
$$P^- + D^+ \rightarrow P + D$$
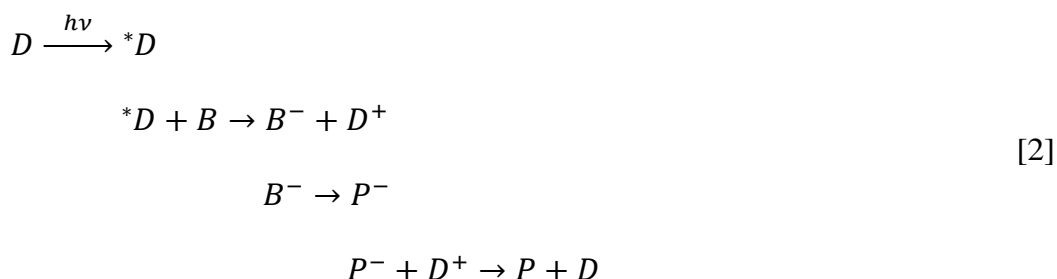
The reaction acting as an electron donor or acceptor is represented in Equation 1.2. The product "P" occurs from the activated substrate throughout the potential energy curve, while a new reaction step is created when the photosensitizer transfers an electron to the substrate. The direct occurrence of electron transfer will be of greater concern when including energy transfer by the excited-state redox reactivity which particularly includes organic photo-catalysis (Cas., 2011).

The difference between a sensitized and a catalyzed photoreaction is (to a certain extent) arbitrary because of the dissimilar and complex mechanisms. Thus, the term, photo-catalysis has been defined as extensively as possible without the specific suggestion of any particular mechanism and represents matter whose function is activated by the absorption of a photon. Accordingly, a photo-catalyst can be described as one involved in quantum yield expression for photochemical reaction without its stoichiometric aspect or, more exactly, it emerges in the quantum yield expression for a reaction from a certain excited state to a power greater than the coefficient in the stoichiometric equation (Sch., 1985).

1.4.1. Heterogeneous photo-catalysis

Heterogeneous photo-catalysis, which has undergone various developments, in relation to energy and the environment, can be actualized in numerous ways such as in the gaseous phase, pure organic liquid phases or aqueous solutions.

The process for classical heterogeneous catalysis can be considered to comprise of the following five steps; (i) transfer of the reactants in the fluid phase to the surface, (ii) adsorption of at least one of the reactants, (iii) the reaction in the adsorbed phase, (iv) desorption of the product(s) and, (v) removal of the products from the interface region. The photocatalytic reaction arises in the absorbed phase. The activation mode is not associated with the rest of the steps for classical heterogeneous catalysis, although photo-adsorption and photo-desorption of reactants do exist mainly as oxygen (Her., 1999).

In the fluid phase, gas or liquid, an inherent spontaneous adsorption happens. Considering the redox potential of each adsorption, an electron transfer occurs towards the acceptor molecules. Whereas, positive photo-holes are turned into the donor molecules as shown in Equations 1.3 to 1.5 (Her., 1999),

$$hv + C \rightarrow e^- + p^+ \hspace{4cm} [3]$$

$$A_{(abs)} + e^- \rightarrow A^-_{(abs)} \hspace{4cm} [4]$$

$$D_{(abs)} + p^+ \rightarrow D^+_{(abs)} \hspace{4cm} [5]$$

Then, either one of the ions reacts and forms the intercessors and final products. The photonic catalyst excitation arises as the primary step of the activation of the whole catalytic system, as a result of reactions given in Equations 1.3 through 1.5. Therefore, the incident photon should be considered as a reactant with two aspects; (i) photon flux of special fluid phase and, (ii) electromagnetic phase. The initial energy, (the photon energy) is transferred to the absorption of the catalyst, not depending on the reactant. The activation of the process goes through an excitation of the solid but not through that of the reactants (Her., 1999).

1.4.2. Homogenous photo-catalysis

In homogenous photo-catalysis, the reactants and photo-catalysts are in the same phase, which is liquid. H_2O_2/UV, O_3/UV, O_3/H_2O_2 and Fenton reaction (H_2O_2/Fe^{+2}) are necessary for the homogenous photo-catalysis so that an advanced oxidation process may occur. Naturally, each of these photo-catalysts have their own process reaction equation and absorption energy to start the reaction. The homogeneous photo-catalysis process can be represented by the basic equation as represented in Equation 1.1. For a process including extra catalytic and UV exposure, and which includes a Fenton reaction, ozone and hydrogen peroxide catalysts Equation 1.2 can be used. However, the steps in this latter process might have radical consumed. This is an undesirable condition in terms of the persistence of the photo-catalysis process (Çal., 2008).

Homogenous photo-catalysts have some disadvantages such as; lesser photocatalytic activity, easy heat transfer, expensive recycling and poor selectivity. Yet, the homogeneous photo-catalysts is commonly used for water treatment and chelation with organic ligands from easily obtainable metal ions (Cie., 2004).

1.5. Band theory for solids and initial energy

The electrons of an atom will begin to interact with each other as the atoms of an element come close to each other. Otherwise, the Pauli exclusion principle, when used to describe the settlement of electrons in atoms to particular energy levels, starts to get in effect. Pauli's exclusion principle states that more than one electron cannot have the same quantum number in an atom. According to this principle, if there cannot be two electrons with the same quantum number in an atom, two electrons with the same quantum number cannot exist in a "macro-molecules" either. Therefore, quantum pockets in the atomic energy levels as atoms are brought closer. Similarly, when a great number of atoms come together to create a solid, atomic energy levels will start to split. If the entire solid is considered, these levels are close to each other and can't be distinguished.

Materials with such energy bands are considered to be continuous structures because of the small energy between the splitted levels. Just as electrons cannot exist between energy levels in atoms, electrons cannot exist in energy levels between two bands in a solid either. Furthermore, there are energy regions (energy bands) in which electrons can and cannot exist. Bands, in which the electrons might be found, are called allowed bands while bands in which electrons cannot be found are designated as the forbidden bands (Cer., 2015).

The energy band containing the valence electrons, outermost orbit electrons, is called the valence band. The valence band is completely filled with the electrons at absolute zero temperature as shown in Figure 1.1. In this case, electrical conduction defined as the

transmission of electrons in the valance band to the conduction band is impossible. Electrons in the valance band may pass through the conduction band by excitation through heat or light. Consequently, they leave their position leaving holes in the valance band. Both electrons in conduction band and holes in the valance band contribute to the electrical conduction.

Meanwhile, since the electrons cannot be positioned in the forbidden bands, the stimulant light has to have a certain minimum energy, a threshold energy, so that the electrons may be excited to the conduction band, as Figure 1.2 demonstrates. This threshold energy is called the band gap energy (labeled E_g) and the band gap energy defines the minimum energy of light required to initiate photo-catalysis. This triggering band gap energy for photo-catalysis, also called initial energy, is another important characteristic property of the materials (Cas., 2011), (Tob., 2013). The band gap energy and band structure of solids forming a crystal structure give vital information about both free electron and free hole behaviors. This information is crucial for understanding the chemical, electrical and optical characteristics of the solid substances (Cer., 2015).
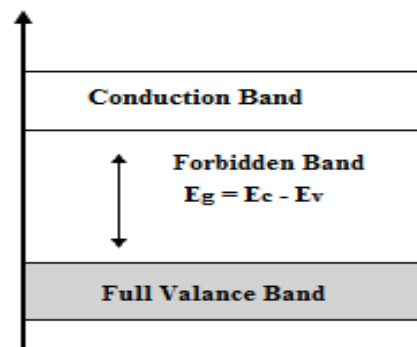
Figure 1.1. Conduction and valance band of intrinsic semiconductor at absolute zero temperature (T=0°K).
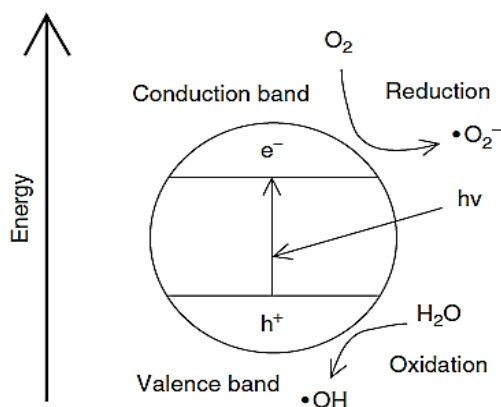
Figure 1.2. Photo-promotion of an electron, reduction of oxygen and oxidation of water (Cas., 2011).

1.6. Photocatalytic activity enhancement for visible light range

Photocatalytic materials are generally semiconductor substances. The most important property of a semiconductor is that electron flow in the material is controllable by the addition of dopants. Impurity (dopant) concentrations lower than 0.0001% can bring about remarkable effects on the optical, electrical and chemical properties of the semiconductor materials (Tur., 2000).

To enhance photocatalytic activity by the light within visible range, the initial energy of photon should correspond to the energy of photon in the visible light energy. However, the band gap energies of almost all intrinsic photocatalytic semiconductors equate to photon energies in the ultraviolet range (Coh., 1977). Photo-catalysis with visible light is possible if the band gap of the photocatalytic materials is adjusted via the most common and easy method utilized for semiconductors i.e. adding impurities (Tur., 2000).

Adding impurities, or doping, is simply the process of introducing impurity atoms, known as dopants, into the semiconductors. The presence of dopants changes not only the electrical properties but also the optical properties of the semiconductor. The dopants are labeled according to their contribution to the holes or electrons in the semiconductor

substance. For example, the inclusion of atoms with valence electrons (donors e.g. phosphorus, arsenic, antimony) is referred to as n-type doping and, in this case, negative free radicals are released. When atoms with valence electrons (acceptors, which include atoms such as boron, aluminum, gallium) are included, extra holes are introduced into the semiconductor, due to the shortage of electron pairing created and this is named p-type doping.

According to Fermi-Dirac statics, n and p-dopants will add new energy levels in which the electrons of impurities are able to locate themselves where they could not be able to position themselves in the loaded valence or conduction bands. These n and p dopant electrons or holes, called donors and acceptors, respectively. They can be easily transferred to the conduction band by applying an energy which is much smaller as compared to the intrinsic semiconductor band gap energy (Cer., 2015).

The photo-catalyst semiconductors require smaller initial energy to start photo-catalysis reaction as a result of doping. This doping should reduce the band gap energy of intrinsic photocatalytic semiconductors from the UV light region to the visible light range according to the Planck-Einstein relation (Coh., 1977).
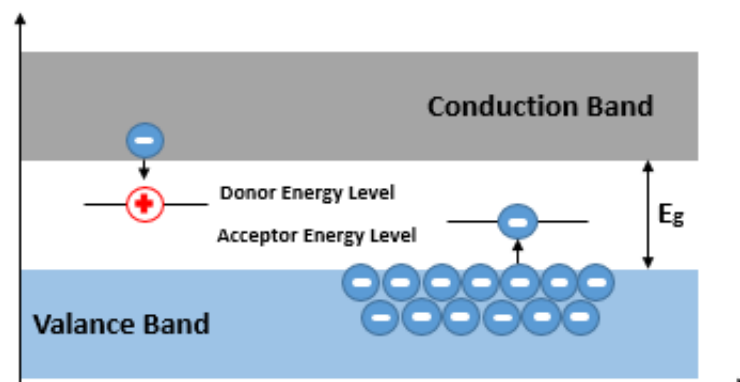
Figure 1.3. Doping in the band structure.

1.7. *Manufacturing techniques for self-cleaning textiles*

Traditional technologies, including coating, finishing, and lamination of textiles, are still used for almost every area of industry and are commonplace in our everyday lives. The lamination of textiles joins a fabric and a prepared film by adhesion, heat, and mechanical bonding and replaces (or supplements) sewing to obtain laminated fabrics with enhanced functionality and more consistent qualities. However, the definitions of coating and finishing can be confusing and require some explanation in definition in the textile manufacturing (J. Hu., 1925).

The finishing process takes place at the end of the textile processing whereas coating can be applied at two different stages; (i) yarn production or (ii) post-treatment. This is shown in Figure 1.4. The coating and finishing processes should be approached in terms of their structural properties.
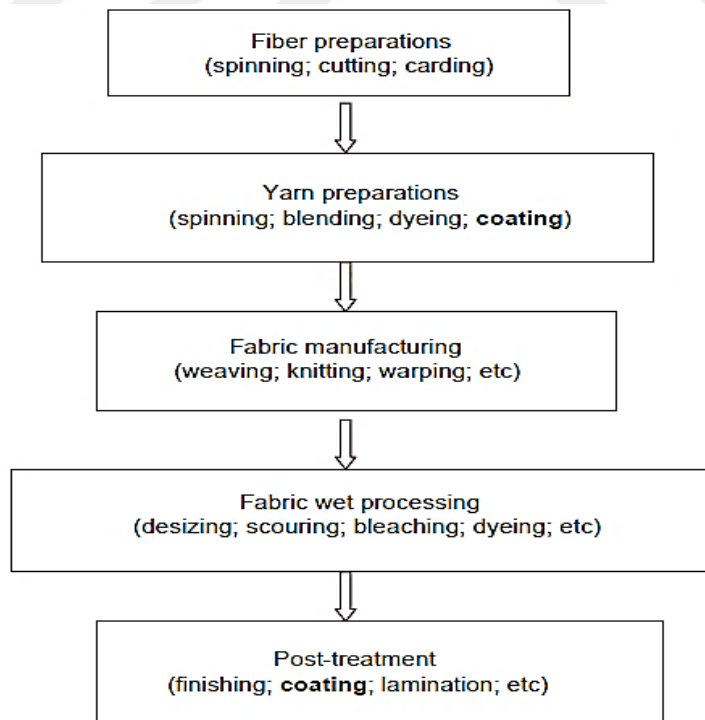
Figure 1.4. Coating and finishing stages in textile processing (J. Hu 1925).

1.7.1. Physical techniques

1.7.1.1. Coating methods

Coating process is a physical method to deposit a new layer, which can provide additional properties to the textile surface. The coating application can also complete the yarn preparation such as in warp sizing.

In the coating process, a thick liquid chemical or paste is utilized to form a continuous film on the yarn or textile surface. Openings between the fiber and yarns may shrink to varying degrees or vanish depending on the features of the liquids used. The traditional textile coatings are usually inactive protections but the new trend is to use a substrate designed with an additional barrier on purpose to be applied on the textile surface. This barrier can actively change the properties of the textile. While some advanced coatings can enable the textiles to exhibit functionalities such as providing wrinkle free, flame retardant, properties etc., an active coating gives textiles intelligent properties more than just the functional performance. As an example, an active coating can sense the environmental changes, and may react accordingly (J. Hu., 1925) (Shi., 2010).

Many traditional coating methods can be implemented in the active textile industry. Although plenty of coating processes exist in industry, the main purpose of all the coating methods is that they produce a stable film with the desired adhesion and designed functionalities on the substrate surface. The new technologies such as nanotechnology, plasma technology and sol-gel technology have been implemented in coating processes to manufacture functional and active textiles. The sol-gel technique is the most promising of these methods and it offers a low-temperature method for material synthesis with both inorganic or organic content. Also, several techniques are possible in order to achieve a

sol-gel process. Dip coating, spray coating, chemical bath deposition are basic techniques used to deposit sol-gel coatings (Shi., 2010).

1.7.1.1.1. Dip-coating

The dip coating method, as one of the various thin film deposition methods, refers to the oldest commercially used coating process. The patent of this process was obtained by Jenaer Glaswerk Schott & Gen. in 1939 for sol-gel derived silica films. The dip coating method can be used for a wide range of applications in industry owing to its cheap and moderate applicability conditions (Bri., 2013).

Basically, the process may be separated into five important technical stages; (i) immersion; the substrate is immersed into the solution of the coating material at a constant speed, (ii) dwell time; the substrate is immersed into the precursor solution at a constant speed followed by a certain dwell time in order to leave a sufficient interaction time for the substrate to become wet with the coating solution, (iii) deposition and drainage; this is achieved by pulling the substrate upward at a constant speed so as to achieve a thin layer of precursor solution, i.e. film deposition. Excess liquid will percolate from the surface and (iv) evaporation; the solvent evaporates from the fluid, forming a deposited thin film, which can be promoted by heated drying, (v) subsequently, the coating may be exposed to further heat treatment in order to hasten drying (Bri., 2013).

In this simple process, the substrate is dipped into a bath of the coating solution, which is normally of low viscosity, and then run back as the substrate emerges (Figure 1.5). This process is frequently used on porous substrates. As a result, the dip-coating method is the most widely compatible among all the potential application (J. Hu., 1925).
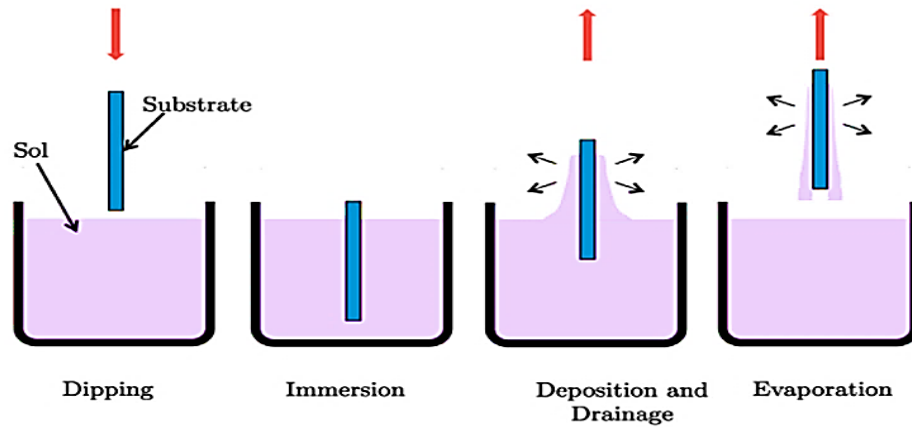
Figure 1.5. Illustration of dip-coating method (Brinker 2013).

1.7.1.1.2. *Chemical bath deposition*

The Chemical bath deposition method (CBD) is one of the useful methods to deposit thin films and nanomaterials, as it does not need expensive equipment investment. It is also a scalable technique applicable to wide area continuous deposition (Kathalingam et al. 2010). The CBD method has two main steps, (i) nucleation and (ii) particle growth. The substrate or target is immersed into a solution and then, via stirring of the solution, settlement of the particles on target occurs (Kat., 2010).The major advantage of CBD is that it requires only one container for the solution, in order to conduct process as shown in Figure1.6. The target (i.e. the substrate) on which the coating is to be deposited is immersed into this solution.

Figure 1.5. Chemical bath deposition process by ultrasonic stirrer.

The main shortcoming of this method is the disposal of the solution after every deposition. Amongst various deposition techniques, chemical bath deposition produces stable, adherent, uniform and hard films with sufficient reproducibility by a moderately simple process (Gov., 2004). The chemical bath deposition method is also one of the suitable methods for preparing highly efficient thin films in a basic media and is commonly used for the deposition of various metal chalcogenide thin film suspensions.

The growth of thin films is based on the growth conditions, such as; duration of deposition, composition and temperature of the solution, and the topographical and chemical nature of the target (Gov., 2004).

1.7.2. Chemical process

1.7.2.1. Chemical finishing methods

The term 'finishing' usually refers to the operations for improving the appearance or usefulness of a textile after fabric wet processing and it also includes washing, bleaching and coloring. The fabric wet processing comes after the fabric manufacturing steps composed of the loom or knitting processes. At the end of the whole process, finishing changes the characteristics of textiles and gives them special properties such as the final soft feeling, hydrophobicity, etc. (J. Hu., 1925).

The purpose of the finishing process is to improve the appearance of the fabric and it is achieved via steps such as calendaring, optical whitening and changing the physical feeling of the fabric by softening as well as improving the physical properties by increasing wearing qualities by making textiles shrink and/or crease resistant. Furthermore, making garments hold their shape and enabling them to be wearable without ironing are among the aims of the finishing process. The finishing is also used for creating

dimensionally stable and stronger, durable fabrics. The chemical finishing process is a method to provide all these objectives for textiles (Sch., 2004), (Tes., 1968).

The finishing solutions used for chemical finishing processes include various acids, alkalis, bleaches, resins, detergents, softeners, and other chemical materials. These chemical substances cause permanent changes in the fiber, yarn or fabric by chemical reactions. Thus, curing time and exposure of finishing solution, is critical if damage to the textile is to be avoided. Also, since the finishing process is a wet procedure, a drying step is necessary after it is completed (Sch., 2004).

The heat applied at this stage is an important consideration for dry step finishing because drying at a high temperature may induce tear, color change and burning (part of fabric) or cause chemical decay of the finishing solution. In order to successfully complete both the coating and the drying steps, a padding machine (Figure 1.7) is an advantageous device since it allows fine control of the timing of both the curing and the drying steps. The timing of these steps may vary for each textile type, which is critical for the finishing process to be successfully completed (Sch., 2004).

Figure 1.6. Padding machine (Atac Makina, 2016).

1.7.2.2. Chemical functionalization for enhanced attachment of functional additives

In recent years, numerous intensive studies on nanotechnology emerged with new potential applications outside of the usual methods. Semiconducting nanostructured materials and other nanostructured materials have generally been consulted versatile chemical methods for the developed production. A major improvement has taken place via the synthesis of desired organic/inorganic nanomaterials for the applications in the areas of energy conversion, sensing, electronics, photonics, and biomedicine (Hee., 2011).

Chemical functionalization is carried out by modification of particles or additives. The modification might be carried out by diverse chemical synthesis techniques. Nowadays, polymeric material based synthesis is widely implemented and is an advantageous procedure to create required particles. These additives can be connected by molecular blocks via directed noncovalent interactions such as hydrogen bonding, electrostatic, metal–ligand, or π– π interactions (Goo., 2017). The size of modified particles and additives is controllable and it is possible to acquire uniform particles in terms of size distribution by some synthesis methods (Stö., 1968). Furthermore, the surface modification of textiles through synthesized particles helps supply incremented surface stability and prevention of agglomeration (Sim., 2007). Naturally, these modifications lead to changing chemical and physical properties of particles such as morphological, optical, and liability of bonding and mechanical durability (Aid., 2012).

The utilization of polymer technology rapidly arises in the textile industry as well. Synthesizing functional polymers with specific compositions, blending polymers with special molecules, designing special structures, and modification with chemical or

physical treatments diversify a response to a narrower range of external stimuli such as heat, water, light, and pressure on textiles.

These polymers can be implemented on textiles through coating and finishing agents depending on the type of the textile fabrics. These agents can also be either polymeric or responsive hydrogels known as finishing solutions or binders. However, there are many types of polymers but many are not suitable for textile applications. The finishing solution or binders are reacted with textiles according to their ingredients for some technological properties. Consequently, they can also be used as solvents to prepare suspensions for curing in coating or finishing processes (J. L. Hu., 2016).

1.8. Composite materials

The ingredients of the finishing solutions used in this study are amino functional silicon micro emulsion, non-ionic softener, nonionic-polyethylene and acetic acid. These chemicals blend to form long polymeric chain by creating hydrogen bonding, electrostatic, metal–ligand, or π–π interactions (Goo., 2017). In this study, the finishing solutions are used not only for classical textile manufacturing purposes, such as calendaring, optical whitening and changing the physical feeling of the fabric, but also as an ancillary agent to increase the stabilization of the photocatalytic particles and for obtaining specific effects through polymerization (Pau., 2001).

Given that the baseline photocatalytic semiconductor activity is known to be in the ultra violet range, the enhancement of the photocatalytic particles activity in the visible range is attributed to the formation of bonds between photocatalytic particles and pure elemental dopants or synthesized particles. In this study, the advanced particles were chosen to be the branched particles due to the practical methods of synthesis and controllable particle size distribution. The branched shell can actively control the binding event by pairing ion,

metal complex recognition and hydrogen-bond recognition (Ran., 2012). Thus, photocatalytic particles will be in certain composite structures as a result of using branched particles and their interaction with finishing solution monomers, as illustrated in Figure 1.8.

Composite materials are structural materials composed of two or more ingredients which are not soluble in each other. One of their ingredients is named the reinforcing phase and the other one that the reinforcing phase material is embedded, is termed the matrix. The matrix is so called because the reinforcing phase material is embedded within it. The reinforcing phase materials may be in the form of particles, fibers, or flakes while the matrix phase materials are generally epoxy resins. The matrix phase materials are usally light and weak. The materials known as reinforcing phase are strong but hard, and may not be light in weight (Cha., 2012).

Both types of composite phases contribute to the mechanical performance on materials. This mechanical performance provides the textile with advantageous properties such as; protecting the surface of the fibers from mechanical degradation, keeping the fibers of the textile in place and protect against impacts from aspects of environment such as chemicals and moisture.
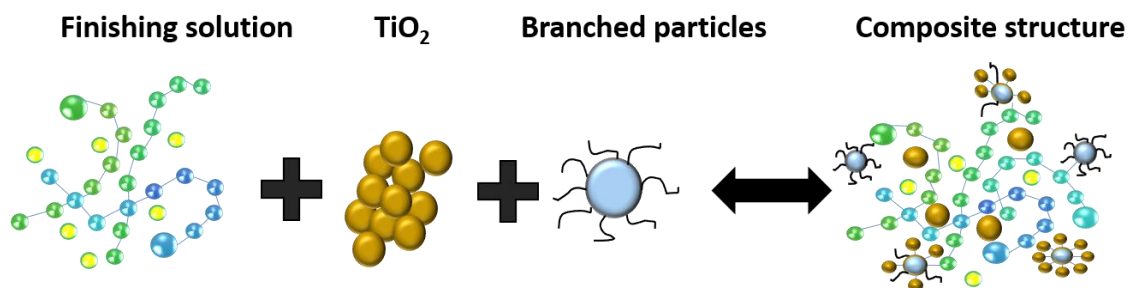
Figure 1.7. Formation of composite particles in this study.

Moreover, the joining of specific particles to form composite structures allows for the design of textiles with novel properties, especially with respect to photocatalysis. In this way, the utilization conditions of self-textiles made from composite materials can be diversified.

1.9. *Utilization of self-cleaning textiles*

Changing lifestyles, increasing requirements of clean clothes, the obligation to protect natural life and the need to reduce energy consumption have increased the demand for self-cleaning textiles. Therefore, photo-catalysis which can occur under normal environmental conditions, (i.e. under daylight and in the presence of oxygen and moisture) is highly desirable.

Self-cleaning textiles would ideally clean themselves in few hours by exposure to light. The time required for self-cleaning of a textile depends on the specific type of fabric, the coating used for photocatalytic material and the environmental conditions. With respect to the type of stain, organic and chemical contaminations can contaminate the self-cleaning textiles. However, these contaminants should not be sedimentary such that the entire surface of textile is shielded from the light necessary to initiate and sustain the self-cleaning action. This sedimentary part i.e. large particles (such as coffee grains) of dirt should be removed from the textile surface before self-cleaning cycle can be initiated.

Also of interest are commercial self-cleaning textiles such as curtains and carpets. Curtains and carpets are basically made from PES, elastin fibers and wool. However, the manufacturers are not explicit about the contents of their products, effectiveness of products for self-cleaning process and user satisfaction in general.

The commercial products are also limited since self-cleaning process may be unstable and slower than usual cleaning techniques. In addition, there are some conditions which might affect the initiation of the photo-catalysis like incident light energy, fabric blend and surface characteristic. Gradually, scholars have come to agree that these unstable conditions can potentially be overcome and which is the scope of self-cleaning textiles in terms of permanently replacing the conventional cleaning methods (Kiw., 2016), (Cas., 2011).

1.10. Objective and scope of study: development of self-cleaning textiles at visible light range

Many reports have been published on self-cleaning textiles over the last few decades. It is generally agreed today that self-cleaning textiles created from photocatalytic materials should be examined in order to achieve innovative and sophisticated high quality functionalized films and consequently increase the potential market applications of self-cleaning processes. For the purpose of this study, photo-catalysis and self-cleaning textiles will be discussed in the context of visible light range activity, the effects of the manufacturing and processing stage and in the creation of possible market production.

As an empirical phenomenon, high efficiencies of intrinsic photo-catalytic semiconductors have repeatedly been observed in the UV light region. Thus, a textile coated with such an intrinsic photo-catalyst will display self-cleaning properties when irradiated with UV light. However, only 8% of the total irradiance, power per area, of indirect window-filtered daylight is in the UV region (300-400nm) (Qui., 2004). Consequently, self-cleaning processes may take too much of a time as compared to the traditional cleaning methods. The self-cleaning efficiency of photocatalytic materials, which make use of light in the visible range might be improved by the chemical

modification of the photocatalytic particles. The chemical modification of the photocatalytic materials might be supplied by synthesis methods or by the synthesized dopants. Recently, the expectation of discovering high performance self-cleaning technologies have been re-addressed as polymer chemistry has accomplished to materials with spectacular properties.

The necessity of modifying the photocatalytic particles is certain, but there is also room for optimizing the coating processes. There is a potential for simplification of the process by incorporating the coating step into the finishing process. As predicted, the manufacturing stages of textiles also include some chemical treatments. They are useful in the pre-treatment of self-cleaning textiles before the coating process (Boz., 2005). This pretreatment is known as a finishing process. Solutions are utilized during the finishing process, which have a chemical crosslinking agent together with a catalyst and a fiber lubricant/softener. Since the coating step is a post-treatment to the finishing process, the compounds used in each step should be physically and chemically compatible.

The market of self-cleaning textiles has been limited as the photo-catalytic activity is restricted to the use within the UV light range. The harmony between the photocatalytic materials and the textile production and manufacturing has been neglected in the development of self-cleaning products and needs to be resolved through rigorous experimentation, analysis and quality measures, if the full potential of self-cleaning textiles is to be realized.

This study has been initiated by noting the possibility of achieving similar results to those in the existing literature but with chemical modifications to the photocatalytic materials, which should bring the mentioned synergy and improvement in photocatalytic activity.

The foregoing discussion has attempted to explain, in outline, self-cleaning materials and photo-catalysis.

In this thesis, the baseline photocatalytic particles were initially analyzed in terms of particle size, measured using two different methods. Next, the suitability of the particle emplacement to the finishing processes in terms of the solution stability was determined and then the photocatalytic activity of textiles coated with the particles was ascertained through absorbance and stain tests. The result of these analyses have been interpreted quantitatively so as to decide on the choice of the photocatalytic material which has the greatest self-cleaning ability as well as compatibility with the finishing process. This photocatalytic material was among the baseline photocatalytic particles and one of the TiO_2 forms and blend of TiO_2 forms. Furthermore, it has been considered that this material is to be used as a possible extrinsic semiconductor dopant so as to enhance photocatalytic activity in the visible light range.

The use of pure boron as p-type dopant for a potential breakthrough in photocatalysis has also been investigated as the second part of this study. Thus, a succession of absorbance tests has been conducted to find optimal photocatalytic performance. This has been done using the Design-Expert software, which uses a powerful statistical method and multifactor testing techniques. The textiles coated with photocatalytic particles doped with the desired amount of pure boron nanoparticles have also been evaluated in terms of initial energy, stability of doping solutions and the photocatalytic efficiency.

The creation of dopants or particles has been done in such a way so as to both enhance the photocatalytic activity in the visible light range and supply a standard solution for self-cleaning textile manufacturing. Promising composite particles were synthesized according to the basic sol-gel methods described in the literature and the effects of these

particles, when used in combination with the baseline photocatalytic material, on self-cleaning action was analyzed by running pre-absorbance tests. The most active solution, as determined by the preliminary tests, was used to coat the textiles in the finishing process using a padding machine based on dip-coating method. The suitability of the coated textiles to be used as market products, was appraised using surface morphology absorbance post-tests, stain tests, physical resistance measurements, water transmittance tests and washing tests based on the related ISO standards.

Consequently, this study serves as a window into the understanding and improvement of self-cleaning textiles irradiated with visible light, the characterization of photocatalytic particles, quality control tests, the combinations of fabrication products and to the increased functionality made possible by photocatalysis.

CHAPTER 2

CHARACTERIZATION OF PHOTOCATALYTIC PARTICLES FOR SELF-CLEANING ABILITY

2.1. Introduction

Self-cleaning ability is one of the attributes of photocatalytic materials. The nature of photocatalysis is based on solid state chemistry and knowledge on crystal structure, imperfections in solid, nonstoichiometric as well as electronic properties of solids for characterization of photocatalytic materials. These relations affect the photocatalysis functionality of materials (Cas., 2011).

Most commonly used photocatalytic materials are zinc oxide (ZnO), cadmium sulfide (CdS), iron(III)oxide (Fe_2O_3), tungsten trioxide (WO_3), tin oxide (SnO_2), zinc sulfide (ZnS) and titanium dioxide (TiO_2). The composites of these main compounds are also used in photocatalytic applications in manufacturing as well. Among these, titanium dioxide (TiO_2) is the most commonly used photocatalyst for the textiles (Pat., 2013).

TiO_2 has attracted attention because of its potential for both homogenous and heterogeneous photo-catalysis (Kim., 2004), (Cas., 2011). The main advantages of TiO_2 are its high chemical stability when exposed to acidic and basic compounds, nontoxicity, and high oxidizing ability. The fact that it can be abundantly found also plays an important role in addition to its low cost, which made it a proper candidate for various photocatalytic applications.

In this chapter, the potentials of two different crystalline forms of TiO_2 were screened to investigate standard photocatalytic activity for self-cleaning ability. The photocatalytic

efficiency of anatase and P-25 (anatase and rutile combination) types TiO_2 were studied by particle size, solution phase absorbance analyses in addition to additives as textile coatings.

2.2.   Materials and methods

Surface chemistry plays a critical importance in photo-catalysis to understand relevant structures, compositions, surface dynamics of atoms and molecules, and the electronic properties of the surfaces. Adsorption and bonding of atoms and molecules on the surfaces are required to be known to understand the mechanisms of self-cleaning ability. Different titanium dioxide forms were chosen as photocatalytic materials for this study to create standardization and to select the most efficient form of titania for the self-cleaning ability. Degussa-P25 and anatase were examined to build a standard background for the testing. TiO_2 has three polymorph forms varying in crystal structures as rutile, brookite and anatase. Degussa-P25 titanium dioxide powder contains anatase and rutile forms blended in a ratio of 3:1.Its band gap energy is 3.26 eV as reported in the literature (Lóp., 2012) and it is commonly used as a benchmark for photo-catalysts (Rui., 2014) (Oht., 2008).

Anatase is the most thermodynamically stable form of titania amid the three nanocrystal types Anatase with higher crystallinity is favored for photo-catalysis, since higher crystallinity provides a smaller quantity of defects acting as recombination sites in the middle of photo-generated electron and hole combination (Fil., 2015). It is more active than the rutile phase as a photo-catalyst, although its band gap value, 3.27 eV, higher than the rutile's band gap which is 3.05eV (Lóp., 2012) (Fil., 2015) (Now., 2012). The tetragonal crystal structure of anatase is shown in Figure 2.1.
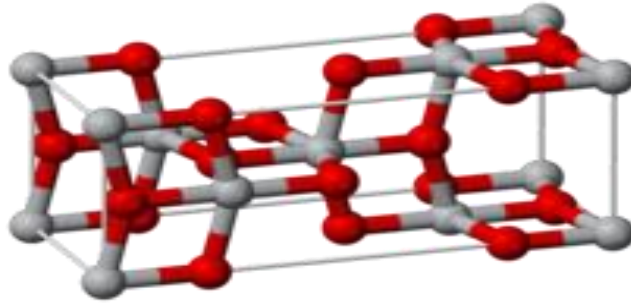
Figure 2.1. Crystal structure of anatase (Yin et al. 2010).
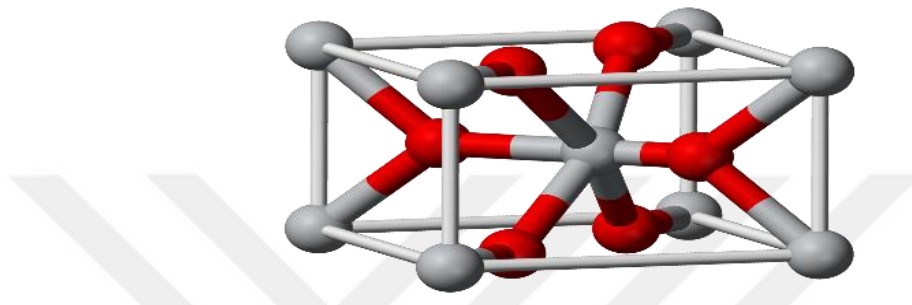
Figure 2.2. Crystal structure of rutile (Yin et al. 2010).

Brookite and anatase can transform exothermically and irreversibly to the stable rutile form upon heating and hence, are thermodynamically metastable forms. The transformation of the amorphous titanium dioxide to anatase form of titanium dioxide has been reported to commence at temperatures as low as 100-150°C, while rutile has been reported to form over the temperature range of 550-800 °C (Bey., 2002). The crystal structure of rutile form of titanium dioxide is illustrated as the tetragonal shape in Figure 2.2.

2.2.1. Principles of TiO$_2$ Photocatalysis

Oxidation and reduction reactions in photo-catalysis of TiO$_2$ also require explanation. TiO$_2$ is known as a semiconductor material and it behaves as a strong oxidizing agent, lowering the activation energy of decomposition reaction of organic and inorganic pollutions. TiO$_2$ induces separation of two types of charge carriers; electrons and holes through illumination on the surface.

Adequate energy needs to be supplied by a photon to produce these two carriers, which in turn excites an electron from the valence band to the conduction band. The excited electron leaves a hole behind in the valence band as illustrated in Figure 2.3.

In the photocatalytic process, recombination of electrons and holes is slower than the electrical conduction recombination movement. Also, the sufficient energy supplied by a photon depends on the band gap energy specific for that material. Photo-induced holes can oxidize a donor molecule (humidity in air) adsorbed on the surface to produce hydroxyl radical as can be seen in Equation 2.1 and 2.2;

$$h\vartheta + TiO_2 \rightarrow e^- + h^+ \qquad\qquad [1]$$

$$h^+ + HO_2 \rightarrow OH^- + H^+ \qquad\qquad [2]$$

These hydroxyl radicals can increase the photocatalytic activity. However, very high humidity will lower the photocatalytic activity by taking up more adsorption sides on the surface (Hen., 2015). The electron in the conduction band reduces an acceptor molecule (O_2) to obtain superoxide ion as seen in, Equation 2.3;

$$e^- + O_2 \rightarrow O_2^- \qquad\qquad [3]$$
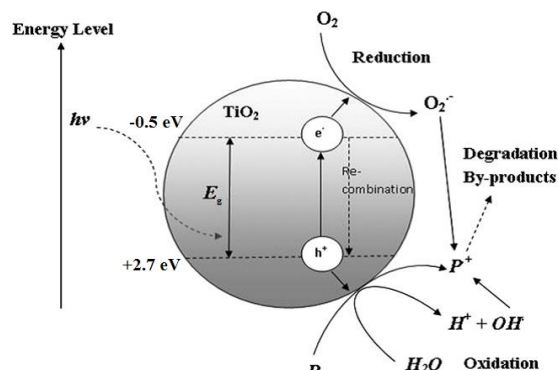
Figure 2.3. Recombination of an electron by illumination in anatase, reduction of oxygen and oxidation of water (Uma., 2013).

The superoxide ions are highly reactive with an ability to oxidize organic materials. Since the superoxide ions are unstable and have relatively little energy, they can easily leave crystal structures to create oxygen vacancies. The oxygen vacancies create excess of electrons turning the intrinsic semiconductor into a n-type semiconductor. Another reason that makes oxygen vacancies important is that the surface of titanium becomes hydrophilic as water or liquid molecules occupy these vacancies. The hydrophilicity and the degradation of organic materials on the titanium surface are reasons for its use in the self-cleaning applications (Hen., 2015).

2.2.2. Stability of photocatalytic particles for textile applications

Most textile finishing suspensions are granular dispersions with particles in the micrometer range. The existence of an interface between the dispersed and continuous phases raises the free energy relative to that of the separate phases. In this manner, the dispersed systems and suspensions are generally unstable in thermodynamic sense. The stability of a suspension is defined in terms of an interval and the important properties due to their lack of thermodynamic stability. Namely, the critical suspension properties do not change over some arbitrary period of time. Physical stability can be described based on three aspects: (i) wetting and dispersion, (ii) sedimentation and its relation to rheology, (iii) prevention of caking (Hud., 1981).

Wetting may be briefly explained as the replacement of a solid-air interface by a solid-liquid interface. Most powders are agglomerated, meaning that the particles are clustered together by relatively weak secondary and physical bonds. However, wetting might not be sufficient to break up agglomerates of solid particles which are surrounded by a liquid medium in a suspension. Mechanical energy may help in separating the primary particles from formation of agglomeration. Whether these particles will be recombined or not

depends on attractive and repulsive forces forming the weak bonds. Usually, separation forces on the particles, referred to as suspension, are not satisfactory to avoid the sedimentation (Hud., 1981).

Suspensions tend to sediment as a result of gravitational pull of particles of micron size and larger except for the very dilute colloidal dispersions. Theoretically, these particles in the suspensions act according to the Brownian motion counteracting gravity and Stoke's equation in fluid dynamics. However, in order to attain stability, it is prominent to slow down the sedimentation rate as much as possible. To reduce the sedimentation rate, it is necessary to increase the shear viscosity, decrease particle size, and match the density of dispersed and continuous phases (Hud., 1981). The sedimented particles are typically made of relatively denser substances and the interaction between the particles is very difficult to be homogenously dissolved by mild agitation such as hand shaking.

In the light of the given summary, intrinsic photocatalytic materials such as Degussa-P25 and anatase were prepared in DI-water and the selected commercial textile finishing solution and their stability were evaluated by means of setting tests as well as particle size measurements.

2.2.3. Particle size measurement

Particle size measurement is one of the indicators of quality and performance of suspensions, emulsions, and aerosols in terms of stability. The size and shape of powders influence flow and compaction properties such as rate of reaction, potential to dissolve, packing density, sedimentation, effectiveness of drug delivery by inhalation as well as product appearance and texture. Particle size measurements for production of self-cleaning textiles were conducted to evaluate the tendency of the prepared suspensions to sedimentation.

The total surface area of the particle is dependent on the particle size and it is also critical in determining the rate of the chemical reactions. Chemical reactions are faster for fine particle suspensions than coarse suspensions due to the increasing total surface area when the particles size is decreased for the given mass of a powder. The influence of particle size on the dissolution rate is similar to the impression of particle size on the reaction rate. By creating finer particles and therefore increasing the total surface area, the physical obstructions to dissolution are weakened, making the process to occur much more quickly. Therefore, the speed of dissolution has direct effectiveness in the performance of chemical drugs, powders and suspensions.

Suspension "stability" is most easily achieved by prevention of sedimentation. Unstable suspensions can lead to inhomogeneous coatings, for example, if the photocatalytic particles settle out of liquid suspension, the particles cannot hold on to the textile surface properly. This will affect consistency of coating and hence a proper dispersion is essential for high performing product preparation.

In this study, the photocatalytic particle size was measured using two methods (i) laser diffraction particle size analyses by Coulter LS 13 320 and, (ii) using an atomic force microscope (AFM). Comparison of particle size measurements through two different methods is critical to verify the results and explain their effectiveness and performance on photo-catalysis activity.

.1.1.2. Light-scattering based particle size analyses

Light-scattering is one of the most widely used methods for measuring the size distribution of particles in a suspension. The technique is fast, flexible, cheap and presents precise measurements that are easily adapted to samples submitted to the analyzer in various forms. This method includes analysis of patterns of scattered light produced when

35

particles of different sizes are exposed to a beam of laser light. This method is very effective in determining the stability of the particles in a given suspension medium.

The measurement of particle size in the suspension was initially carried out by the laser diffraction particle size analyzer Coulter LS 13 320, which utilizes Rayleigh Scattering, Mie Theory, Fraunhofer Theory and extends the light-scattering based size distribution analyses down to 40 nm by use of Polarization Intensity Differential Scattering (PIDS) technology by polarizing the laser light.

2.2.3.2. *AFM micrographs for size evaluation of photocatalytic particles*

Atomic force microscopy (AFM) is one of the scanning probe microscopy techniques, which was utilized for surface morphology analyses in this study. AFM was developed in 1986 during laboratory studies at IBM and is based on the principle of a tip in atomic size that scans the surface. Interplay between surface and tip is measured by the interaction forces between the surface and the tip. The tip might slide through the surface or pulse when it is moving. The most important feature of this technique is obtaining a 3D image of the examined sample at an atomic or molecular scale without requirement of sensitive sample preparation and vacuum environment, as is the case with conventional electron microscopy techniques.
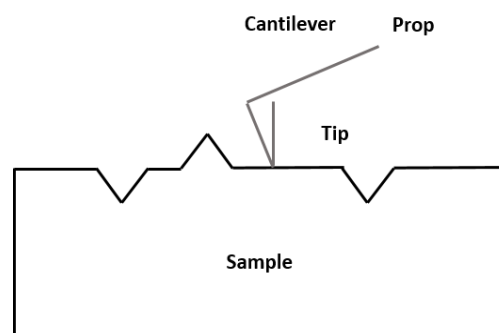
Figure 2.4. Basic schema of the AFM scanning sample surface.

The AFM measurement enabled the scan of the individual particles to be compared to the size distribution measurements of the solutions obtained by the light scattering technique.

The interaction forces change according to the nature of the sample, properties of the tip and the distance between the surface and the tip. This technique monitors the sample surface with a precision of around 10^{-10} to 10^{-4} meters in a range (Hau., 2012).

2.3. *Experimental Approach*

2.3.1. Screening of standard photocatalytic particles for self-cleaning

2.3.1.1. Stability of photocatalytic particles for textile applications

2.3.1.1.1. Photocatalytic particle stability in DI-water

Initially, the photocatalytic particle solutions were prepared by using distilled water and evaluated for stability. The solutions of photocatalytic materials, anatase and Degussa-P25 particles, were prepared at varying concentrations of 0.1wt%, 0.01wt% and 0.001wt% solids content.

The anatase and Degussa-P25 powders were weighted with a high precision balance Ohaus Pioneer series ($\pm$ 0.001 mg precision). Millipore Elix UV 10 DI-water unit was used for the DI water source. After wetting of anatase and Degussa-P25 powders with distilled water in separate bottles labelled according to their weight percentages, solutions were ultra-sonicated in Elmasonic S 100H ultrasonic bath for 30 minutes. Subsequently, the precipitation behaviors of the solutions were observed for a duration of 22 hours in graduated cylinders prepared as 20 ml suspensions.

2.3.1.1.2. Photocatalytic particle stability in textile finishing solution

The finishing solution is used at the last step of the textile manufacturing. The anatase and Degussa-P25 particles were evaluated to be introduced at this step according to the stability of the particles in the finishing solution. To observe the stability, settling tests were conducted in the textile finishing solutions.

Finishing solutions are typically chosen based on the textile blend since the finishing solutions interact with the textile according to their nature (Schindler and Hauser 2004). Finishing solution is also used to prevent static on the textile surface and gives the textile a selected specific property and durability. Also, the finishing solution is commonly used for sports-wears by the textile manufacturers. As it was introduced earlier, the finishing solution is composed of Setasil KF 1320 (amino-functional cationic micro silicon emulsion) Setas Chemicals, Serisoft 210 (non-ionic softener) Serboy Chemicals, Walline PE (polyethylene) Geochem Chemicals and acetic acid (Sigma- Aldrich for pH balance) at a total concentration of 2.7% (w/v) in DI-water and measured pH of 3.52 (Akb., 2016).

2.3.1.2. Particle size measurements

2.3.1.2.1. Light scattering measurements

Particle size of anatase and P-25 powders prepared in DI-water and finishing solutions into proper suspensions at the given solids concentrations were measured after proper dispersion in the ultra-sonicating baths.

2.3.1.2.2. AFM micrographs for size evaluation

The particles properly dispersed in DI-water as a dilute solution were dropped on the freshly cleaved mica surfaces to prepare them for the AFM scanning. After drying of the particles on freshly cleaved mica substrate, the samples were scanned with AFM

(Nanomagnetics Ambient AFM/MFM) in contact mode to determine the individual particle size.

2.3.1.3. *Effect of the photocatalytic particle concentration on photocatalytic cleaning efficiency*

The efficiency of photocatalytic particles was evaluated by comparing and contrasting their effectiveness in terms of self-cleaning on the textiles. ISO standards were utilized in this study to compare the photocatalytic activity of various particle types.

The ISO published a few standards about semiconductor photo-catalysis, which have received remarkable attention from a large and growing number of research groups and industries. For this study, the ISO 10 678 standard, published in 2010, was used to determine the photocatalytic particle concentration efficiency on cleaning. The standard is called as "Determination of photocatalytic activity of surfaces in an aqueous medium by degradation of methylene blue" and it has been derived by using methylene blue (MB^+) as the staining agent. This is a simple method that requires the measurement of the rate of photocatalytic bleaching of MB^+ in aqueous solution via UV/VIS spectrometry (Mil., 2007). The ISO 10 678 standard conditions were implemented on the textile samples in this study.

2.3.1.3.1. Absorbance tests on textiles coated with photocatalytic particles

The textiles coated with anatase and P-25 particles in DIW and finishing solution at different concentrations were analyzed to verify their photocatalytic efficiencies. The analyses were carried out by preparation of samples based on the ISO 10 678 standards. Accordingly, the coated textile samples were prepared as 10 cm square and dipped in a beaker full of 100ml, 2×10^{-4} M MB^+ solution and kept in the dark for 12 hours. The

methylene blue has large molar absorptivity at 665 nm wavelength of light (Mil., 2012). This helps to noticeably and easily measure the color change from blue to a transparent range as the photocatalytic cleaning takes place. The system was irradiated by a UV lamp at 365nm in a UV cabin and during the irradiation solution was mixed via stirrer. The spectrometer (Shimadzu UV1280 UV-visible spectrometer) measurements were performed at absorbance mode at 665nm, which were repeated every 20 minutes of UV light illumination.

2.3.1.3.2. Stain tests on textiles coated with photocatalytic particles

The stain tests were performed according to the ISO 10 678 standards. The textile samples were prepared as 10cm squares as in the absorbance tests. The methylene blue solution prepared in distilled water at $2x10^{-5}$ M concentration was used to stain the textiles. The coated textiles were dunked in the methylene blue solution for 20 seconds and dried at $36^{o}C$ (human body temperature) for a 12-hour period to evaluate stain performance in ambient equivalent to the conditions in daily life. Afterwards, the stained textiles were exposed to UV light at 365nm wavelength using a UV cabin as shown in Figure 2.5. The stain bleaching was observed by taking a picture every 24 hours throughout a week duration.

Figure 2.5. UV bleaching test set-up performed on textile in UV cabin.

2.4. Results and Discussions

2.4.1. Stability of photocatalytic particles for textile applications

2.4.1.1. Photocatalytic particle stability in DI-water

The settling of the suspensions prepared in the graduated cylinders were followed by taking photographs as illustrated in Figures 2.6 to 2.8 as a function of time. Suspension height was plotted according to the total height versus time. These graphs are given in Figures 2.7 through 2.9. It was observed that all the suspensions were stable except for the suspensions prepared at 0.01 and 0.1 wt.% after settlement time of 22 hours and later.
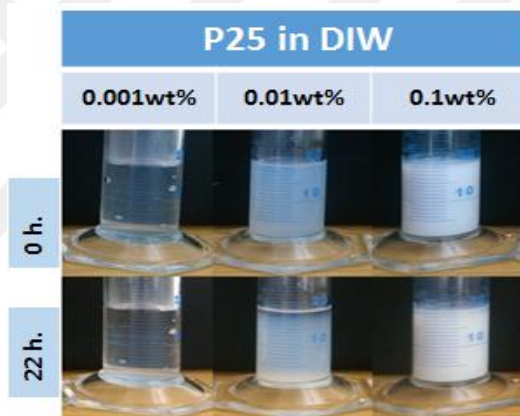
Figure 2.6. P25 particle settling behavior as a function of time in DI-water.
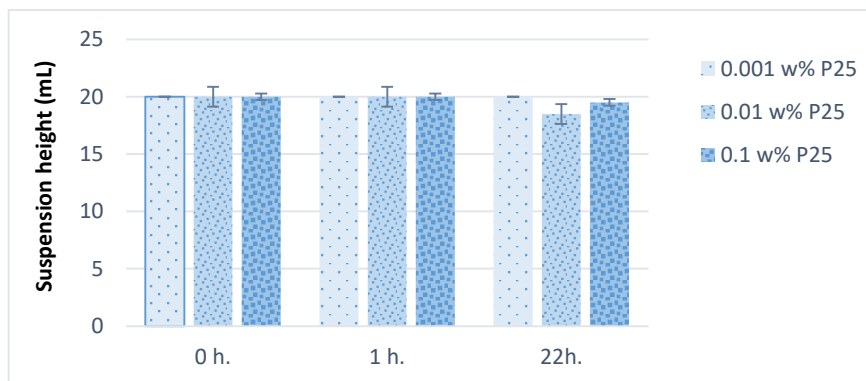
Figure 2.7. Suspension height of 0.001, 0.01 and 0.1 wt.% P25 in DI-water as a function of time.
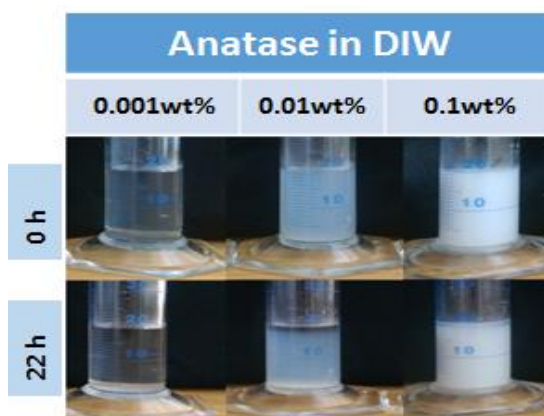
Figure 2.9. Anatase particle settling behavior as a function of time in DI-water.
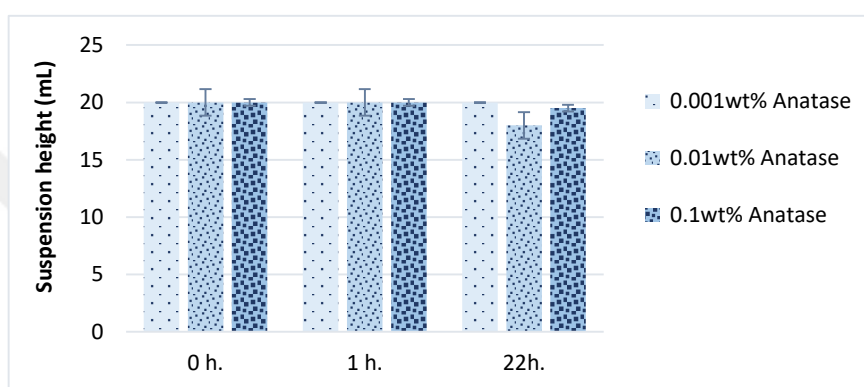
Figure 2.8. Suspension height of 0.001, 0.01 and 0.1 wt.% anatase in DI-water as a function of time.

2.4.1.2. Photocatalytic particle stability analyses in textile finishing solution

The suspensions in finishing solution were prepared the same way as in the DI water testing. The photocatalytic particles at 0.1wt%, 0.01wt% and 0.001wt% were added into the finishing solutions in graduated cylinders at 20 ml and their settling behaviors were observed for 22 hours as given in Figures 2.10 through 2.12. Figures 2.11 through 2.13 demonstrate the graphs of suspension height versus time. It can be seen that better stability was observed in finishing solution both for P25 and anatase particles even after 22 hours of settling test.
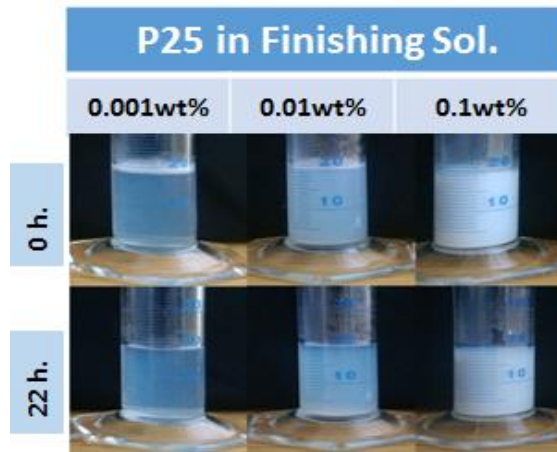
Figure 2.10. P-25 particle settling behavior as a function of time in finishing solution.
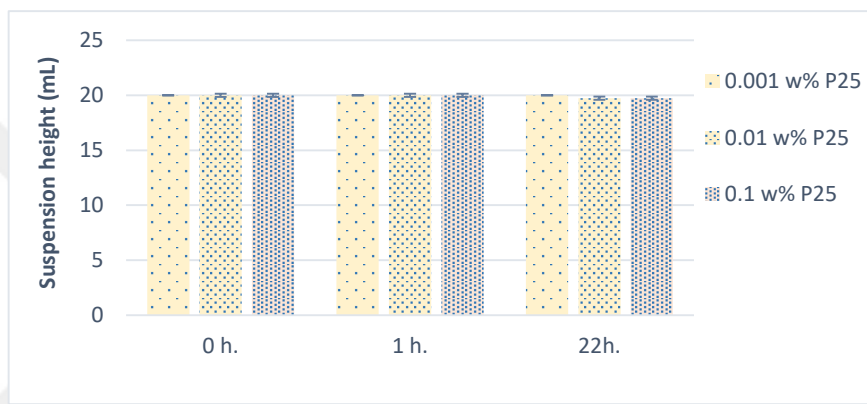
Figure 2.11. Suspension height of 0.001, 0.01 and 0.1 wt.% P25 in finishing solution as a function of time.
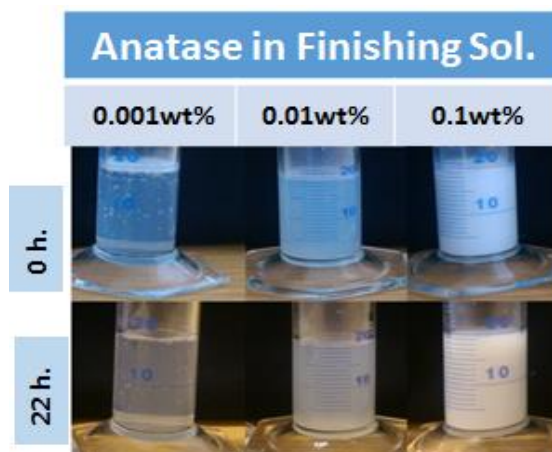
Figure 2.12. Anatase particles settling behavior as a function of time in finishing solution.
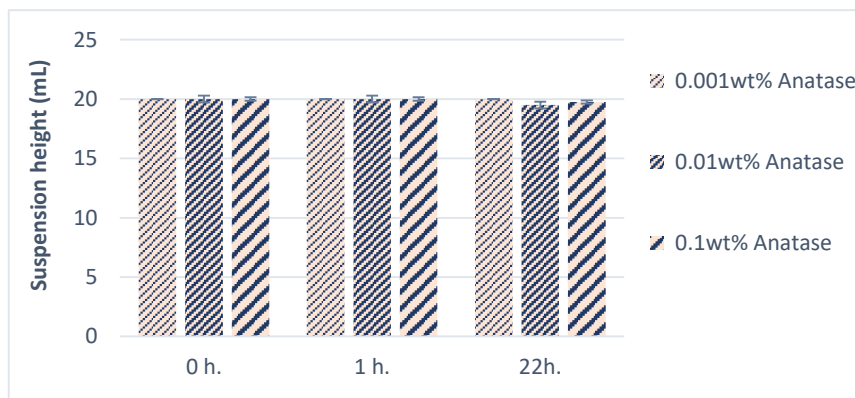
Figure 2.13. Suspension height of 0.001, 0.01 and 0.1 wt.% anatase particles in finishing solution as function of time.

The suspensions have faced reduction in height due to the reduced solution stability. As it can be seen in the related figures, although the settling behavior of the photocatalytic particles was negligible for suspensions prepared in the finishing solution, the settling behavior in the DI-water was much more pronounced. However, since the textiles are always treated in the finishing solution for the commercial applications in the manufacturing operations, more focus was given to the suspensions in the finishing solution and the DI water treatment was used as a baseline comparison in the evaluations.

2.4.2. Particle size measurements

2.4.2.1. Light scattering measurement results

The results of consecutive runs of particle size analyses are presented as overlays of volume and differential number percent versus particle diameter graphs in Figure 2.14 (a) and (b).
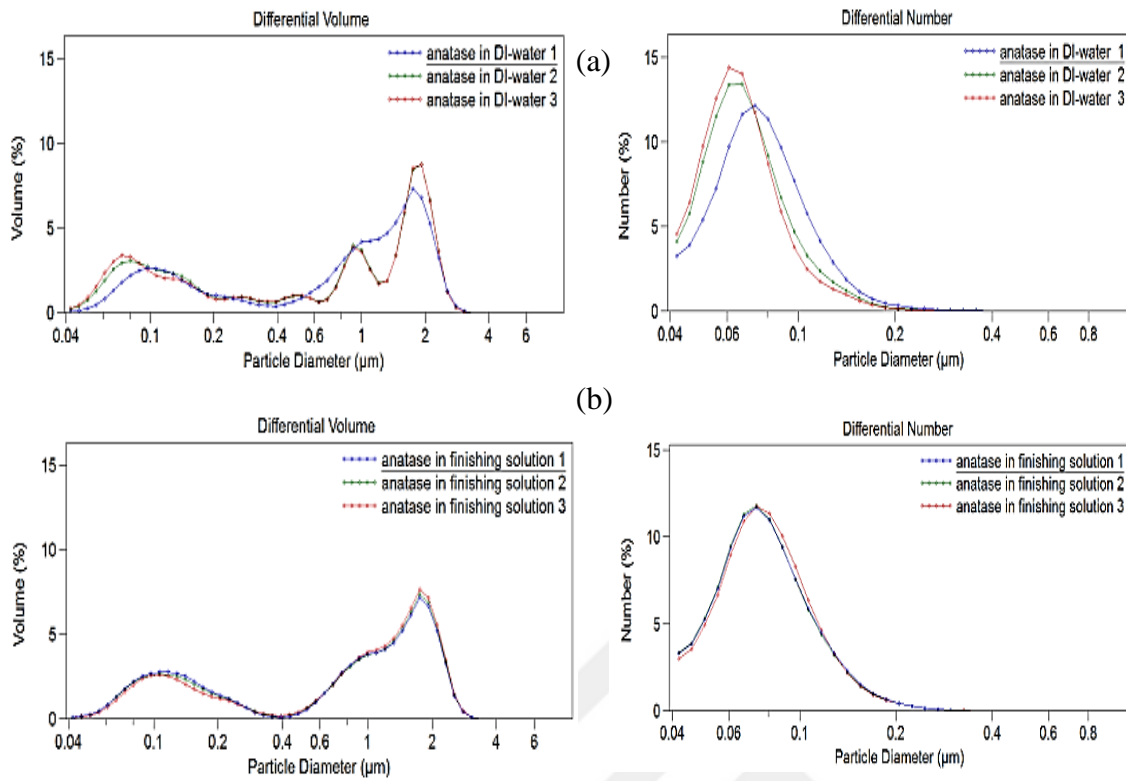
Figure 2.14. Static light scattering particle size measurement results for (a) anatase in DI-water, (b) anatase in finishing solution measured by %Volume and %Number distributions.

Generally, volume % particle size distributions help demonstrate the suspension stability illustrating both the primary particles and the agglomerated particles. However, due to the nature of the finishing solution, the contents in the finishing solution have shown additional peaks, which belong to the silicon content of the finishing solution.
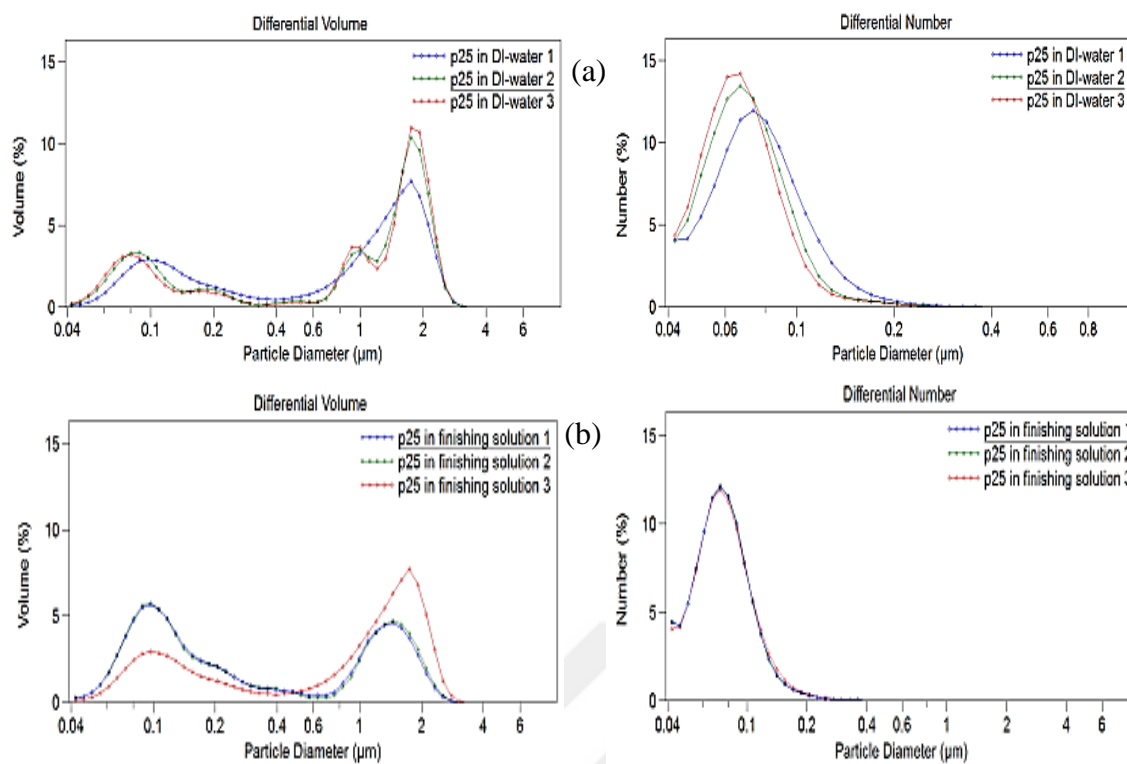
Figure 2.15. Static light scattering particle size measurement results for (a) P-25 in DI-water, (b) P-25 in finishing solution measured by %Volume and %Number distributions.

Table 2.1. Photocatalytic particle size mean values by Coulter LS 13 320.

Photocatalytic particle	Mean Particle size (µm)	Standard Deviation (µm)
Anatase in DIW	0.087	0.005
Anatase in finishing solution	0.084	0.001
P-25 in DIW	0.075	0.006
P-25 in finishing solution	0.081	0.001

The measured mean sizes of the photocatalytic particles are summarized in Table 2.1. It can be seen that the particle size measurement results have lower standard deviation for the particles prepared in the finishing solution as compared to the DI-water. The mean particle size values were observed to be similar to the measurements in the distilled water. The finishing solution may help particle dispersion on the grounds that it is a more viscous

liquid (Hud., 1981). It also was observed that the finishing solution have a positive affect on the particle size distribution as per reduction of the settlement of suspensions during the coating process.

2.4.2.2. AFM based particle size evaluations

The particle size of anatase and P-25 particles were also evaluated by analyzing 2D cross sections of the scanned particles for size and height. The anatase and P-25 particles deposited on the mica substrates were scanned with 5×1 μm and 3×3 μm scan areas. The particle sizes were reported as the average width of the five chosen particles and their standard deviations.
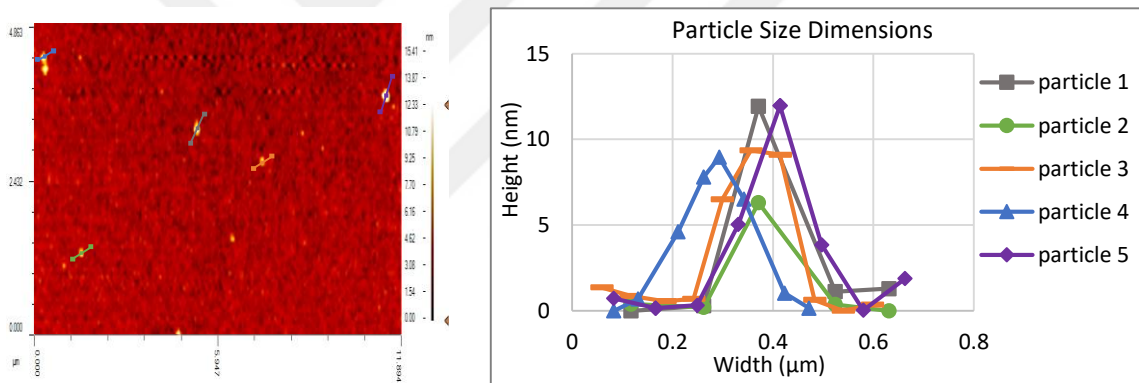
Figure 2.17. AFM picture and cross section of anatase particles on mica substrate.
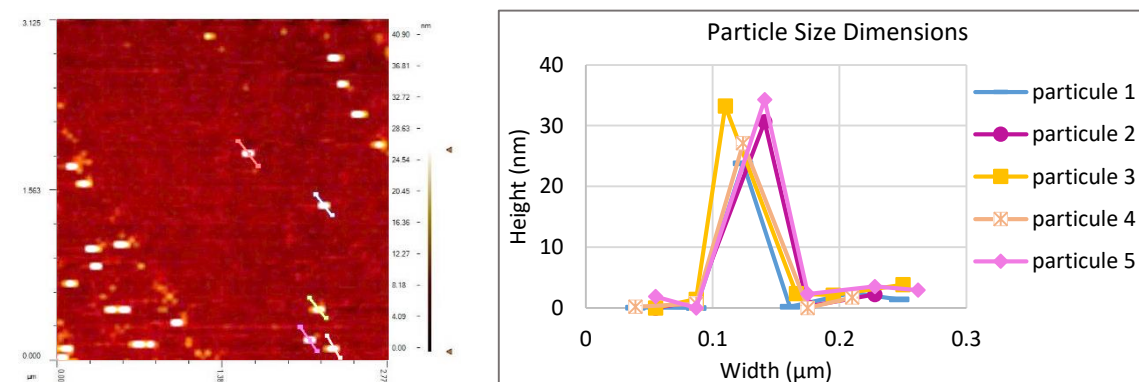
Figure 2.16. AFM picture and cross section of P25 particles in finishing solution.

Table 2.2. Photocatalytic particles size measurement results with AFM.

Photocatalytic particles	*Particle size average (nm)*	*Standard deviation (nm)*
Anatase	277.6	35
P-25	83.4	6.5

The AFM based particle size measurements for P-25 particles showed similarity with the results of light scattering analyzer. The AFM particle size of the anatase particles, however, were measured to be 277.6 nm, which is almost four times larger than the particle size measured by Coulter LS 13 320 indicating that the anatase particles dried on the freshly cleaved mica substrate and agglomerated. These differences can further be attributed to the tendency of different particle size measurement techniques to measure sizes with minor differences and the fact that the anatase particles being notoriously prone to agglomeration (Gom., 2014). This observation is also supported by the particle size analyzer volume% based measurement graphs, where the volume dispersion graphs illustrate a second peak indicating agglomeration.

2.4.3. Effect of the photocatalytic particle concentration on self-cleaning efficiency

2.4.3.1. Absorbance tests on textiles coated with photocatalytic particles

The textile samples were prepared for the absorbance tests according to the ISO 10 678 specifications. Spectrometer measurements were performed at 665nm wavelength and repeated every 20 minutes for the textiles coated with P-25 and anatase in both DIW and finishing solutions. The results of the absorbance analyses have been presented with arbitrary absorbance units versus wavelength graphs.
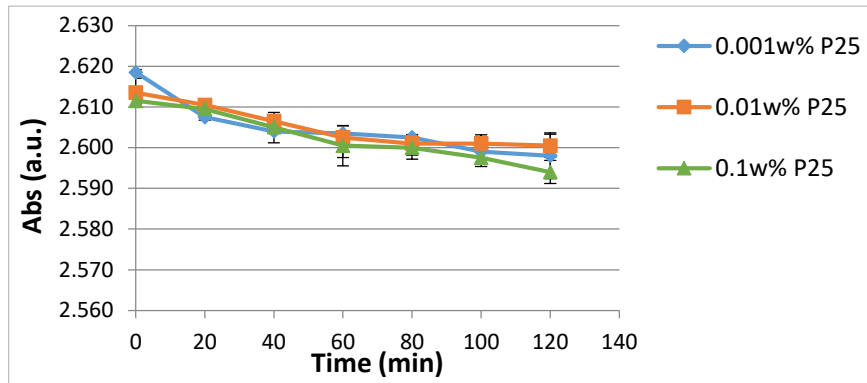
Figure 2.18. Absorbance results for textiles coated with P25 particles at 0.001, 0.01 and 0.1wt% concentrations in DIW.
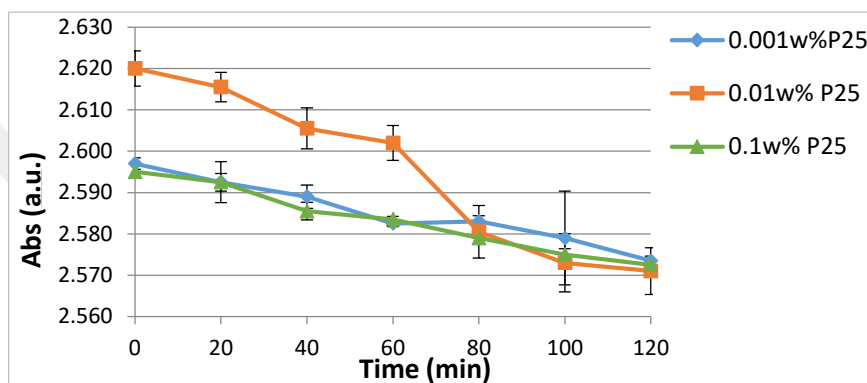
Figure 2.19. Absorbance results for textiles coated with P-25 particles at 0.001, 0.01 and 0.1wt% concentrations in finishing solution.

The textiles coated with photocatalytic particles in DI-water water and the finishing solutions were evaluated for their photocatalytic activity by absorbance tests and the stain tests according to the ISO 10 678 standard. The transmittance is inversely proportional to the absorbance and as the methylene blue solutions are degraded by the textiles coated with the photocatalytic particles, the absorbance decreases because of the color change of the methylene blue solution from blue through being colorless and transparent. Therefore, the reduction of the absorbance value by time can give an idea related to the cleaning ability of the coated textiles (Mill., 2012), (Mil., 2007). According to these observations, the absorbance test results were evaluated and the suspensions prepared in the DI-water resulted in lesser absorbance change as compared

to the ones prepared in the finishing solutions. The increase in the anatase particle concentration in the finishing solution created higher change in absorbance, which is a sign of better cleaning ability of anatase in the presence of active agents in the finishing solution. Among the tested concentrations the 0.1wt% anatase concentration in the finishing solution was observed to be the most effective in degrading the methylene blue solution by 0.076 units in the absorbance delta. This was a favorable result in terms of retaining the solution stability as well as the agglomeration prevention.
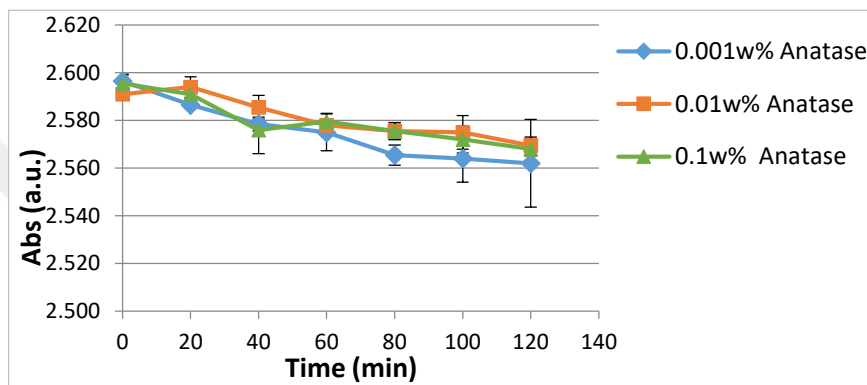
Figure 2.20. Absorbance results for textiles coated with anatase particles at 0.001, 0.01 and 0.1wt% concentrations in DIW.
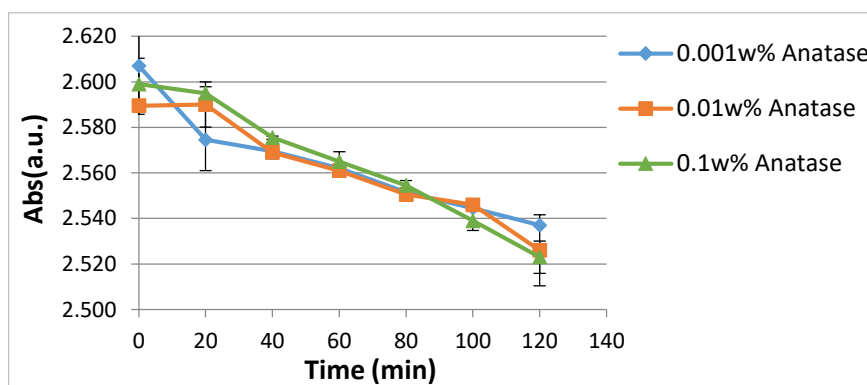
Figure 2.21. Absorbance results for textiles coated with anatase particles at 0.001, 0.01 and 0.1wt% concentrations in finishing solution in finishing solution.

50

Table 2.3. Absorbance variation of photocatalytic particles on textiles

Photocatalytic	Absorbance t=0	Absorbance t=120	Delta
P-25 in DIW	2.612	2.594	0.018
P-25 in finishing	2.594	2.571	0.023
Anatase in DIW	2.596	2.562	0.034
Anatase in	2.599	2.523	0.076

2.4.3.2.   Stain tests on the textile coated with the photocatalytic particles

To observe the cleaning efficiency, textiles stained with the methylene blue solutions were also exposed to the UV light. The change in the stain color was compared by visual perception of observations on the photographs taken by daily basis as given in Figures 2.21 through 2.24.
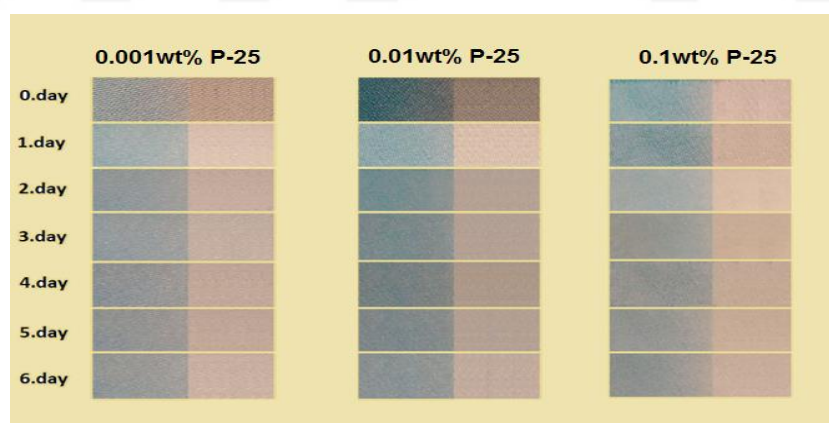
Figure 2.22. The stain bleaching tests on textiles coated with P-25 particles at 0.001, 0.01 and 0.1wt% concentrations in finishing solution.
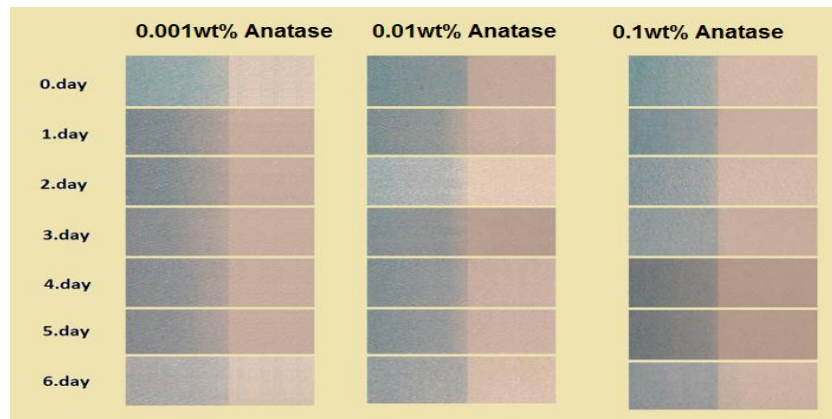
Figure 2.23. The stain bleaching tests on textiles coated with anatase particles at 0.001, 0.01 and 0.1wt% concentrations in DIW.
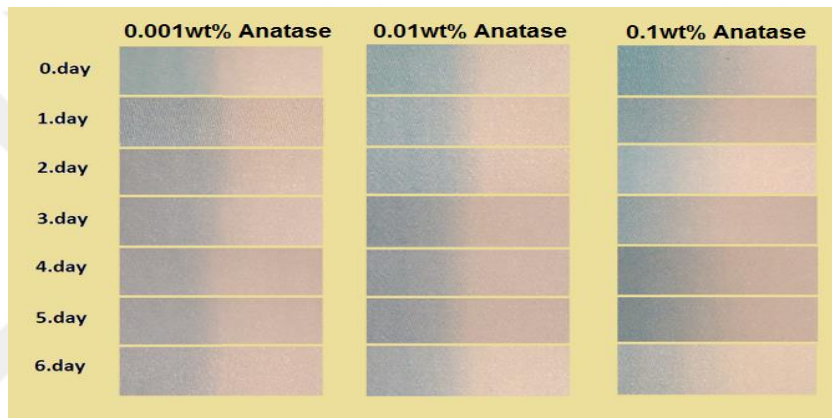
Figure 2.24. The stain bleaching tests on textiles coated with anatase particles at 0.001, 0.01 and 0.1wt% concentrations in finishing solution in finishing solution.
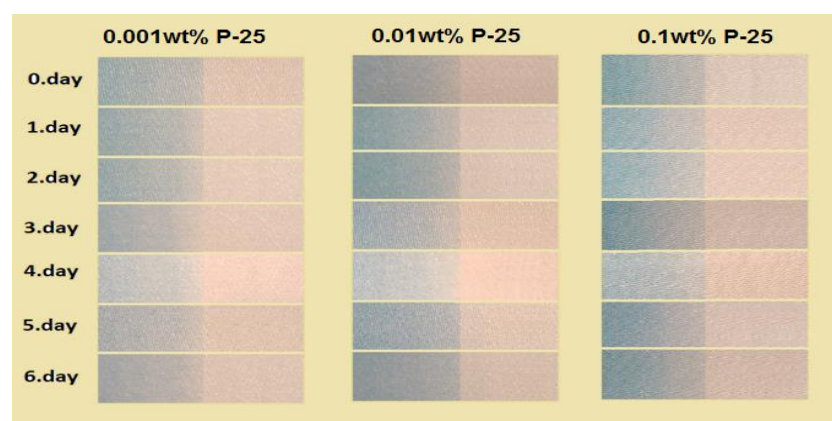
Figure 2.25. The stain bleaching tests on textiles coated with P-25 particles at 0.001, 0.01 and 0.1wt% concentrations in finishing solution.

In parallel to the absorbance results, anatase particles in DI-water and P-25 particles (both in DI-water and finishing solution) didn't show cleaning activity on the coated textile surfaces. Yet, the textiles coated with the anatase particles in the finishing solution changed the stain shade with respect to the color of the initial stain as demonstrated in Figure 2.4. The most effective bleaching was observed for the textile coated with 0.1wt% anatase in the finishing solution in parallel to the absorbance measurements in the solution cleaning tests.

2.5. Conclusions

The alternative naturally photocatalytic particles were evaluated in terms of the stability of their solutions, particle size measurement by using two different methods and analyzing the effects of the particles coated on textiles on the methylene blue absorbance as well as stain bleaching ability of the particles on the textiles. The results of these analyses showed that finishing solution helps photocatalytic particles for their solution stability, preventing their agglomeration and activating their cleaning ability. The anatase suspensions prepared in the finishing solution were determined to be more active than any other combinations. The 0.1wt% anatase in finishing solution was found to be the most efficient among the tested anatase concentrations in the finishing solution. The photocatalytic effectiveness of this particular sample may be further increased to visible range by doping additives. Furthermore, in implementation of the anatase in the coting process, a finishing solution was observed to be practical by introducing the photocatalytic particles in the finishing solution during the finishing process which is the last step of the manufacturing. Thus, it can be concluded that the self-cleaning textile may be produced without changing the textile manufacturing process significantly.

CHAPTER 3

EVALUATION OF A P-TYPE DOPANT FOR ENHANCED PHOTOCATALYTIC ACTIVITY

3.1.   Introduction

Titanium dioxide is a typical n-type semiconductor (Heb., 2013). It is usually doped with n-type dopants such that the dopants only change the band gap without limiting its photocatalytic ability. It is also plausible to increase its photocatalytic activity by doping with minerals which have similar crystal structure and chemical availability for photocatalytic reaction using secondary bond interactions. The activity and feasibility of the use of some dopants with baseline photocatalytic particles may not be sufficient for daily use and require more investigations. Therefore, in this study, the p-type dopants were evaluated for their ability to enhance the photocatalytic activity of titanium in the visible light range as a new alternative.

The photocatalytic activity of metal doping is usually diminished due to thermal instability and a rise in carrier-recombination. Therefore, many researchers have started to use anionic nonmetal dopants to widen the photocatalytic activity into the visible-light region because the related impurity states are near the valence band edge and do not act as charge carriers. Their recombination function might be minimized when compared with the cationic dopants (Din., 2009).

The choice of p-dopant was made according to its availability in the region of fabrication and its suitability for creating secondary bonds. Boron has met these needs among the p-block elements as a standard dopant for the semiconductor technology. This study evaluates the optimum amount of boron concentration through a series of experiments

conducted by using the Design Expert software. In these experiments, the band gap energy and the photocatalytic efficiency of the doped titania were evaluated.

3.2. *Materials and methods*

3.2.1. Statistical design of experiments

In this study, crystalline boron, a p-type dopant, was chosen among the p-block elements on the grounds that it is easy to find, a general need to investigate boron effects on photocatalysis (Akb., 2016), (God., 1991). Nano-boron was obtained as the nano powder with 50nm particle size from Nabond Chemistry Inc. (China). Determination of optimum dopant concentration is time consuming because of the need to analyze the photocatalytic efficiency of all the possible concentrations. By applying a powerful statistical method, the Design Expert software, we were able to experiment for the elusive spots via multifactor testing techniques. Therefore, the design expert software was used by a choice of central composite design which enables to extending the response surface out of the surface of the cube for the selected responses.

 The design levels for central composite design were chosen for three factors; nano-boron concentration, anatase concentration and their UV exposure time. The proper values of each design variable was chosen according to the software recommendation once the high and low values were set as shown in Figure 3.1.

	- alpha	Low		High	+ alpha	
	-1.68	-1	0	1	1.68	
Nano-boron	0	0.04	0.1	0.16	0.2	wt%
Anatase	0	0.02	0.05	0.08	0.1	wt%
Time	20	40	70	100	120	Min
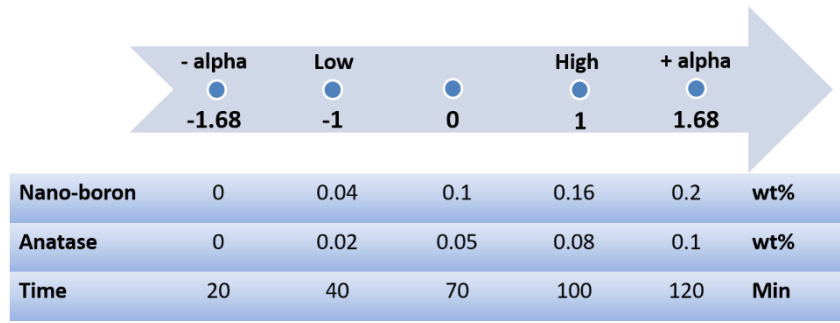
Figure 3.1. Central composite design variables with low (-1) and high (1) concentrations used to compose the design.

3.2.2. Initial energy determination

Initial energy is critical for a photocatalytic reaction to initiate. The light energy which initiates a photocatalytic reaction must be at least equal, or higher, than the energy band gap. The band energy plays a role as the threshold energy for the photocatalytic reaction. Therefore, the absorption method was utilized for the determination of the band gap energy for anatase doped with the nano-boron particles.

The absorption method is used for identification of forbidden band energy, simply known as the band gap energy. In this method, specification of the forbidden band energy is evaluated from the relation between the absorption coefficient and the forbidden band energy, as given in Equation 3.9.

$$(\alpha h v)^n \approx (h v - E_g) \tag{1}$$

Where, h, v and α represent the Planck constant, the frequency and the absorption coefficient, respectively. In this method, a graph of $(\alpha h v)^n$ versus $h v$ is drawn. The energy value, $[(\alpha h v)^n = 0]$, is determined by Tauc plot through plotting to the linear portion of $h v$ representing the band gap energy of examined material as demonstrated in Figure 3.2 against $(\alpha h v)^n$ ((God., 1991). When the n value in the Equation 3.1 is chosen to be 2, direct band gap energy of material can be determined.

If the n value is 1/2, the determined value is defined as the indirect band gap value of the material (Swa., 1983).

In addition to the determination of band gap energy, the thickness of the nano-boron doped films were also determined. The thickness of a thin film plays an important role in characterization of the electrical, optical and structural specification of the films. The optimized solutions after simulation of Design Expert software were deposit on ultrasonically cleaned glass substrates by using Chemical Bath Deposition method in ambient conditions. Transmittance measurements were conducted with UV-VIS spectrometer for the determination of the thickness of the thin films.
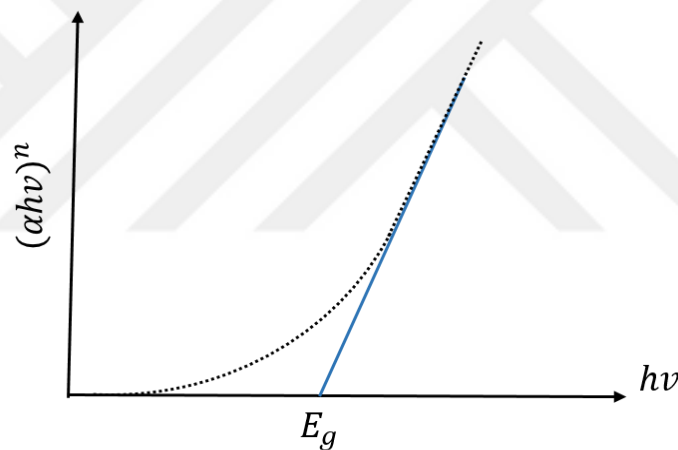
Figure 3.2. Absorption variation graph of $(\alpha h v)^n$ versus $h v$.
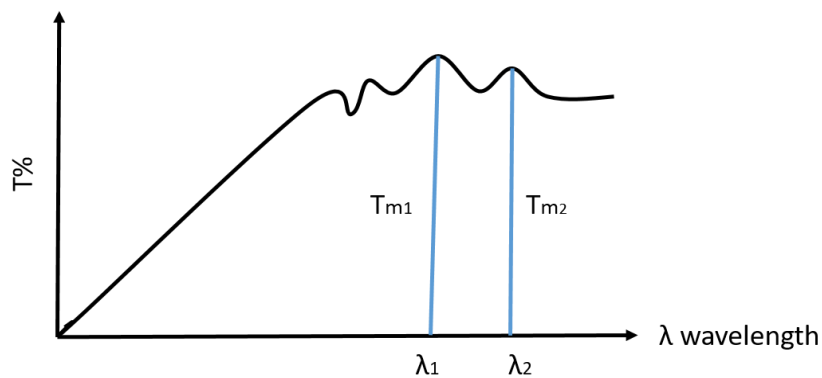
Figure 3.3. Transmittance graph showed maximum points.

57

$$n_f = \left[\left(\frac{n_s(2-T_m)+2n_s(1-T_m)^{\frac{1}{2}}}{T_m}\right)\right]^{1/2} \qquad [2]$$

$$t = \left(\frac{(\lambda_1\lambda_2)}{2(n_{f1}\lambda_2 - n_{f1}\lambda_1)}\right) \qquad [3]$$

The maximum or minimum peak of the transmittance graph was obtained from the UV-VIS spectrometer and was used for analysis of thin film thickness according to the Equations 3.2 and 3.3. The thickness of the thin films was calculated by substituting T_{m1} and T_{m2} values in Equation 3.2 and replacing the values in Equation 3.3. The n_s represents refractive index of the glass used to coat the nanoparticle solutions (Swa., 1983).

3.3. Experimental approach

3.3.1. Statistical design of experiments

The Design Expert Software configured with 3 variables and the central composite design generated 20 experiments and, the nanoboron and anatase containing solutions were prepared with concentrations generated by the software. The Methylene blue solution at $2x10^{-4}$M was used for staining to evaluate photocatalytic activity according to ISO 10 678 standards. 15 ml volume of photocatalytic suspensions with designed concentration were stained with 0.5 ml methylene blue solution and were exposed to UV light at 365nm wavelength to observe the cleaning efficiency.

3.3.2. Initial energy determination

To determine the band gap of anatase doped with nano-boron, solutions prepared with anatase and nano-boron concentrations in DI-water were deposited on the glass target to benefit from transparency of the glass as the textiles aren't suitable for being

analyzed with spectroscopy due to their inhomogeneous opaque structure. The Chemical Bath Deposition method was used to deposit the solutions on the ultrasonically cleaned glass target and the drying of thin films was carried out in confined glass petri cups at room temperature. The deposited film thickness was measured with a Shimadzu UV1280 UV-visible spectrometer by positioning the glass slide perpendicular to the light direction.

3.3.3. Stability of nano-boron doped photocatalytic suspensions

The nano-boron particles used as dopants were mixed into anatase in DI-water and finishing solution according to the statistical design. The stability tests were carried out under the same conditions as detailed in the previous chapter. The solutions were selected as concentration series containing 0.16w% anatase doped with 0.08w% nano-boron to determine the most active photocatalytic concentration. Each concentration was prepared in DI-water and finishing solution to compare the efficacy of using a finishing solution with respect to the baseline DI water environment. The solution preparation process involved mixing the particles into the solvent (DI-water or finishing solution) and stabilization in an ultrasonic bath. Afterwards, the solutions were poured into a graduated glass cylinder to evaluate precipitation of the suspension as a function of time over a total period of 24 hours.

3.3.4. Evaluation of photocatalytic efficiency

3.3.4.1. Stain tests

The specific textile, which is a blend of 35% elastin and 65% cotton and named "Melody" by the manufacturer was chosen for coating with nanoboron-TiO_2 suspensions as well as the baseline solvents by using a padding machine (Atac Makina ATC-GK40C/S). The ISO 10 678 standards were used to evaluate stain bleaching and

photocatalytic activity for anatase doped with nano-boron particles. To prepare the textiles for a stain test, the textiles coated with anatase doped with nano-boron particles were cut into $10cm^2$ pieces and dipped into a $2x10^{-5}$ M methylene blue solutions for 20 seconds. The stained textiles were dried in an oven at 36℃. Afterwards, the samples were exposed to UV light at 365nm wavelength for a week and stain bleaching was determined by taking pictures by daily basis.

3.3.4.2. *Absorbance tests*

The ISO 10 678 test conditions were used to evaluate the absorbance performance of the coated textiles to sort out their photocatalytic activity. The absorbance tests were carried out to compare samples which indicated more effective stain bleaching based on the stain tests. The samples were cut into $10cm^2$ and dipped into a beaker filled with a $2x10^{-4}$ M MB^+ solution. The methylene blue solution in the prepared solutions were collected to analyze absorbance every 20 minutes as the samples were exposed to UV light.

3.4. Results and Discussions

3.4.1. Statistical design of experiments

The 20 experiments generated by the Design Expert software were carried out under the stated conditions. The main photocatalytic response was chosen as the absorbance delta between the absorbance value of the prepared photocatalytic solutions before and after the UV exposure. The evaluated responses based on the conducted design are given in Figure 3.4.

The software fitted the absorbance values to alternative models one is polynomial and the other is quadratic. Between these, the polynomial model is suggested due to its

better R^2 fitness value. The absorbance mean and standard deviation values were determined to be -0.0274 and 0.0334, respectively. The negative delta value is a sign of the rise of absorbance. The model graphs are represented in 3D and are shown in Figures 3.5 through 3.9.

Run	Factor 1 A:NB g	Factor 2 B:Anatase g	Factor 3 C:Time min	Response 1 UV-Vis abs
1	0.04	0.02	100	-0.002
2	0.1	0.05	70	-0.062
3	0.16	0.02	40	-0.001
4	0.1	0.05	120	0.007
5	0.04	0.02	40	-0.01
6	0.1	0.05	20	-0.086
7	0.1	0.05	70	-0.062
8	0.16	0.08	100	0.008
9	0.1	0.1	70	-0.064
10	0	0.05	70	0.001
11	0.1	0	70	-0.036
12	0.04	0.08	100	-0.008
13	0.2	0.05	70	-0.001
14	0.16	0.08	40	0.001
15	0.04	0.08	40	0.009
16	0.16	0.02	100	0.006
17	0.1	0.05	70	-0.062
18	0.1	0.05	70	-0.062
19	0.1	0.05	70	-0.062
20	0.1	0.05	70	-0.062

Figure 3.4. The data definition page for 20 different experiments offered by the design expert software.
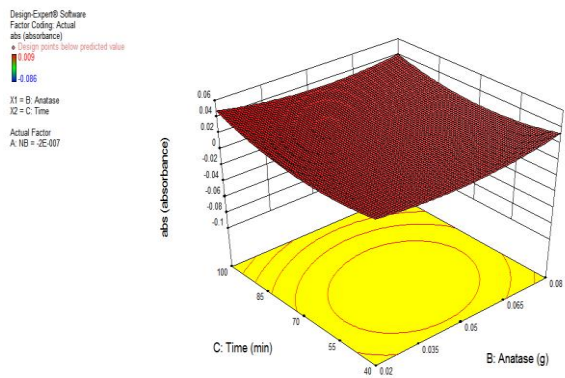
Figure 3.7. Absorbance box plot as a function of time of UV exposure and anatase concentration.
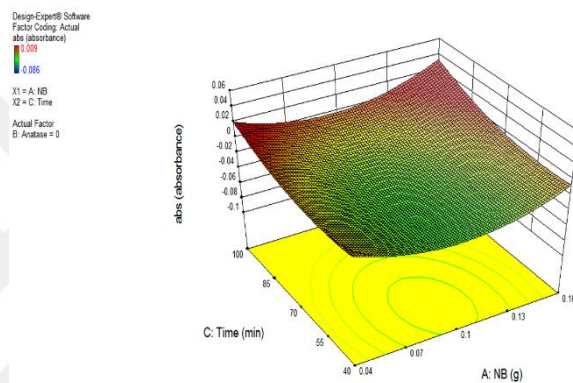
Figure 3.6. Absorbance box plot as a function of time of UV exposure and boron concentration.
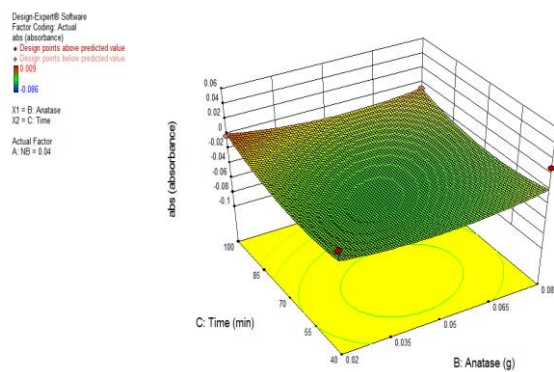
Figure 3.5. Absorbance box plot as a function of time of UV exposure and anatase concentrations doped with 0.04wt% boron.
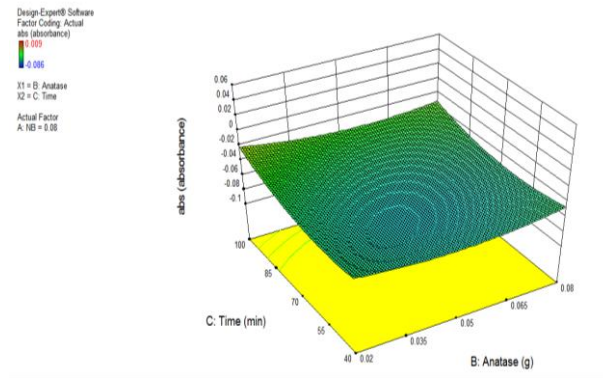
Figure 3.8. Absorbance box plot as a function of time of UV exposure and anatase concentrations doped with 0.08wt% boron.
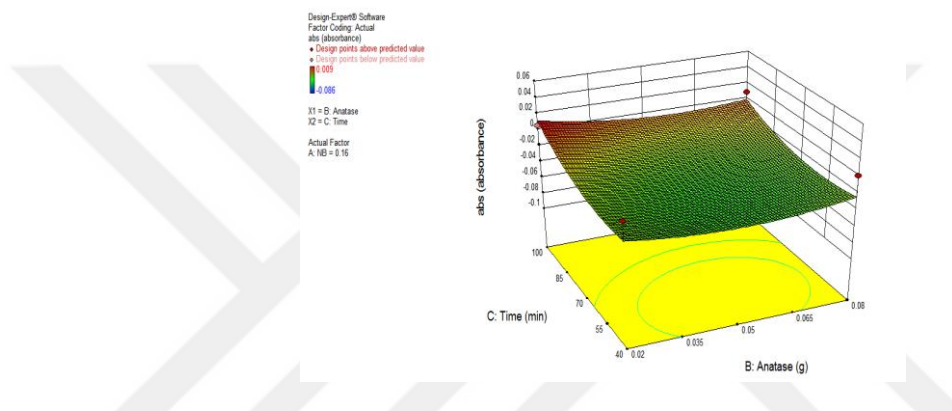
Figure 3.9. Absorbance box plot as a function of time of UV exposure and anatase concentrations doped with 0.16wt% boron.

Table 3.1. Absorbance delta values of photocatalytic particles showed positive delta.

Photocatalytic particles in solutions	Absorbance delta
0.05wt% Anatase (70 mins)	0.001
0.08wt% Anatase +0.04wt% Nano-boron (40 mins)	0.009
0.05wt% Anatase +0.1wt% Nano-boron (120 mins)	0.007
0.16wt% Anatase +0.08wt% Nano-boron (100 mins)	0.008
0.08wt% Anatase +0.16wt% Nano-boron (40 mins)	0.001
0.02wt% Anatase +0.16wt% Nano-boron (100 mins)	0.006

In Figure 3.9, the absorbance plot as a function of time of UV exposure and anatase concentrations doped with nano-boron powder, demonstrates two regions which have high absorbance delta values after 100 minutes of exposure. The positive delta indicates a reduction of absorbance, which is inversely proportional to the transmittance. In other words, the solution becomes more transparent due to the photocatalytic activity taking place. The solutions with positive absorbance values are listed in Table 3.1. To determine the most optimal desirability for the nano-boron amount, the criteria were adjusted to (i) minimize the anatase concentration to get closer to the most effective concentration of TiO_2 as determined in the previous chapter (0.1wt%) (ii) maximize the absorbance delta value to attain a high photocatalytic activity. Based on the set criteria, the desirability was attained from the Design Expert software for 100 minutes of exposure to the UV light as shown in Figure 3.10. However, due to the fact that the exposure time is another factor to be considered in order to evaluate the desirability, the absorbance was also plotted against the anatase and nano-boron concentrations at the exposure times highlighted on Table 3.1 as shown in the Figures 3.11 through 3.13.
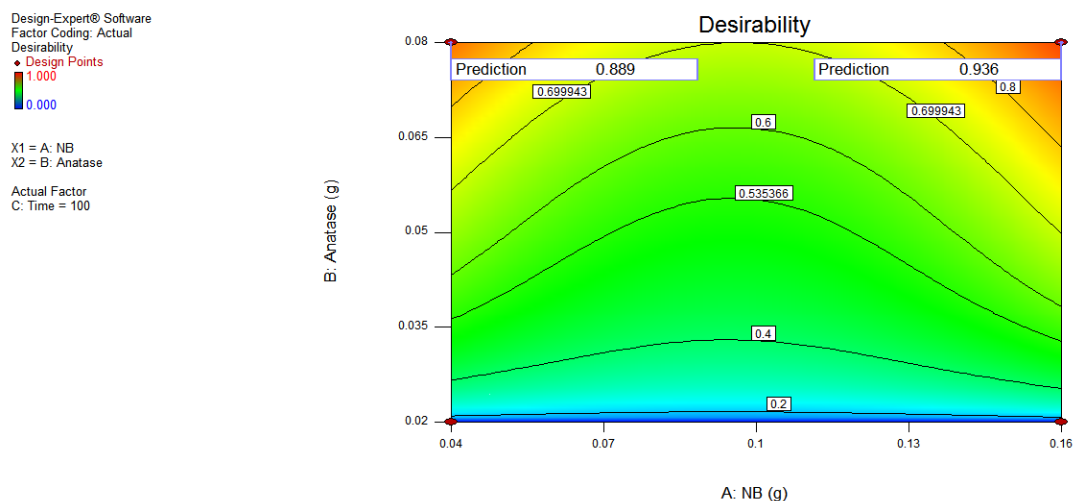
Figure 3.10. Desirability graph as function of anatase concentrations and nano-boron concentration for 100 minutes.
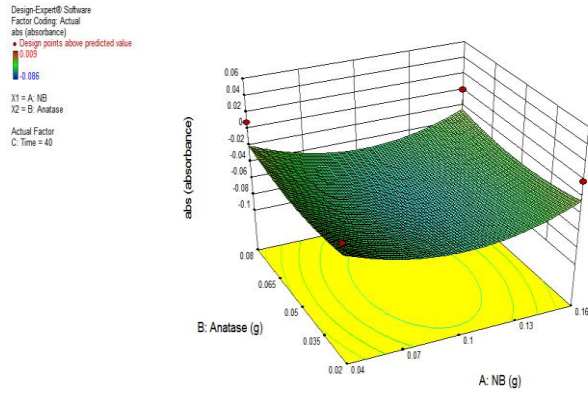
Figure 3.11. Absorbance box plot as a function of UV exposure for 40 minutes, anatase and boron concentrations.
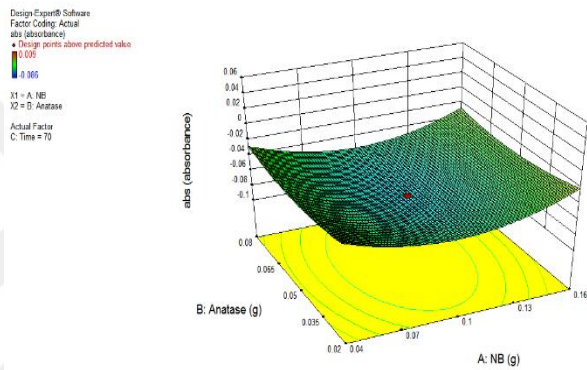
Figure 3.12. Absorbance box plot as a function of UV exposure for 70 minutes, anatase and boron concentrations.
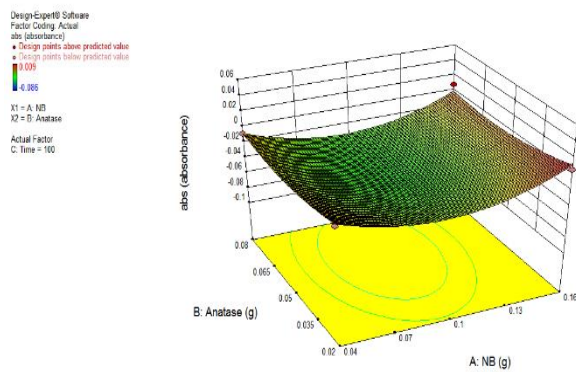
Figure 3.13. Absorbance box plot as a function of UV exposure for 100 minutes, anatase and boron concentrations.
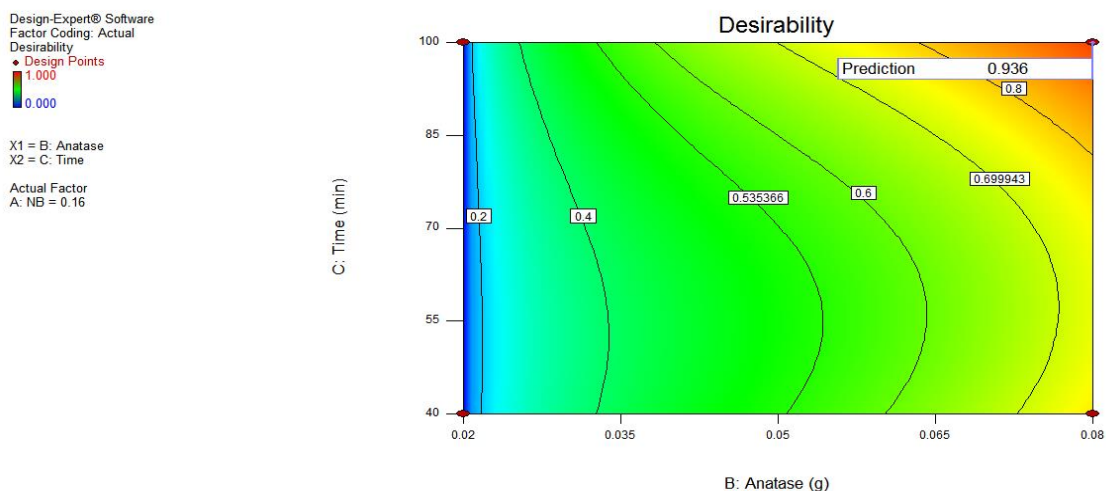
Figure 3.14. Desirability graph as function of time and anatase concentrations for 0.16wt% nano-boron concentration.

The desirability graph as a function of anatase and nano-boron concentration for 100 minutes of exposure time (Figure 3.10) showed two active regions where the desirability was high. Between these, the anatase concentration was observed to be similar, whereas the absorbance values were high either at the low or the high end of the nanoboron particle concentration. Implementation of the desirability criteria at the configured optimum dopant concentration according to Figure 3.10 show maximum desirability to be attained at the higher concentrations of anatase and nanoboron at the relatively longer UV exposure times to be 0.936 as shown in Figure 3.14.

The experiments designed by the Design Expert software showed that the photocatalytic activity of the solution with 0.08wt% anatase and 0.04wt% nano-boron exposed to UV light for 40 minutes is more effective according to the absorbance results given in Table 3.1. However, the photocatalytic activity of solution with 0.16wt% anatase and 0.08wt% nano-boron exposed to UV light for 100 minutes appears to the be the
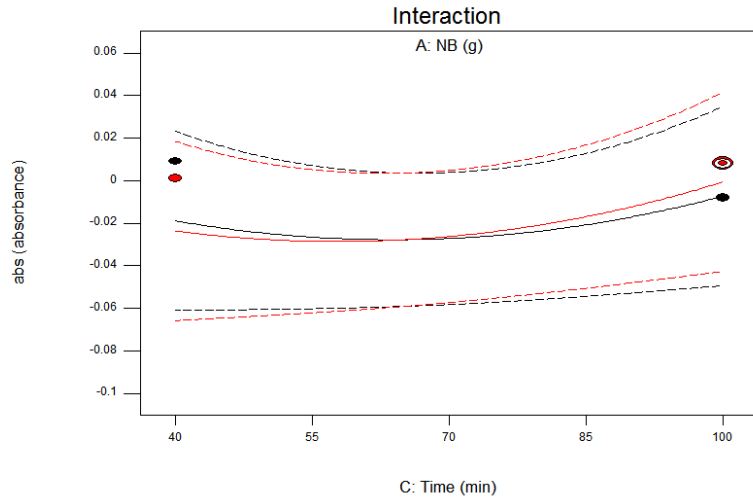
Figure 3.15. Interaction graph as function of time and absorbance changes with nano-boron concentration.

most desirable sample according to the Design Expert software based on the chosen criteria. All interactions were further evaluated and plotted in a graph as demonstrated in Figure 3.15.

Figure 3.15 illustrates the interaction of absorbance by time as a function of nanoboron concentartion within the chosen optimization criteria. The black lines and points represent the high absorbance values and most desirable sample for the selected absorbance criteria. The red lines and points symbolize the high anatase concentration criteria and proper sample for this criteria. The experiment Run#8, which was conducted at 0.08wt% anatase and 0.16wt% nano-boron concentration, is in the middle of these upper and lower limits. Hence, it can be referred as the optimum sample with 0.08wt% anatase and 0.16wt% nano-boron addition.

3.4.2. Initial Energy determination

To understand the photocatalytic efficiency limitation of the most desirable sample according to the Design Expert software results, this sample's band gap energy determination was carried out under the given experimental conditions. Accordingly,

67

transmittance and absorbance of thin films prepared with solutions composed of 0.08wt% anatase and 0.16wt% nano-boron and 0.24wt% anatase in DI-water were measured to determine thickness and band gap energy and are shown in Figures 3.16 through 3.19.
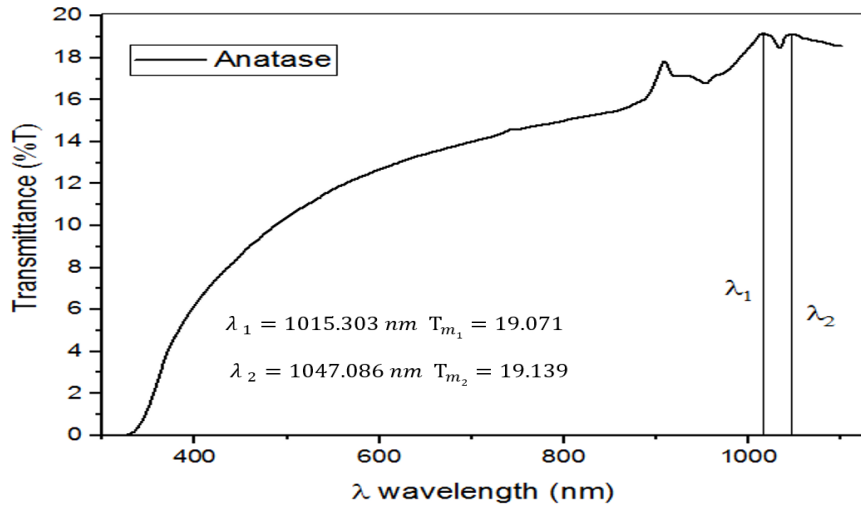
Figure 3.16. Maximum values of transmittance graph of anatase thin film on glass.
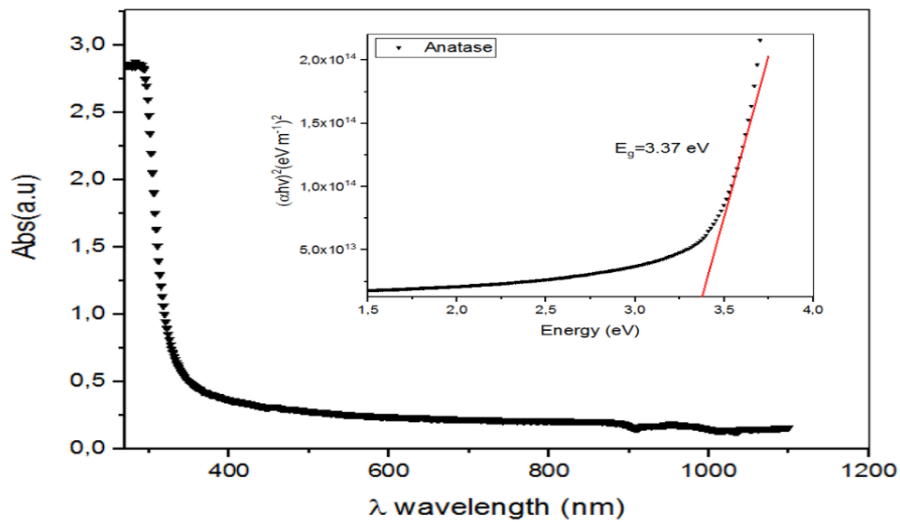
Figure 3.17. Absorbance and energy graphs of anatase thin film.
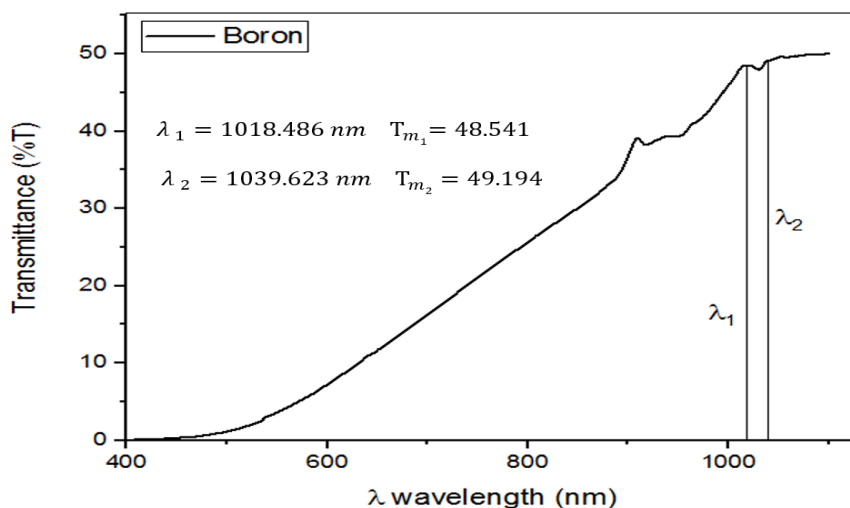
Figure 3.18. Maximum values of transmittance graph of anatase doped with nano-boron thin film on glass.
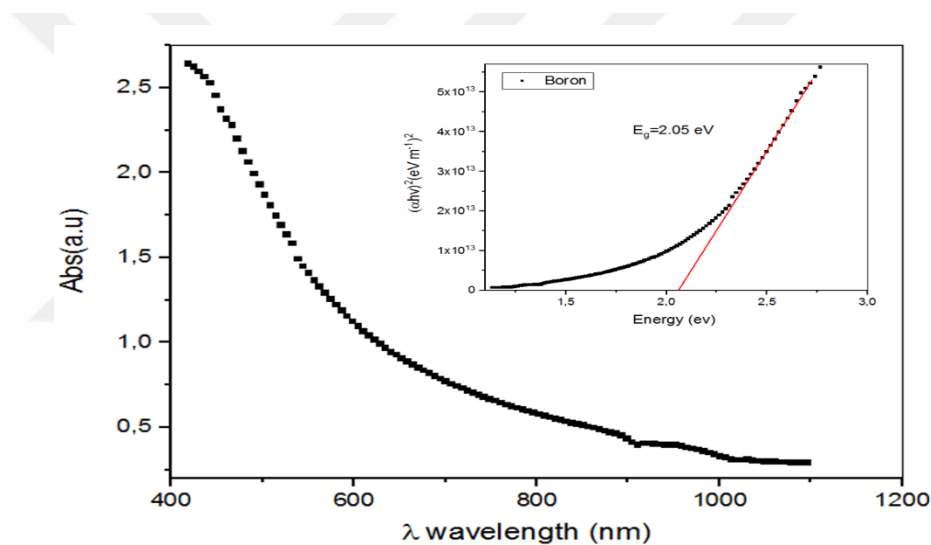
Figure 3.19. Absorbance and energy graphs of anatase doped with nano-boron thin film.

Table 3.2. Initial energy and film thickness of photocatalytic particles measured on glass.

Photocatalytic particles as thin film	Band gap(eV)	Thickness(nm)
0.24wt% anatase in DI-water	3.37	182.23
0.08wt% anatase +0.16wt% nano-boron in DI-water	2.05	323.16

69

The film thicknesses were attained by placing peak values of transmittance into Equation 3.2 and 3.3. The calculated values were found to be in the nanometer range indicating that the selected solutions are capable of creating nano-scale thin films when they are coated on the textile surface. Thus, the coating will not constitute structure which can change the fabric softness. Moreover, the energy band gap of thin film generated from 0.16wt% anatase doped with 0.08wt% nano-boron in DI-water was 2.05 eV, which corresponds to the visible light range according to the Plank-Einstein relation. Although the band gap energy, initial energy for photocatalysis, was in the visible light range, which means that the photocatalytic activity is plausible under the visible light conditions, some sedimentation was observed on the film surface. When the thickness is considered, the band gap energy of the generated film was similar to the anatase as given in the literature (Now., 2012), (Lóp., 2012).

3.4.3. Stability of nano-boron doped photocatalytic suspensions

For stability tests, a series of suspensions were prepared based on the concentration of the optimum sample suggested by the Design Expert software results. The stability of the prepared DI-water and finishing solution based suspensions were observed by taking pictures of the suspensions immediately after they were poured into graduated cylinders and after 24 hours of the time lapse. The results are presented in Figures 3.20 through 3.25.
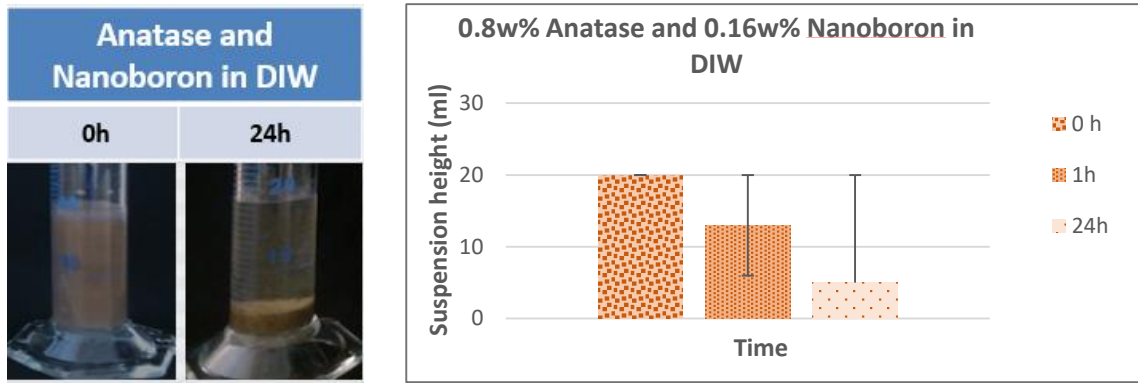
Figure 3.21. Stability test conducted on 0.8w% anatase doped with 0.16w% nano-boron in DI-water.
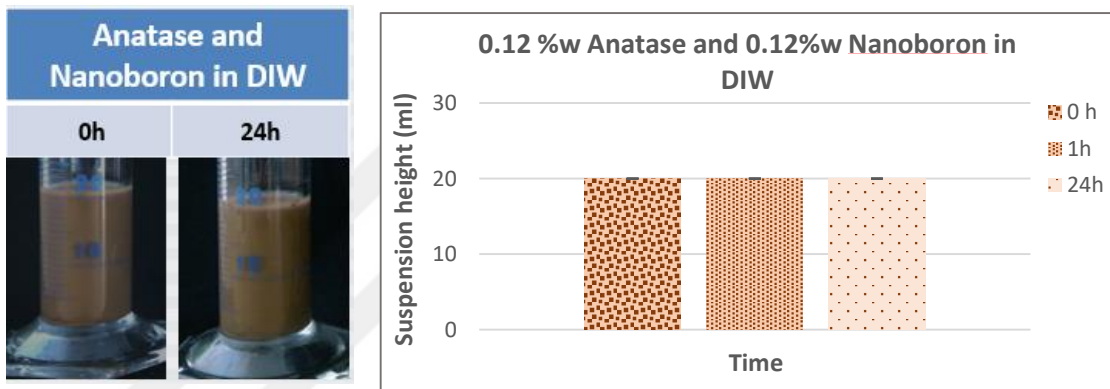
Figure 3.22. Stability test conducted on 0.12w% anatase doped with 0.12w% nano-boron in DI-water.
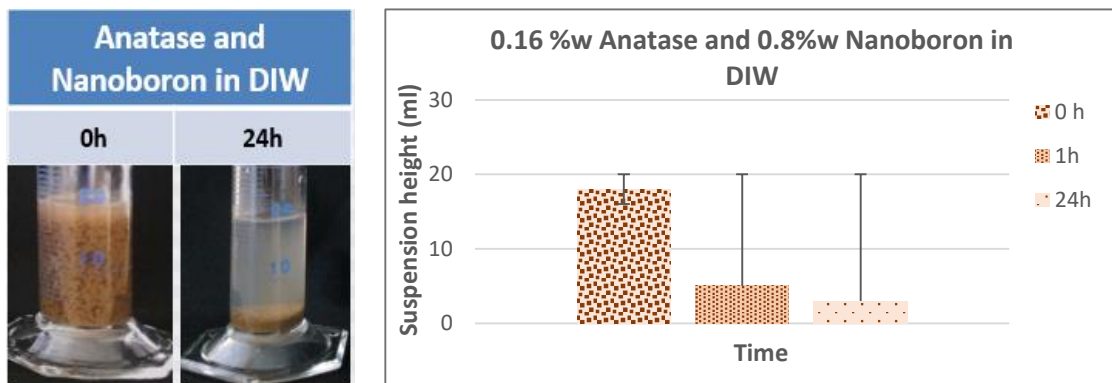
Figure 3.20. Stability test conducted on 0.16w% anatase doped with 0.08w% nano-boron in DI-water.

71
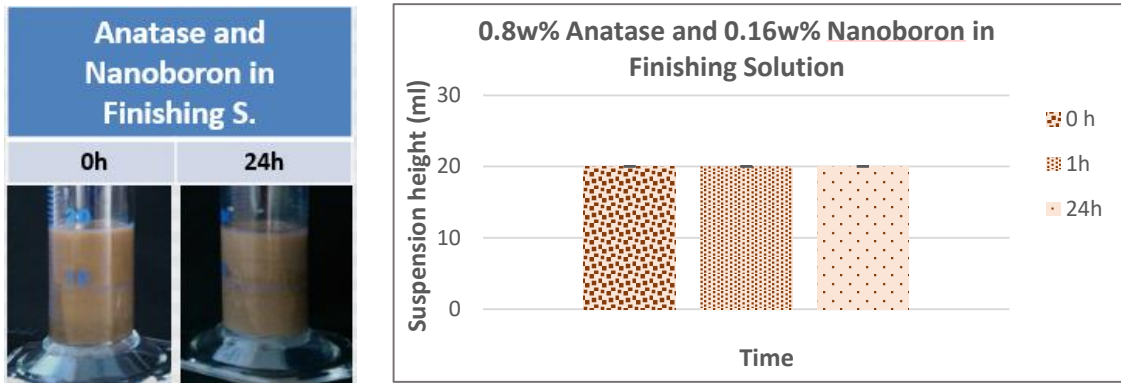
Figure 3.25. Stability test conducted on 0.8w% anatase doped with 0.16w% nano-boron in finishing solution.
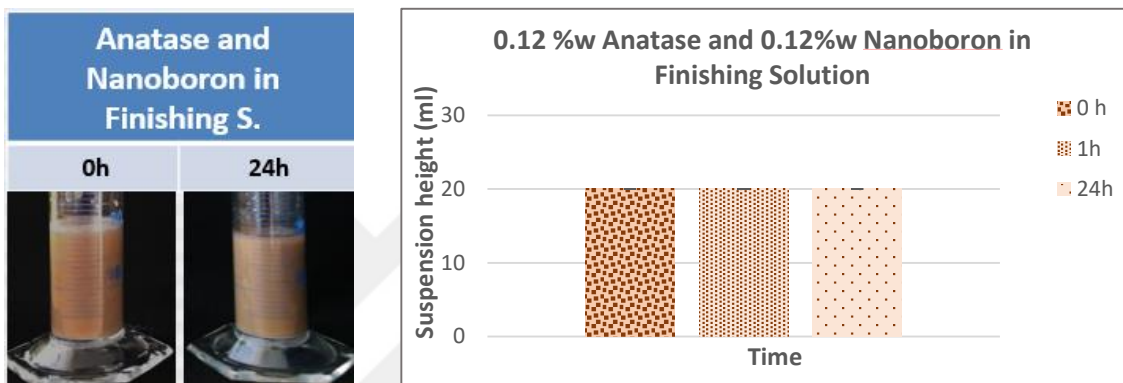
Figure 3.24. Stability test conducted on 0.12w% anatase doped with 0.12w% nano-boron in finishing solution.
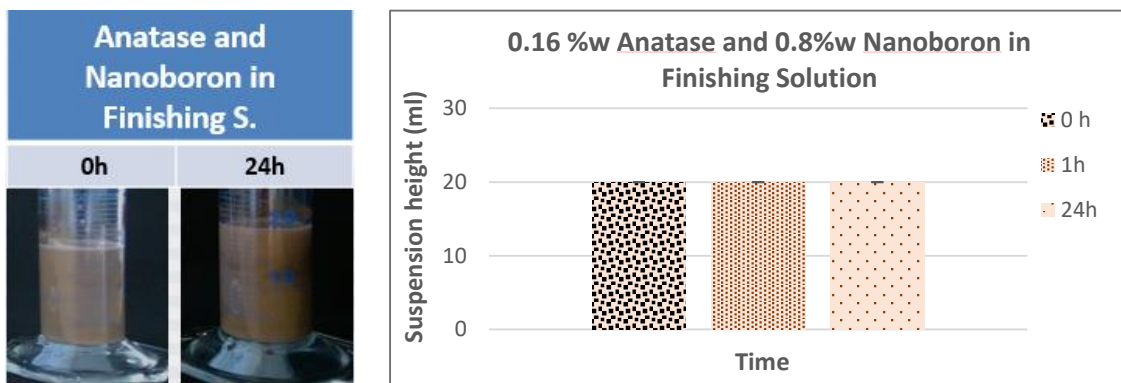
Figure 3.23. Stability test conducted on 0.16w% anatase doped with 0.08w% nano-boron in finishing solution.

The suspensions have demonstrated different stability behavior in DI-water, while the stability of doped anatase suspensions in the finishing solution showed consistent performance. These solutions were used to coat textiles to observe the photocatalytic activity as well as the textile appearance evaluations.

3.4.4. Evaluation of photocatalytic efficiency

3.4.4.1. Stain tests

The textiles coated with solution series of the most desirable anatase and nanoboron combinations chosen by the Design Expert software were exposed to the stain tests procedure to evaluate their photocatalytic activity. The results of the stain test are illustrated in Figures 3.26 through 3.29.
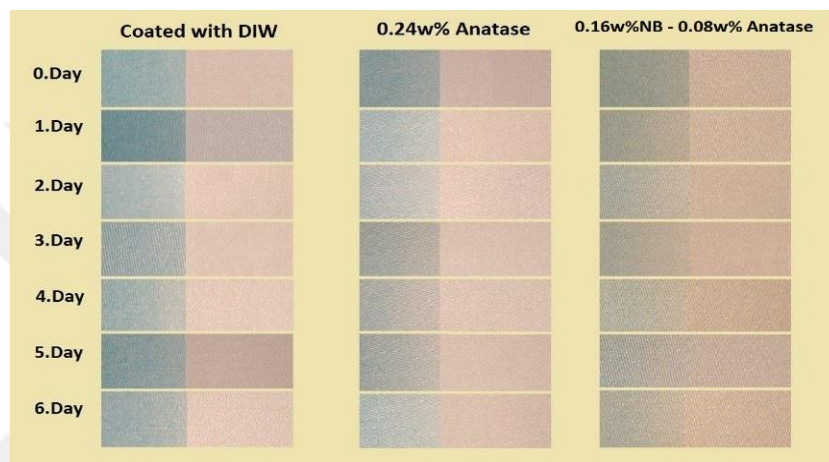
Figure 3.27. The stain bleaching tests conducted on DI-water as compared to 0.24wt% anatase and 0.08wt% anatase doped with 0.16wt% nano-boron.
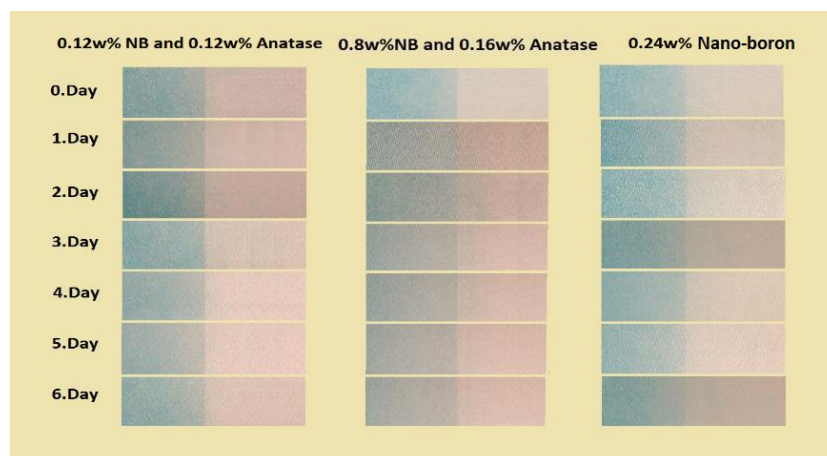
Figure 3.26. The stain bleaching tests conducted on DI-water as compared to 0.24wt% nano-boron, 0.16wt% anatase doped with 0.0 8wt% nano-boron and 0.12wt% anatase doped with 0.12wt% nano-boron.
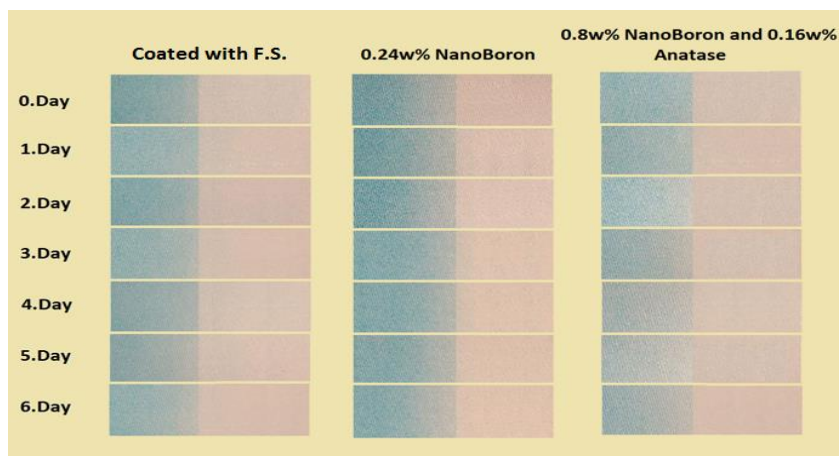
Figure 3.29. The stain bleaching tests conducted on the finishing solution as compared to 0.24wt% anatase and 0.16wt% anatase doped with 0.08wt% nano-boron.

Figure 3.28. The stain bleaching tests conducted on finishing solution as compared to 0.24wt% nano-boron, 0.0 8wt% anatase doped with 0.16wt% nano-boron and 0.12wt% anatase doped with 0.12wt% nano-boron.

The stain bleaching tests conducted on textiles coated with anatase doped with nano-boron in finishing solution did not show any remarkable discoloring of methylene blue stain. Yet, the stain bleaching tests conducted on 0.08wt% anatase doped with 0.16wt% nano-boron and 0.24wt% anatase in DI-water resulted in a remarkable stain bleaching performance which can be distinguished by the human eye as shown in Figure 3.26. In order to verify these observations, the absorbance tests were also conducted as given in the next section.

74

3.4.4.2. Absorbance tests

The absorbance tests performed on the 0.08wt% anatase doped with 0.16wt% nano-boron and 0.24wt% anatase in DI-water showed the greatest stain discoloration. Figure 3.30 shows the absorbance test results for the solutions of the methylene blue as they were exposed to the UV light in the presence of the textile pieces coated with these selected concentrations. It can be seen that the textiles coated with 0.08w% anatase and 0.16w% nano-boron in DI-water couldn't provide higher absorbance delta as compared to the textile coated with only 0.24wt% anatase in DI-water. As a results of that, we can state that the doping anatase with nano-boron cannot provide the expected improvement for self-cleaning ability. Furthermore, it must be noted that the pure nanoboron powder has a brownish dark color that is not favorable on the optic white textiles.
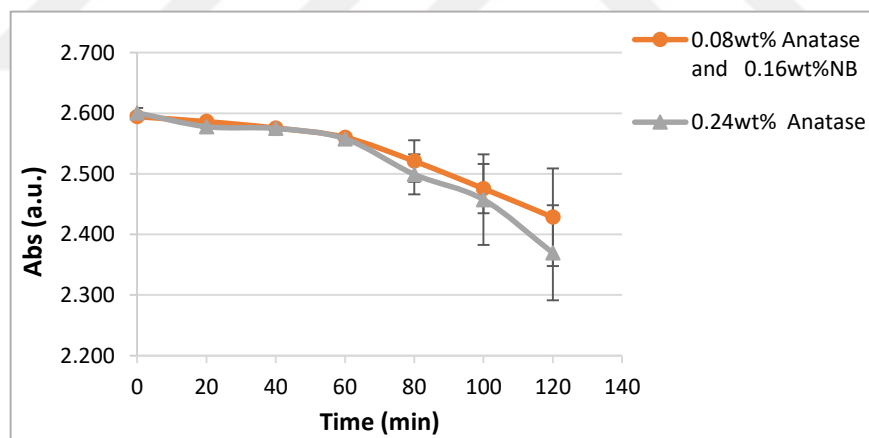
Figure 3.30. Absorbance results for textiles coated with nano-boron doping in DI-water.

Table 3.3. Absorbance delta data for nano-boron doped textiles.

Photocatalytic particles on textiles	Absorbance
Anatase in DI-water (2.4wt%)	0.231
0.08wt% anatase doped with 0.16wt% nano-boron in DI-water	0.166

Yet, the anti-microbial properties of the nanoboron powders have been proven earlier and it can be suggested that the biological evaluations are worth being conducted on the coated textiles although it is beyond the scope of this thesis.

3.5. *Conclusions*

The design expert software was used to determine absorbance performance of the textiles coated with anatase in combination with nanoboron as a p-type dopant. The software initially showed that 0.16wt% anatase doped with 0.08wt% nano-boron in DI-water is the most desirable sample.

The optical characterization of anatase and nano-boron doped anatase in DI-water was performed by coating the suspensions on a glass substrate. The band gaps of 0.24w% anatase and 0.08wt% anatase doped with 0.16wt% nano-boron were determined to be 3.37 and 2.05 eV, respectively. However, sedimentation of the nano-boron doped suspensions negatively affected the film coating due to the agglomeration of the particles on the coated glass surface. Hence, the band gap for nano-boron doped anatase thin films could not be determined properly.

The settling stability tests of the prepared suspensions were conducted by taking daily pictures of the suspensions placed into the graduated cylinders. The results showed that the solutions prepared by finishing solution were more stable as compared to the suspensions prepared in the DI-water. This can be attributed to the presence of secondary bonds between the nano-boron and anatase (Dev., 2013). The particles maybe binding to each other by secondary bonds and are liable to sedimentation due to anatase's well known agglomeration tendency (Gom., 2014). The contents of finishing solution with hydrophobic silicon, however, help stabilize the nano-boron particles to stay in the suspension.

Despite the sedimentation of suspensions prepared in the DI-water, they were used for coating the textiles. The textiles coated with nano-boron doped suspensions prepared in both distilled water and finishing solution were analyzed for their stain tests and bleaching performances at the optimized 0.24w% anatase and 0.08wt% anatase doped with 0.16wt% nano-boron concentrations. The textiles coated with 0.24w% anatase in DI-water were observed to be photo-catalytically more active than the textiles coated with nano-boron as a dopant. Although the band gap energy of nano-boron doped thin films correspond to the visible range, the doping of anatase didn't improve the photocatalytic efficiency in the visible light range. The natural dark color of nano-boron created a problem for stain bleaching tests, changing the transparent color to brown. This is disadvantageous for wide spread use of nano-boron as a dopant in standard textile manufacturing. Yet, the nano-boron's antimicrobial activity has been demonstrated in our group's earlier work and can be further investigated when it is doped with titania on the textile surfaces (Akb., 2016).

CHAPTER 4

EVALUATION OF NOVEL NANOPARTICLES FOR ENHANCED PHOTOCATALYTIC ACTIVITY

4.1. Introduction

The need for developing robust photo-catalysts with faster self-cleaning kinetics is clear to make the textiles functional and sustainable. The trials with nanoboron as a dopant for TiO_2 have shown limited photocatalytic activity and self-cleaning properties due to slow activation in addition to the negative aspects concerning the color of the nanoboron particles. Most self-cleaning films are deposited from colloidal suspensions onto the surfaces that are subsequently heated to diffuse or anneal the active particulates onto the surfaces at temperatures that fabrics and polymer films may not resist (Kiw., 2016). Also, the friction of a finger or a piece of cloth may easily wipe out the non-uniformly deposited and low-adhesive colloidal TiO_2 films because of their insufficient mechanical stability (Kiw., 2016).

The synthesis of high-quality functionalized films would seem to require more sophisticated nano-technological approaches involving innovative composite phases. This might be the key for the self-cleaning textile production, which is active in the visible light range. When the functionalized particles are sufficiently combined with an improved coating method to facilitate the proper dispersion and active diffusion of particles, self-cleaning textile manufacturing can be optimized to meet the industrial demands.

From this point of view, effects of different combinations of functional particles on photo-catalytic textile surface, their stability and quality control in textile manufacturing are focused in this chapter to improve the fabrication processes in terms of enhancing self-

cleaning ability under visible light. Therefore, a novel branched silica/titania synthesis was performed in this chapter and a composite titania and branched silica photocatalytic particle suspension was formulated in addition to the development of the most effective method of deposition and absorbance and stain removal evaluations in this chapter.

4.2. *Materials and methods*

4.2.1. Zeta Potential Measurements on the Coating Suspensions

The textiles coated with photocatalytic particles in contact with a liquid show a change in the surface charge as compared to the baseline textiles. The coated textile surface forms a different electrochemical double layer where; (i) there are charge carriers, which are fixed on the solid/liquid interface and (ii) there are additional charge carriers attracted to the surface and subject to thermal movement. These layers are separated from each other by a shear plane and the potential of the interface in between the immobile and the diffuse layers is called the electrokinetic or zeta (ζ) potential.

The zeta potential is a sign of the charge formation at the solid/liquid interface. The surface charge is constituted by the interaction of the solid surface (textiles for this study) with the liquid. In the solution environment, based on the surface functional groups, the solid surface acts like a weak acid or base. The formation of surface charge is related to the pH value of the electrolyte solution. The experimental results reported in the literature on different material groups are summarized in Table 4.1 in terms of zeta potential. The results draw a prediction about the solution stability based on the zeta potential. It can be seen that the stability is lowest in the vicinity of point of zero charge where the value of the zeta-potential is approximately equal to zero (Ney., 1973).

Table 4.1. Change of material stability depending on zeta-potential size.

Assessment of stability (Sal., 1992)	Zeta Potential (mV)
Maximal agglomeration and precipitation	0…..+3
Region of strong agglomeration and precipitation	5…..-5
Beginning of agglomeration	-10…..-15
Beginning of peptization (dispersing)	-16…..-30
Medium stability	-31…..-40
Good stability	-41…..-60
Very good stability	-61…..-80
Extremely good stability	-81…..-100

If the material is to be destabilized, one of the ways to do this is to lower the zeta-potential and isoelectric point to reduce the electronegativity of a particle and reduce the electrical repulsion in between the particles (Sal., 1992).

4.2.2. Particle morphology

The branched silica particles were utilized in this study to be able to improve photocatalytic activity as well as the solution stability and surface attachment enhancement. The branched silica and titania were synthesized by using a combination of the Stöber silica process and esterification of the grown silica particles. Since various silica synthesis procedures described in the literature tend to result in different particle shapes (Bao., 2016), Scanning Electron Microscope (SEM) was also used for monitoring the particle shape and morphology.
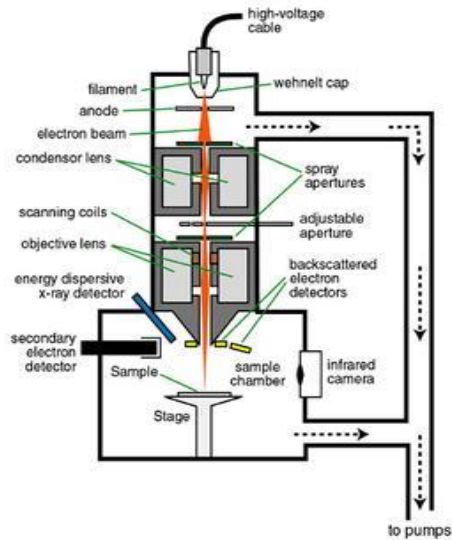
Figure 4.1. SEM Schematic (Ter., 2017) .

In SEM technique, the electrons are thermionically emitted (or, alternatively, via the mechanism of field emission) from a tungsten cathode filament and leading beam to focus on a condenser and the objective lens, respectively. The beam is directed to a sample surface, in a vacuum environment, and many scattering electrons leave the sample surface as illustrated in Figure 4.1. The electrons emitted from the sample surface are detected by the electron detectors.

Generally, the secondary electrons originating from no deeper than a few angstrom of the sample are recorded by the detectors. A Photo-multiplier amplifier is used for enhancing the signal and a resolution of approximately 50Å can be achieved with the SEM devices. SEM is not only used for taking surface images but also the thickness of sample layers can be measured. This technique is useful for getting a close and atomic scale image of a substance.

4.2.3. Contact angle and wetting property measurement of textiles

The wetting shows a vital role in many industrial processes, such as oil recovery, lubrication, liquid coating, printing, and spray quenching (Bra., 2013).
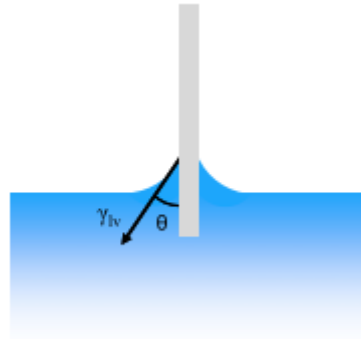
Figure 4.2. Illustration of the Wilhelmy balance method (Bra., 2013).

In recent years, an increasing interest in the study of super-hydrophobic surfaces has taken place due to their potential applications in, for example, self-cleaning, nano-fluidics, and electro-wetting (Nan., 2010).

Wettability studies encompass the measurement of contact angles as the main data, which specifies the degree of wetting from the interaction between a solid and a liquid. Small contact angles ($\ll 90°$) is a sign of the high wettability, while large contact angles ($\gg 90°$) represent low wettability (Bra., 2013). The Wilhelmy contact angle measurement method was chosen for analyzing the textile wettability due to the porous structure of the textiles. It is a method in which the textile sample is oriented perpendicularly towards the liquid surface during the measurement. The principle of the method is illustrated in Figure 4.2 and the sample is moved towards the liquid surface until the meniscus connects with it.

4.2.4. Water vapor transmission rate analyses on textiles

The methods of measuring water vapor transmission rate (WVTR) are a response to the growing need for films that are highly permeable to water vapor. The highly permeable films are generally used in products presented for human use such as self-cleaning textiles. In order to provide human skin respiration continuity after the coating procedure, the water vapor transmission rate is an important measurement. Thus, the technique was used to measure water vapor transmission rate which is a modification of

the wet cup method described by the ASTM E 96-95 standard (Y. Hu., 2001). In this method, the textile sample is a covered on a cup full with DI-water and the change in mass is recorded as a function of time. The weight change was used, according to Equation 4.1 to determine the water vapor transmission rate.

$$WVTR = \frac{mass\ lost}{time.area}$$ [1]

4.3. Experimental Approach

4.3.1. Synthesis of branched titania and branched silica particles

The synthesis of branched particles was performed according to a tendency of creating secondary bonds without changing chemical characteristic of the anatase particles. The branching procedure also serves as a simple surface modification technique to avoid irreversible agglomeration of the titanium dioxide nanoparticles and create uniform size particles.

In this study branching was induced on both the titania and the silica particles to be combined with the standard anatase particles. While branched titania is an amorphous form, the silica (SiO_2) was selected since it is a possible dopant in the textile coatings. To create uniform sized particles and ensure the secondary bonds between the anatase and silica, dendrimers with ester functions were used due to their easy accessibility, facility in branching, versatility, solubility, processability, and applicability as inexpensive raw materials.
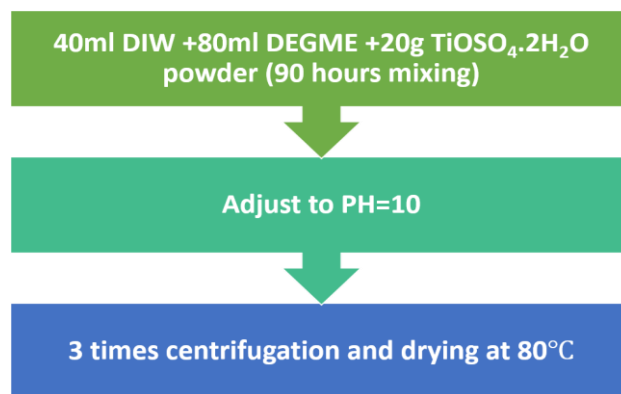
Figure 4.3. Synthesis procedure of the branched titania particles.

The procedure for synthesis of branch titania powder originates from a study by S.A. Simakov and Y. Tsur. The technique is based on the hydrolysis-precipitation procedure, by using $TiOSO_4.H_2O$ as a precursor and water as a hydrolyzed preparation medium. Diethylene glycol monomethyl ether (DEGME) is used as a surface modifier (Sim., to form the desired branches utilized for stability as well as enhanced attachment onto the textile surface.

The preparation procedure was carried out in a continuously stirred closed glass flask at room temperature (Figure 4.3). For the preparation of a surface modified titania powder, 20 g of $TiOSO_4.2H_2O$ powder ($\geq$29% Ti (as TiO_2) basis Sigma-Aldrich) was added to a solution, which contained 180 ml of diethylene glycol monomethyl ether ($\geq$99% Sigma-Aldrich) and 40 ml DI-water. After mixing for 90 hours, the solution pH was increased by the dropwise addition of a dilute NH_4OH solution (diluted from ammonium hydroxide solution of 26% obtained from Sigma-Aldrich) up to pH 10. Upon the addition of the NH_4OH solution, the mixture turned into a white color suspension. The resulting white precipitates were separated by centrifugation technique. After centrifugation, powders were washed three times with a diluted NH_4OH solution and, finally, by distilled water. The procedure was performed in order to avoid creating bonds with the counter-ions of the salt used as a ligand structure (SO_4^{-2}). The solution was centrifuged after each washing

step to separate the precipitates without significant loss and to remove the counter-ions and ligand structure within the remaining solution. Finally, the precipitates were dried at 80℃, resulting in a white powder to be obtained (Sim., 2007).

The Stöber process was used for the preparation of the spherical silica particles of uniform size by means of hydrolysis of alkyl silicates and subsequent condensation of silicic acid in alcoholic solutions as a sol-gel process. Ammonia was used as a morphological catalyst (Stö., 1968). DEGME was added into the Stöber process creating the dendrimers with ester functions to facilitate branching to uniformly sized silica particles. For the preparation of a surface modified silica powder (Figure 4.4), 50ml of ethanol (≥99.8% GC, Sigma-Aldrich) and 0.44ml distilled water were added into a Florence flask and then continuously stirred while adding 2ml NH_4OH and 4ml Tetraethyl orthosilicate (≥99% GC, Sigma-Aldrich). For branching of these particles, 7.5 ml of diethylene glycol monomethyl ether (≥99% Sigma-Aldrich) was added to the solution and then stirred with the Stöber silica particles for ester functionalization for 24 hours. After mixing for 24 hours, the pH was decreased by the dropwise addition of a 0.1M HNO_3 into the prepared solution (65% Sigma-Aldrich) adjusting pH to 7 for precipitation of the prepared particles. The resulting white precipitates were separated by centrifugation. After centrifugation, the pulp was dried at 100℃ for 2 hours.
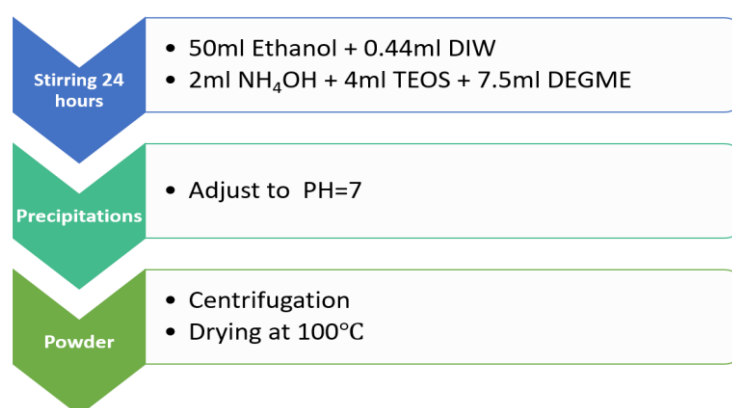
Figure 4.4. Synthesis procedure of branched silica particles.

Finally, dried particles were pounded to attain a powder. The exact dosages of the used chemicals were determined according to the Stöber silica particle synthesis performed in the previous studies (Bao., 2016).

The synthesized particles, both branched titania, and silica were characterized for their particle size and size distributions, photocatalytic activity, stain removal efficiency as well as stability after coating and standard quality testing after pilot scale manufacturing.

4.3.2. Characterizations of the synthesized novel dopants

4.3.2.1. Particle size analyses

The particle size and size distribution of the synthesized particles was determined by light scattering particle size analyzer (Coulter LS 13 320) and AFM measurements. The samples for particle size analysis were prepared as dilute solutions for each type of branched particle both in DIW and the textile finishing solution as carried out for anatase and P-25 particles in the previous chapter.

4.3.2.2. Particle morphology

For SEM analysis, the particles in DI-water were deposited on freshly cleaved mica surface as very dilute suspension and dried by keeping them in a petri cup under the ambient condition. The solutions were prepared under the same conditions as the samples prepared for AFM. SEM measurements were carried out at the TUBITAK MAM laboratories.

4.3.3. Optimization of photocatalytic activity with methylene blue solution

To observe the efficiency of doping branched particles into the best performing anatase particles, the branched particles were mixed into anatase containing solutions. Solutions of photocatalytic components were prepared as 10 ml and 2ml MB^+ solution at

$2x10^{-4}$ M concentration was added into these solutions. The samples were exposed to 365 nm UV light for 5 minutes for observing the discoloration of methylene blue by degradation of the methylene blue. The appearances of solutions were compared by taking photograph before and after the UV light exposure.

The active solutions were prepared at 30 ml volume to and by adding $2x10^{-4}$ M methylene blue to the solutions in 10 ml steps determine absorbance change due to the methylene blue degradation. These solutions were exposed to two different light sources, which are UV at 365 nm and cool light 580-600nm wavelengths. After exposure of light sources at certain time intervals, the absorbance spectrums of the solutions were attained using a Shimadzu UV1280 UV-visible spectrometer as methylene blue degradation takes place.

4.3.4. Evaluation of photocatalytic efficiency

4.3.4.1. Absorbance tests

The textile samples were prepared under the ISO 10 678 conditions as in the previous chapters. The samples were cut as 10 cm square and settled into a beaker full with 100 ml MB^+ solution and exposed to the UV light at 365nm wavelength. During the exposure of UV light, the methylene blue solution absorbance at 665nm wavelength was measured every 20 minutes.

4.3.4.2. Stain tests

Stain tests were also performed under the ISO 10 678 conditions as in previous chapters. The samples were cut as 10 cm square and put into a beaker full with 100 ml of MB^+ solution for 20 seconds. The stained textiles were dried at 36℃ overnight. Afterwards, the stained samples were exposed to the UV light to observe discoloration of the stain. The change in stain color was followed by taking daily photographs.

4.3.4.3. *Solid color spectroscopy*

The discoloration of baseline and coated samples exposed to the stain tests were also followed by XriteCi7800m benchtop sphere solid spectrophotometer, which is one of the advanced instruments for exactly determining color consistency or change as a function of time after exposure to the light source. This tool helps manufacturing consistent colors and it is suitable for measurements of various surfaces. The data collected from the XriteCi7800m benchtop sphere spectrophotometer was evaluated with X-Rite Color iQC quality control software by comparing first day color to the colors obtained as a function of time (daily) under UV exposure.

4.3.5. Surface properties of coated textile

4.3.5.1. *Zeta potential determination of the textile samples*

The zeta potential of the baseline and coated fabrics were measured by using Electro Kinetic Analyzer (Anton Paar SurPASS) as a function of pH of the circulating electrolyte. The textile samples were settled in the middle of a cylindrical cell with supporting disks, which have holes to allow the liquid flow. After the placement of the textile sample into the cylindrical cell, the cylindrical cell was placed in between the electrodes to bind to mobile pistons to allow variation in the distance between the electrodes and adjusting pressure applied to the textile sample. The liquid flow was provided with a 1mM KCl solution and the pH titration was performed by adding 50mM HCl solution at each time interval, as directed by the Attract 2.0 software data analyzer of the SurPASS instrument. The same software also provides the graph of zeta potential as a function of pH value after the analyses are conducted successfully.

4.3.5.2. Isoelectric points

The isoelectric points are defined as zeta potential of materials at the zero pH value (Y.Hu., 2001). With reference to this, the data attained from Attract 2.0 software, which is a scatter graph of zeta potential as a function of pH, were plotted as a polynomial correlation by utilizing MS Excel software. The isoelectric points were determined through replacement of zero value for pH in the equation generated by Excel.

4.3.5.3. Surface morphology analyses by AFM characterization

The textiles coated with 0.1wt% anatase doped with 0.001wt% branched silica in the finishing solution was cut into 1cm square to scan via ezAFM by NanoMagnetics in the dynamic mode. The measurements were carried at NanoMagnetics laboratories by scanning 5μm and 8μm area on the textile.

4.3.6. Wettability measurements of the coated textiles

To perform meniscus contact angle measurements, the textiles were cut into a width of 0.3 cm to analyze with Attension, Tetha optic tensiometers. The contact angle determination of coated textiles was conducted by using DI-water for the liquid interaction evaluations determining the wettability.

4.3.7. Evaluation of the self-cleaning efficiency of the textiles for daily use

4.3.7.1. Resistance tests

Resistance tests were carried out at Kivanc Textile laboratories according to the conditions adopted by textile standards, which are BS EN ISO 13936-1, BS EN ISO 13934-1, BS 4303, DUPONT TTM 076, BS EN ISO 12945-2.

4.3.7.2. Washing tests

The textiles were cut into 10cm squares to perform washing tests. The textiles were washed in a beaker full with 200ml DI-water settled in an Elmasonic S 100H ultrasonic bath for 30min. Before and after the washing process, the textiles were weighed with a high precision balance Ohaus Pioneer series ($\pm$ 0.001 precision) to determine any particle loss during the washing procedure.

*4.3.7.3. Water transmission test*s

The textiles were prepared for water transmittance tests by cutting 10cm square samples to cover the top of the beakers after adding 100ml DI-water in each beaker. The system was weighed to follow the mass change in weekly periods.

4.3.7.4. Water-absorbance tests

The textiles were exposed to the absorbance test procedure after an initial wash and then after a second and a third wash cycle was performed. The absorbance tests and the associated conditions followed the established procedures as detailed in the previous chapters.

4.4. *Results and discussions*

4.4.1. Characterization of novel dopants

4.4.1.1. Particle size measurements

The particle characterization of branched particles was performed in terms of particle size and particle morphology by particle size analyzer using light scattering phenomenon and AFM scanning, respectively.

The particle size analyzer results for particles dispersed in both finishing solution and DI-water are presented in Figures 4.5 and 4.6. The calculated average particle size and standard deviation, based on these results, are further summarized in Table 4.2. It can be seen that the volume% measurements indicate an agglomeration in the solutions whereas the number% measurements give close results to the real particle size of the synthesized branched particles.
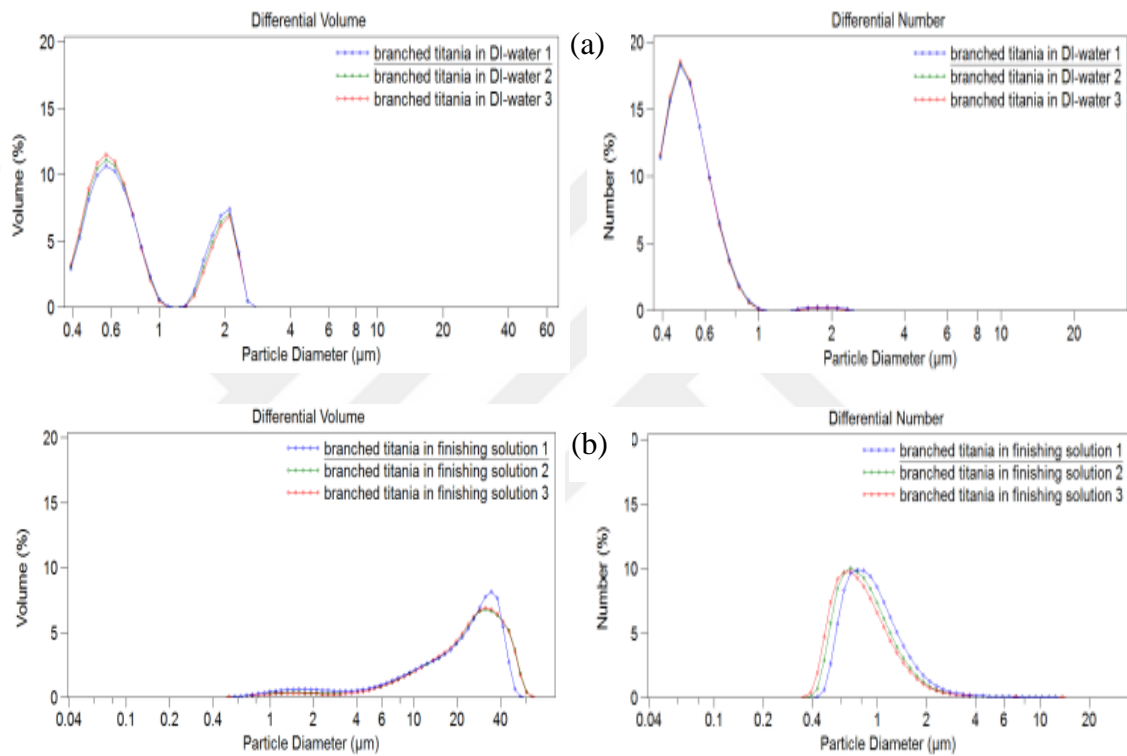
Figure 4.5. Static light scattering particle size measurement results for (a) branched silica in DI-water, (b) branched silica in finishing solution measured by %Volume and %Number distributions.
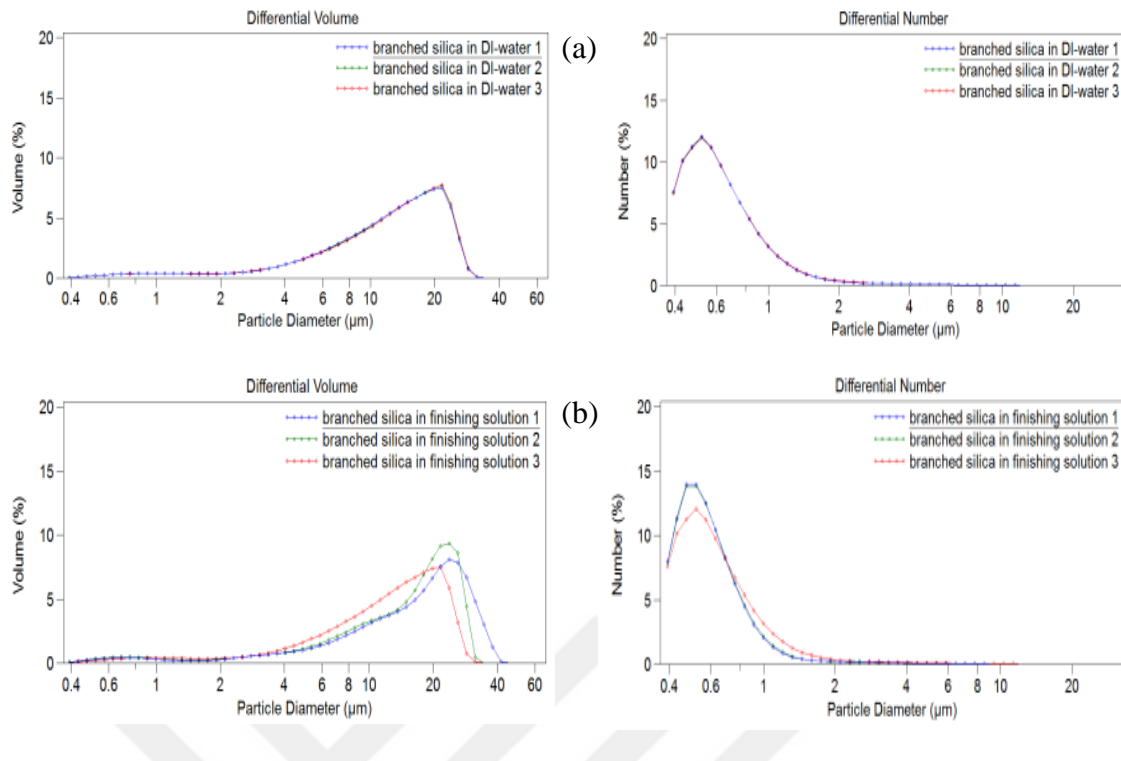
Figure 4.6. Static light scattering particle size measurement results for (a) branched titania in DI-water, (b) branched titania in finishing solution measured by %Volume and %Number distributions.

Table 4.2. The particle size of modified particles with particle size analyzer

Synthesized particle	Particle size(μm)	Deviation
Branched titania in DIW	0.541	0.003
Branched titania in finishing	1.029	0.058
Branched silica in DIW	0.750	0.002
Branched silica in finishing solution	0.671	0.006

The morphology analyses with AFM were conducted by scanning 5μm square on the mica substrate coated with the particles prepared as a solution in DI-water as shown in the Figures 4.7 and 4.8. The provided dimension of the particles from the AFM measurement were calculated and reported in Table 4.3.
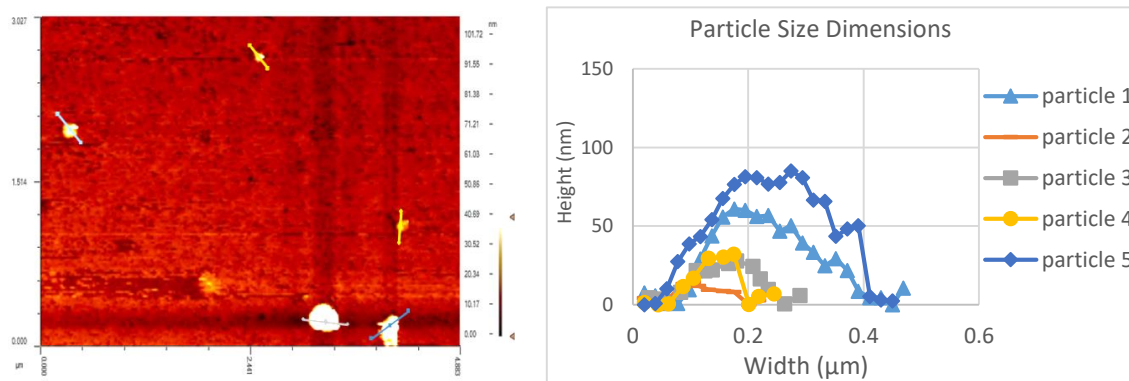
Figure 4.7.AFM picture and cross section of branched titania particles in DI-water.
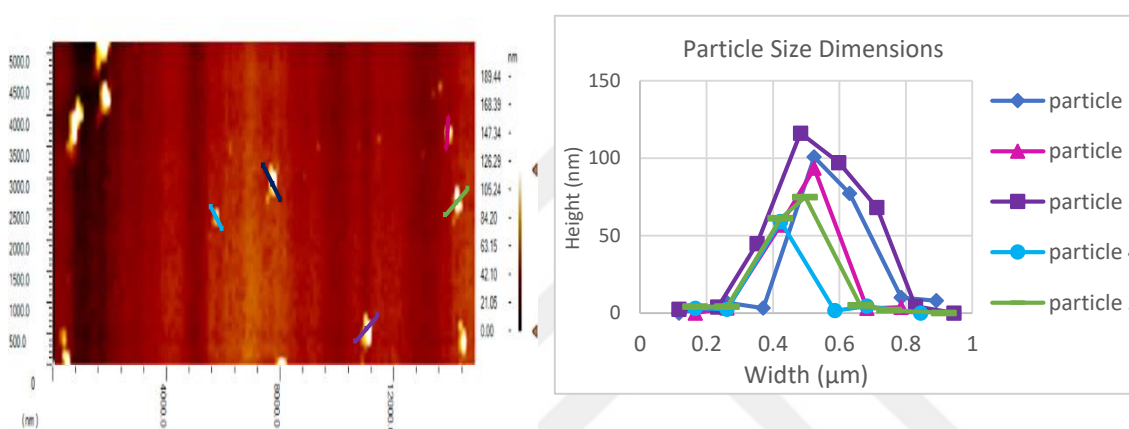
Figure 4.8.AFM picture and cross section of branched silica particles in DI-water.

Table 4.3. Modified particle size analyzed with AFM.

Synthesized particle	Particle size(nm)	Deviation
Branched titania	0.244	0.118
Branched silica	0.468	0.069

The standard deviation of particle size measurements obtained with light scattering is lower as compared to the AFM while the particle sizes measured with AFM is almost two times smaller than the particle size determined by the Coulter LS 13 320. This can be attributed to the fact that the branches attached to the main particle can be extended effectively in the solution environment for the light scattering measurements whereas, the dried particles used for the AFM testing have these polymeric branches attached on the

particle core. Furthermore, the presence of the finishing solution with the added branched silica might result in the measurement of the silica component in the finishing solution itself as a particle.

4.4.1.2. Particle morphology analyses

The diluted branched silica solution was deposited on the mica substrate for the SEM measurements to study their surface morphology clearly. Figures 4.9 and 4.10 show the SEM micrographs at various magnifications.
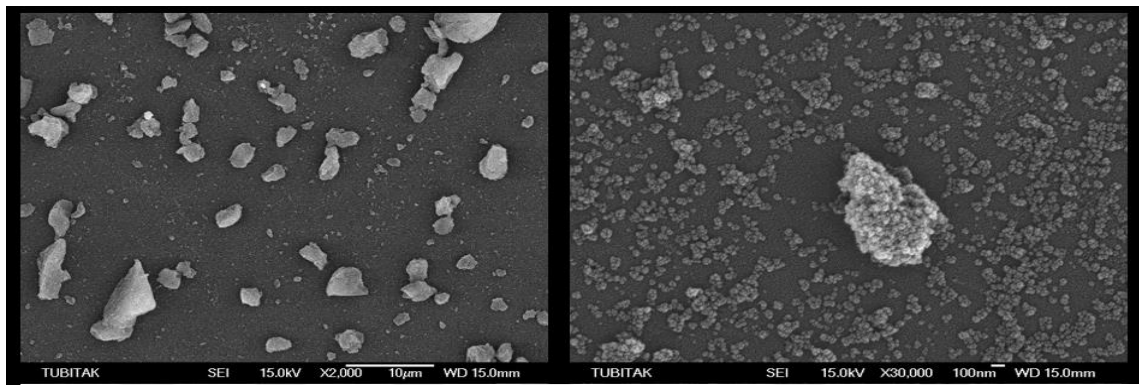
Figure 4.10.SEM image of branched silica film at 2,000 and 30,000 magnifications, respectively.
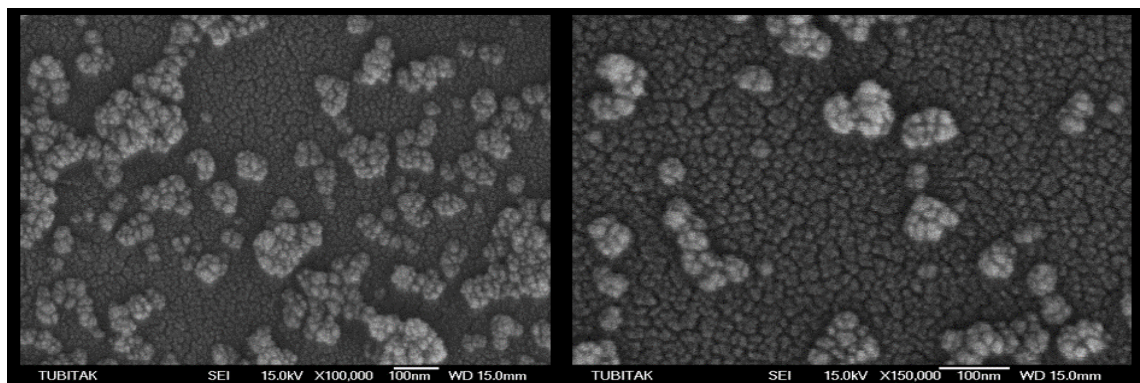
Figure 4.9.SEM image of branched silica film at 100,000 and 150,000 magnifications, respectively.

The SEM analyses verified that the synthesized branched silica particles have a spherical shape. The particles are also prone to agglomeration when dried as observed from the figures.

4.4.2. Optimization of photocatalytic activity with methylene blue solution

The optimization of photocatalytic activity initially studied by using MB^+ and the experimental setup adopting ISO 10 678 conditions. The pictures of the solutions before and after exposure to UV light are presented in the Figures 4.11 through 4.14.
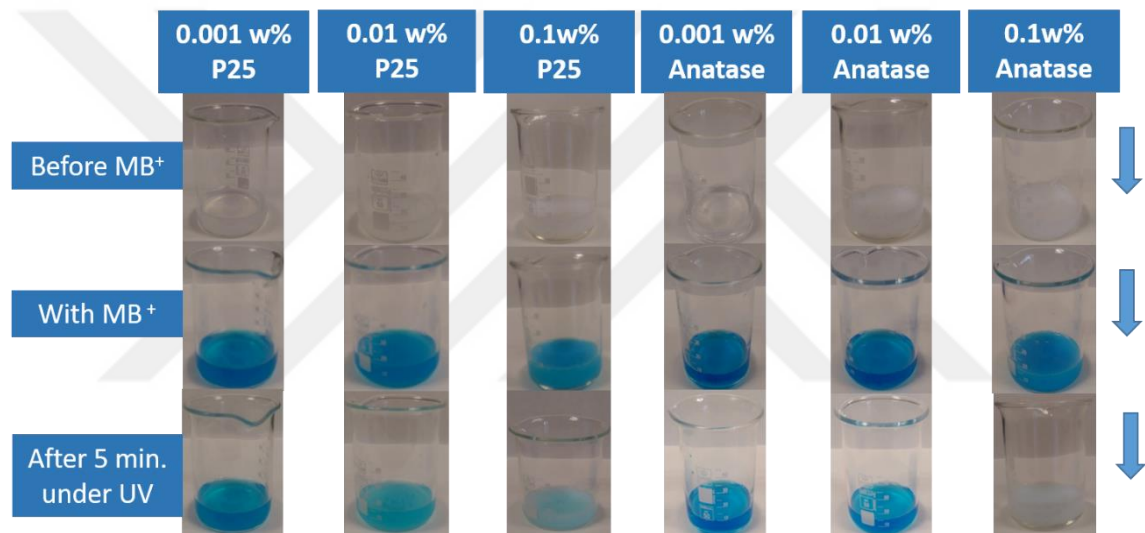
Figure 4.11. Optimization test conducted on anatase and P25 concentrations in finishing solution.
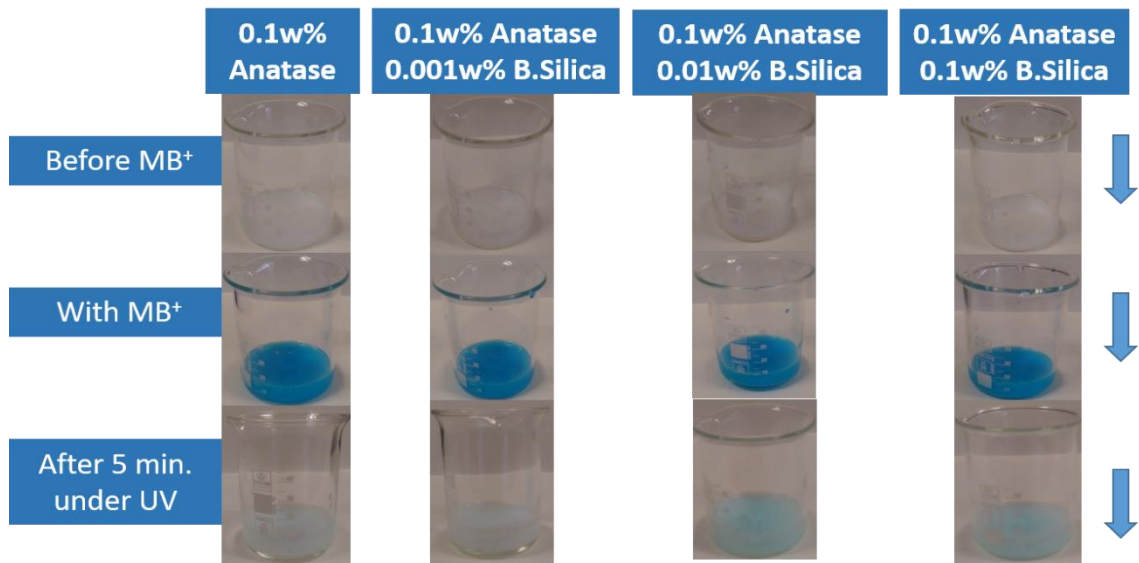
Figure 4.13. Optimization test conducted on 0.1wt% anatase and 0.1wt% anatase doped with branched silica concentrations in finishing solution.
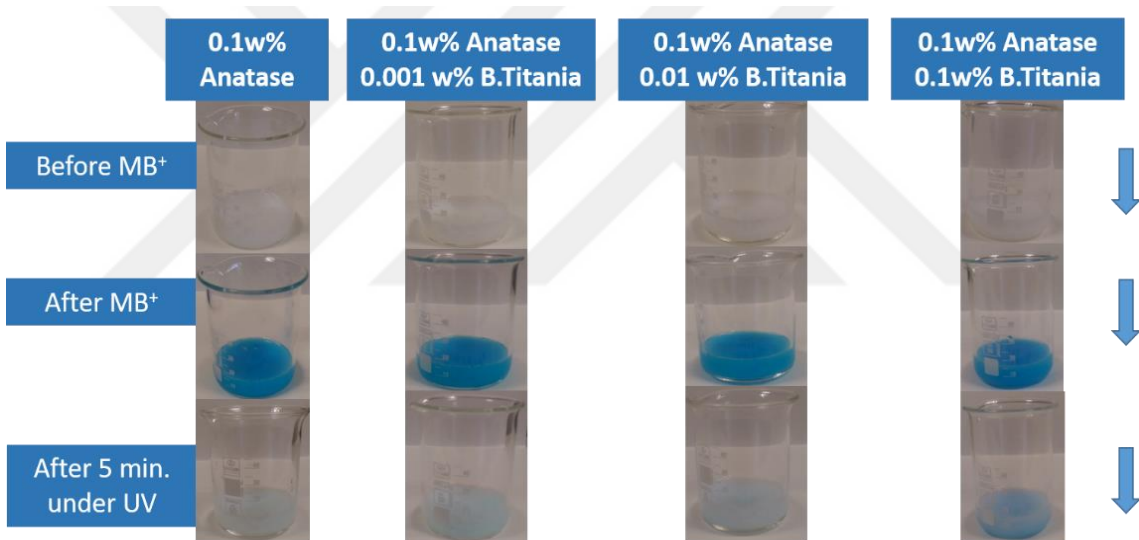
Figure 4.12. Optimization test conducted on 0.1wt% anatase and 0.1wt% anatase doped with branched titania concentrations in finishing solution.

Initially, the optimization tests were performed for baseline photocatalytic materials in finishing solution since the particles showed better methylene blue degradation according to the results presented in the previous chapter. Figure 4.11 demonstrates methylene blue color change from blue to transparent for anatase and P-25 concentrations in the finishing solution.

	0.1wt% Anatase+ 0.001w%Colemanite	0.1wt% Anatase+ 0.001w% N.B.	0.1wt% Anatase+ 0.001w% Sulphur	0. 1 w% P25-Fe doping+ 0.001w% B.Silica
Before Stain				
After Stain				
5 min. under UV				
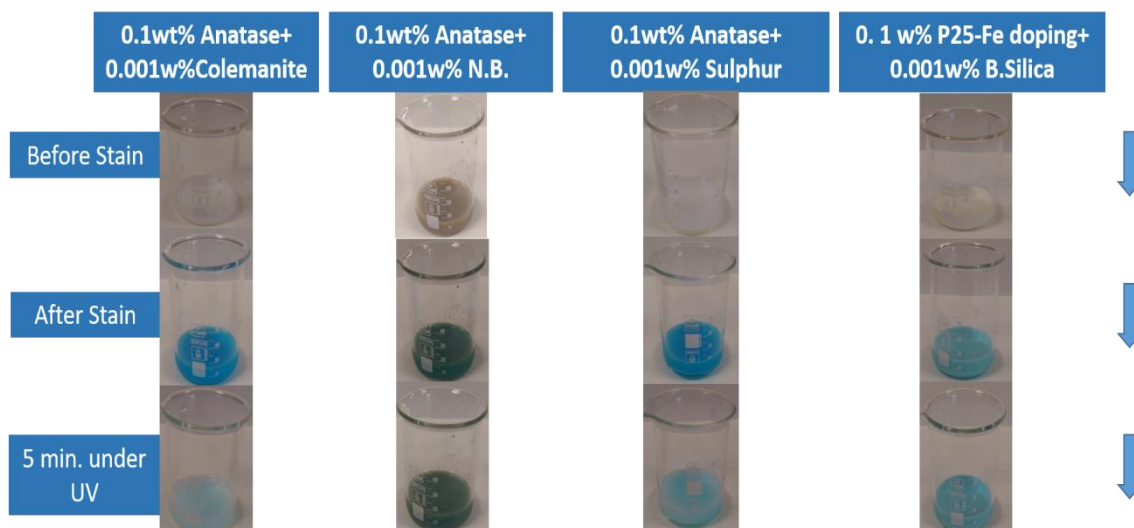
Figure 4.14. Optimization test conducted on 0.1wt% anatase doped with 0.001wt% colemanite, nano-boron and sulphur and 0.1wt% P25-Fe doping and 0.001wt% branched silica in finishing solution.

The 0.1wt% anatase in the finishing solution, which was chosen to be the most efficient material in the previous chapter was further optimized by doping with various materials including branched silica and titania, colemanite and nanoboron as well as the iron doped P25 titania (P25-Fe) and evaluated in the finishing solution for methylene blue degradation. The optimization of solutions resulted in improvements in discoloration due to the methylene blue degradation for 0.1wt% anatase, 0.1wt% anatase doped with 0.001wt% branched silica and 0.1wt% anatase doped with 0.001wt% branched titania in the finishing solution. However, since the determination of the solutions photocatalytic activity according to the color change is based on visual perception, the methylene blue degradation was also observed by following the decrease in the absorbance values as a function of time as shown in the Figures 4.15 through 4.17. The decrease in the absorption is an indication of the better transmittance and hence indicates the cleaning of the solution.
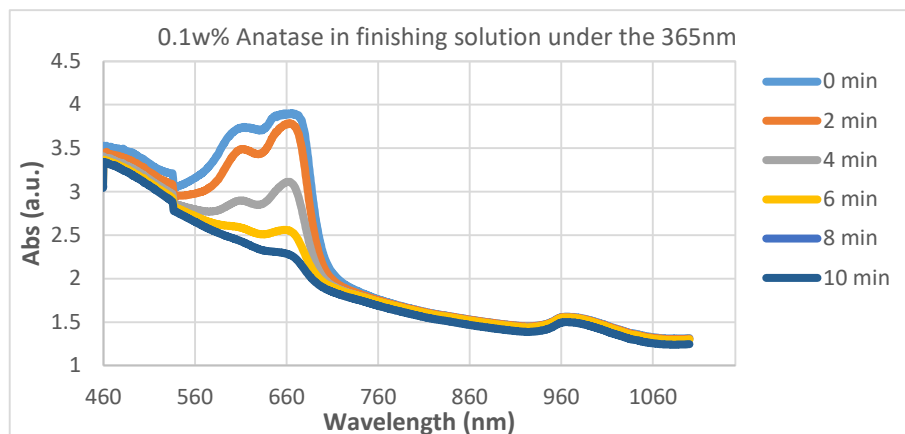
Figure 4.15. Absorbance lines of MB$^+$ degradation with presence of 0.1wt% anatase in

finishing solution by the time as exposed to UV light.
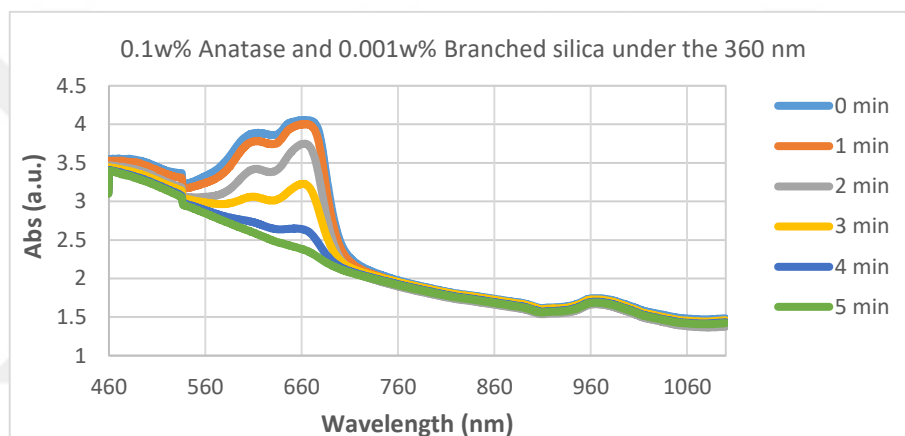
Figure 4.16. Absorbance lines of MB$^+$ degradation with presence of 0.1wt% anatase and

0.001wt% branched titania in finishing solution by the time as exposed to
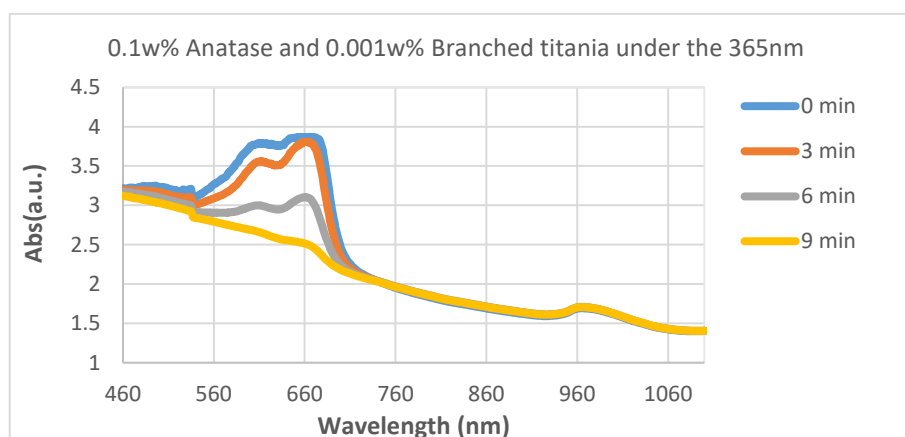
Figure 4.17. Absorbance lines of MB$^+$ degradation with presence of 0.1wt% anatase and

0.001wt% branched silica in finishing solution by the time as exposed to
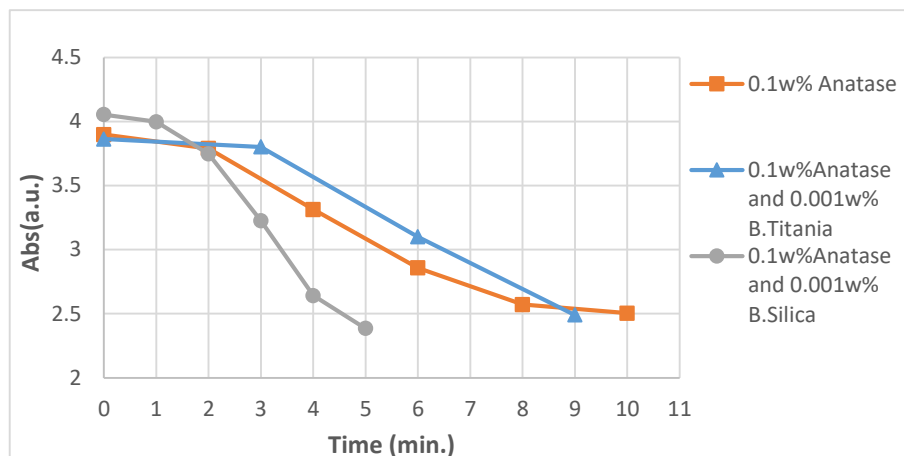
Figure 4.18. The absorbance level at 665nm as function of time as exposure UV light.

Figure 4.18 demonstrates the methylene blue peak variation at 665nm wavelength as the degradation occurs. The quickest degradation and lowest absorbance level has been observed at 0.1wt% anatase doped with 0.001wt% branched silica in the finishing solution environment after 5 minutes and an absorbance value of 2.386 was recorded. 0.1wt% anatase doped with 0.001wt% branched titania in the finishing solution showed the second quickest MB^+ degradation. Although 0.1wt% anatase in finishing solution leads to a low level of absorbance change, the absorbance levels achieved for MB^+ degradation in the presence of 0.1wt% anatase and 0.1wt% anatase doped with 0.001wt% branched titania in finishing solution are quite close in the final absorbance value which are 2.504 and 2.490, respectively.

Branched titania was not evaluated further for the MB^+ degradation tests with cool light source due to its limited functionality. Thus, the degradation tests with cool light source were carried out for 0.1wt% anatase and 0.1wt% anatase doped with 0.001wt% branched silica in the finishing solution. In order to observe the response of 0.1wt% anatase doped with 0.001wt% branched silica in the finishing solution to cool light source, the degradation results are presented in the Figures 4.19 and 4.20. comparing the photocatalytic performance.
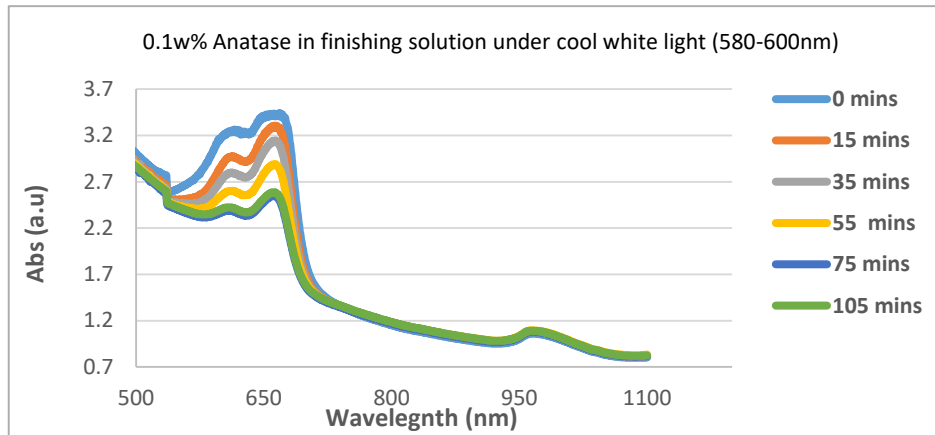
Figure 4.21. Absorbance lines of MB$^+$ degradation with presence of 0.1wt% anatase in finishing solution by the time as exposed to cool light.
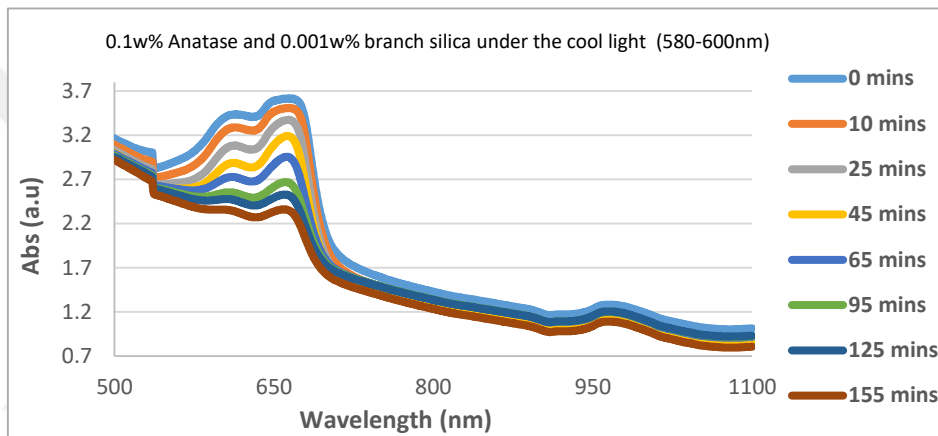
Figure 4.20. Absorbance lines of MB$^+$ degradation with presence of 0.1wt% anatase and 0.001wt% branched titania in finishing solution by the time as exposed to cool light.
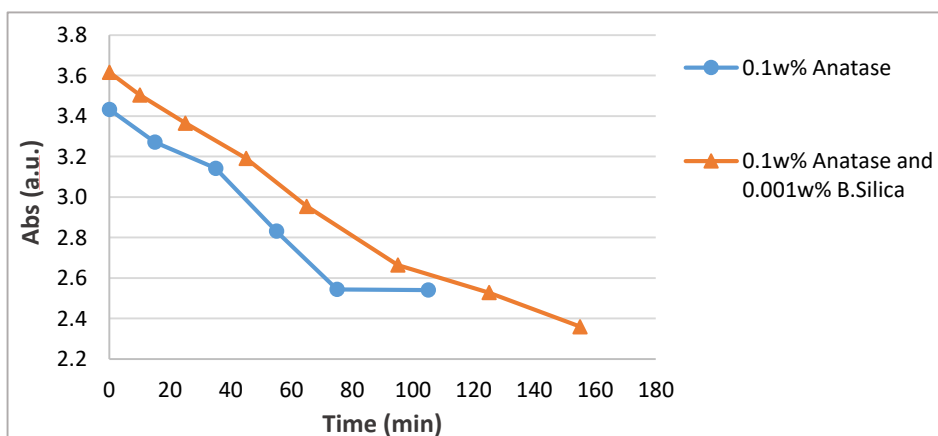
Figure 4.19. The absorbance level at 665nm as function of time for exposure cool light.

Figure 4.21 illustrates the change in the absorbance level at 665nm for MB$^+$ degradation as a function of time. The 0.1wt% anatase doped with 0.001wt% branched silica in the

finishing solution changed the color of the methylene blue solution from blue to transparent as a result of the photocatalytic efficiency under the cool light (580-600nm). On the other hand, the anatase in finishing solution also showed photocatalytic efficiency under the cool light. However, the photocatalytic efficiency of anatase stopped improving after 80 minutes under the cool light while 0.1wt% anatase doped with 0.001wt% branched silica in the finishing solution continued the degradation of methylene blue solution even after 80 minutes of exposure. Consequently, the doping of anatase with branched silica in the finishing solution has clearly improved the photocatalytic activity in the visible range. To follow up, the photocatalytic activity of textiles coated with the selected photocatalytic solution were further evaluated with absorbance tests after the coating process.

4.4.3. Evaluation of photocatalytic efficiency

4.4.3.1. Absorbance tests

Absorbance tests on the coated textiles were conducted to choose the nano-particle combination with the best photocatalytic activity. Hence, the absorbance tests were performed for textile samples coated with (i) 0.1wt% anatase, (ii) 0.1wt% anatase doped with 0.001wt% branched silica and (iii) 0.1wt% anatase doped with 0.001wt% branched titania in the finishing solution. The results of the absorbance tests were compared in the graph given in Figure 4.22. Among the selected coatings, the textile coated with 0.1wt% anatase doped with 0.001wt% branched silica in the finishing solution degraded the methylene blue solution most effectively with a high drop in the absorbance value which indicating photocatalytic activity occurred most effectivelly in the presence of this particular concentration textile coating in the MB solution.
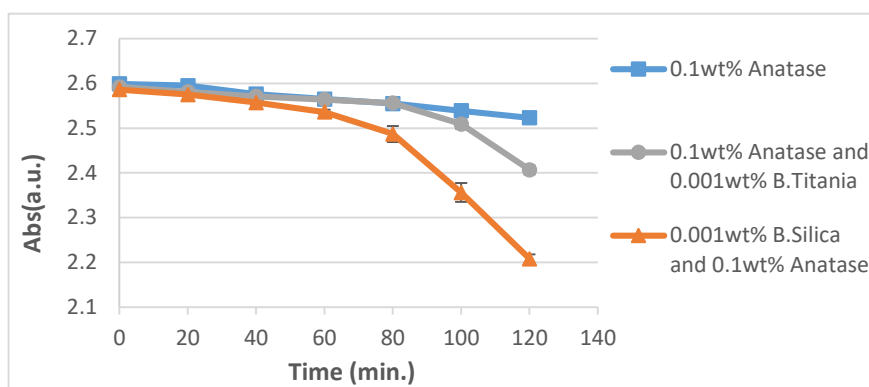
Figure 4.22. Absorbance results for textiles coated with 0.1wt% anatase, 0.1wt% anatase doped with 0.001wt% branched silica and 0.1wt% anatase doped with 0.001wt% branched titania finishing solution.

Table 4.4. Absorbance variation of photocatalytic particles on textiles.

Photocatalytic particles on textiles	Absorbance t=0	Absorbance t=120	Delta
0.1wt% anatase	2.599	2.523	0.076
0.1wt% anatase+0.001wt%B.silica	2.586	2.208	0.378
0.1wt% anatase+0.001wt%B.titania	2.592	2.407	0.185

Thus, the textiles coated with 0.1wt% anatase doped with 0.001wt% branched silica in finishing solution was determined to be the most effective sample in terms of photocatalytic activity. Textile sample coated with 0.1wt% anatase doped with 0.001wt% branched titania in the finishing solution has shown the second most active absorbance change. The following stain removal studies were concentrated on the combination of 0.1wt% anatase doped with 0.001wt% branched silica and baseline 0.1wt% anatase as the branched silica has shown the most effective cleaning efficiency when coated on the textiles.

4.4.3.2. Stain tests

The stain tests were performed based on the visual inspection to observe how the textiles look like after the stain was exposed to the UV light. The stain tests were preliminary carried out with different sources of stain including, tea, coffee, sour cherry juice, etc., which are common sources of the stains in daily life. However, these solutions were pretty light in color to observe any discoloration by human eyes from the pictures taken. Hence, only methylene blue solution was used for the stain tests at the preferred concentration as supported by the literature.

The stain tests performed for the textiles coated with 0.1wt% anatase and 0.1wt% anatase doped with 0.001wt% branched silica in the finishing solution are given in Figure 4.23.
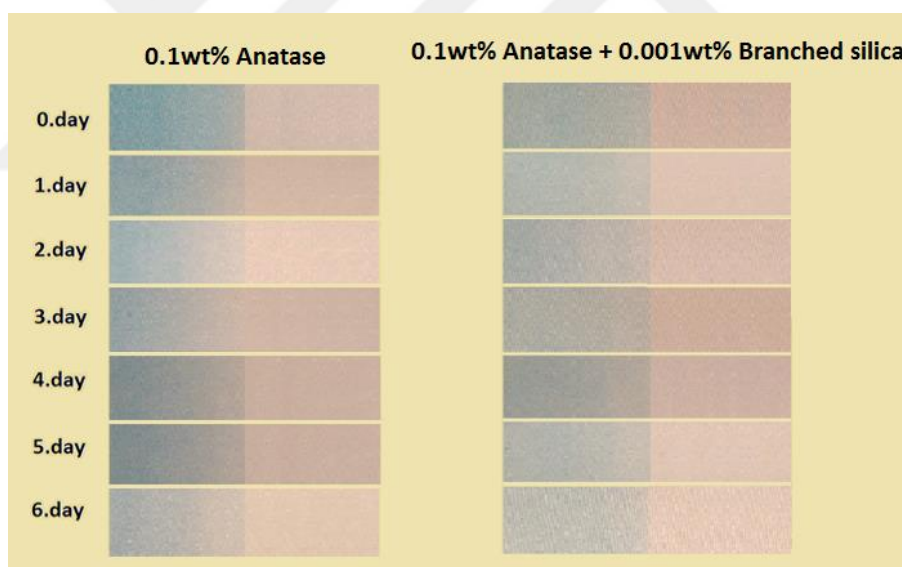
Figure 4.23. The stain bleaching tests conducted on the finishing solution as compared 0.1wt% anatase and 0.1wt% anatase doped with 0.001wt% branched silica in finishing solution.

The stain tests results pointed out that the textile coated with 0.1wt% anatase and 0.001wt% branched silica in the finishing solution created the maximum level of stain discoloring based on the visual judgement of stain bleaching by the human eye.

4.4.3.2. Solid color spectroscopy

To be able to quantify the stain test results properly, solid color spectroscopy was used for analyzing stain discoloration as the stained textiles were exposed to the UV light. The color spectrometer measures the bleaching amount by comparing the stain color measured at the first day to the consecutive days. The stain color was observed change through the lighter shades of the adopted scale as given in Figures 4.24 and 4.25.
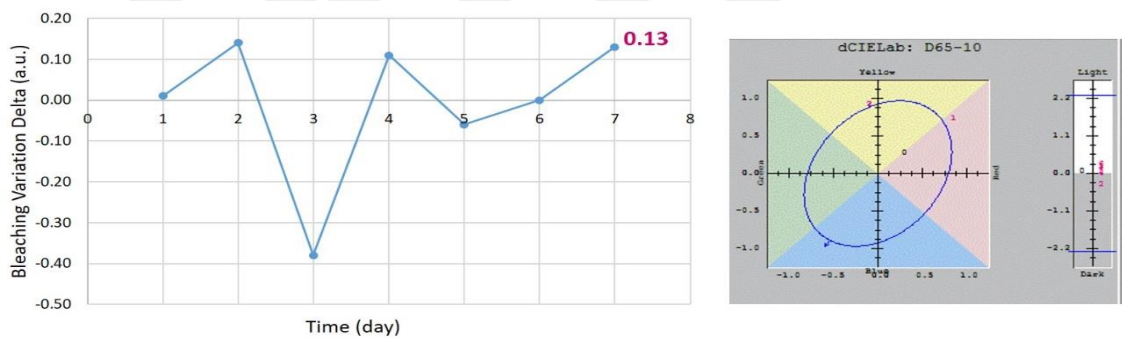
Figure 4.24. The solid color spectroscopy analyses conducted on stain test for textile coated with 0.1wt% anatase in finishing solution.
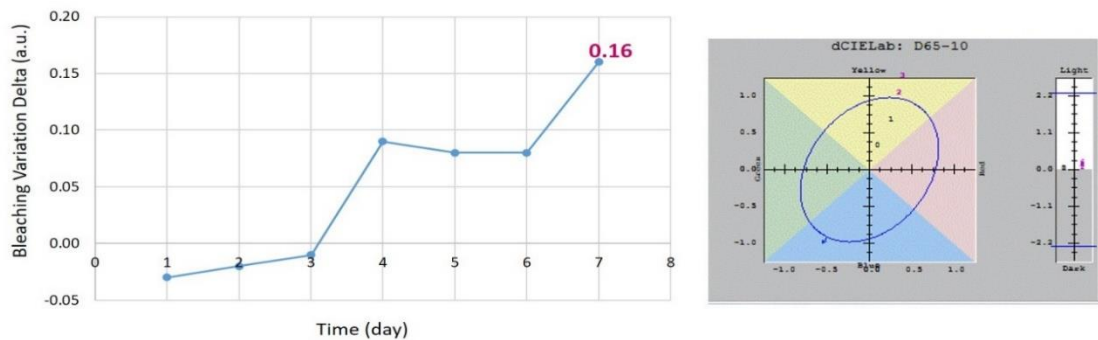
Figure 4.25. The solid color spectroscopy analyses conducted on stain test for textile coated with 0.1wt% anatase doped with 0.001wt% branched silica in finishing solution.

The solid color spectroscopy analysis with X-Rite Color iQC quality control software shows bleaching amount of the samples and their comparison circles as lighter or darker as compared to the first day stain shade as illustrated in the Figures 4.24 and 4.25. The positive values at the given graphs represent the lighter hues, and the negative values represent the darker hues. In this context, the textile coated with 0.1wt% anatase doped with 0.001wt% branched silica in the finishing solution illustrated the highest amount of stain discoloration in the stain tests according to the solid color spectroscopy analyses results provided in Figure 4.25.

4.4.4. Surface properties of coated textiles

4.4.4.1. Zeta potential of textiles

The zeta potential analyses of the baseline and the coated textiles were carried out for the textiles coated with anatase, branched silica and anatase concentrations doped with 0.001wt% branched silica in the finishing solution and the results are presented in the Figures 4.26 through 4.28.
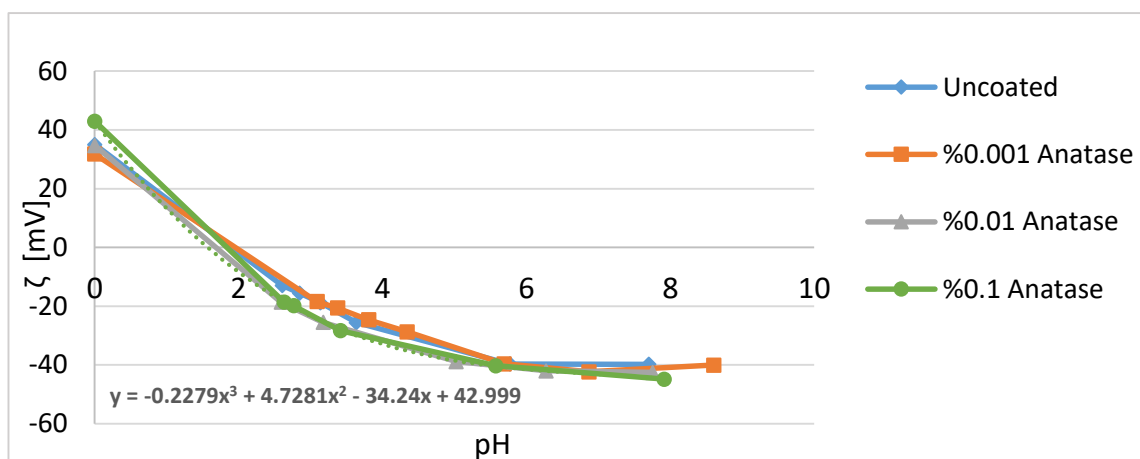
Figure 4.26. The zeta potential as function of pH of textiles coated with anatase concentrations in finishing solution.

$$y = 0.0321x^3 - 0.027x^2 - 6.9758x + 8.696$$
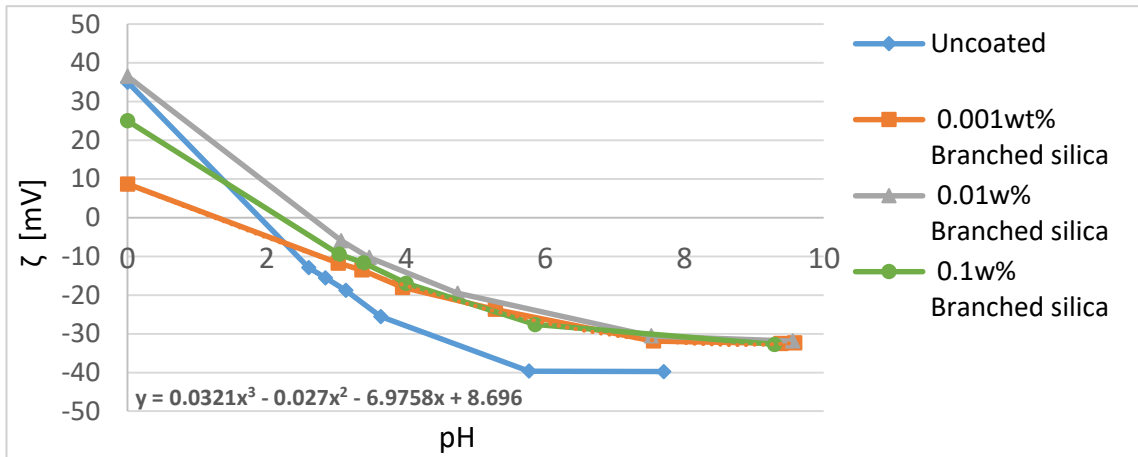
Figure 4.27. The zeta potential as function of pH of textiles coated with branched silica concentrations in finishing solution.

$$y = -0.0666x^3 + 1.6412x^2 - 14.314x + 32.428$$
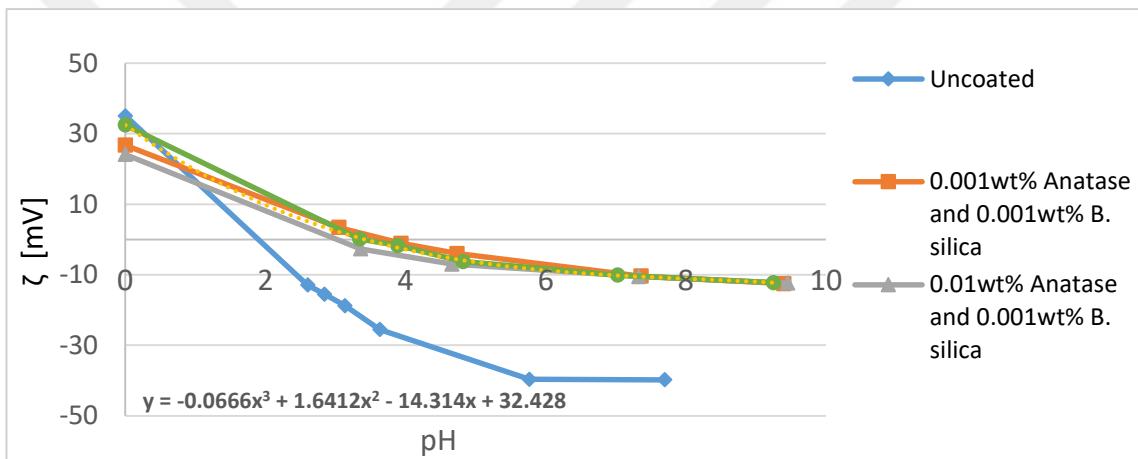
Figure 4.28. The zeta potential as function of pH of textiles coated with anatase concentrations doped with 0.001wt% branched silica in finishing solution.

Generally, the coating process resulted in the textile surface charges to turn into less negative values. It can be seen that when the surface is coated, the textile becomes less negatively charged as a results of the interactions between the anatase and the branched silica affect on the textile/water interface in addition to the cationic additives in the finishing solution (Kos., 2001), (Sal., 1992).

4.4.4.2. Isoelectric points of textiles

The isoelectric points of textiles are calculated as a numerical value of the pH where the electro-kinetic surface potential adds-up to zero in the equations provided for the zeta potential plots in Figure 4.26 through 4.28. One (Walline PE, polyethylene) of the finishing solution integrands added in the finishing solution that is used to prevent linting of textile surfaces resulted in the electro-kinetic charge to get lower for the samples prepared in finishing solution.

Both the baseline and coated textiles have an acidic behavior in the liquid system and differences might originate from interactions between the branched silica and anatase and from the presence of functional groups on the textile surfaces (Gum., 2006).

4.4.4.3. Surface scanning of the most efficient textile sample by AFM imaging

The textile coating which was determined to be the most active photo-catalytically, (coated with 0.1w% anatase and 0.001w% branched silica in finishing solution) was scanned by ezAFM to analyze the surface morphology and the particle dispersion on the textile surface on two locations as illustrated in Figures 4.29. and 4.30. The roughness parameters of these two regions were similar in morphology. Furthermore, the AFM analyses conducted on the textiles with the optimum anatase/branched silica combination showed homogenous coating structure of the particles in the provided scan images.

Roughness Parameters	
Coefficient	Value
Average (Ra)	59.58 nm
Root Mean Square (Rq)	77.09 nm
Skewness (Rsk)	-0.306
Kurtosis (Rku)	3.721
Maximum (Rp)	626.21 nm
Minimum (Rv)	0.00 nm
Peak to peak (Rt)	626.21 nm
Ten Point Heinz (Rz)	625.44 nm
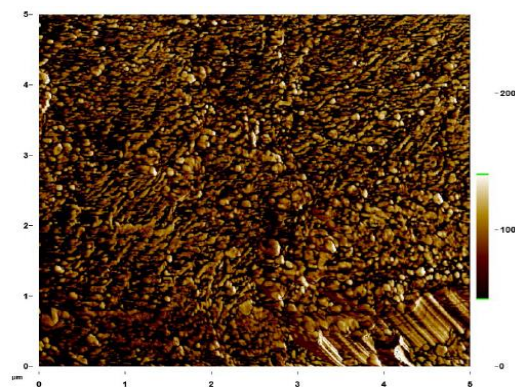
Figure 4.29. The appearance of scanned region as 8μm square and the roughness parameters for this region

Roughness Parameters	
Coefficient	Value
Average (Ra)	320 nm
Root Mean Square (Rq)	420 nm
Skewness (Rsk)	-0.784
Kurtosis (Rku)	3.214
Maximum (Rp)	2030 nm
Minimum (Rv)	0.00 nm
Peak to peak (Rt)	2030 nm
Ten Point Heinz (Rz)	2020 nm
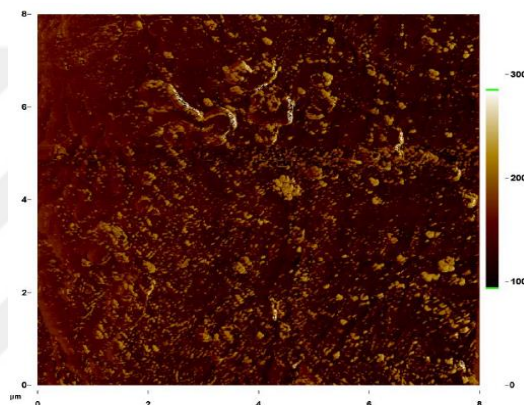
Figure 4.30. The appearance of scanned region as 5μm square and the roughness parameters for this region.

4.4.5. Wettability analyses of the coated textiles

The baseline and coated textiles' contact angle measurements were evaluated to observe the effects of coating on the wettability of the textiles. Monitoring of the contact angle measurement with the selected measurement technique is shown in Figure 4.31. The contact angle analyses were assessed as the average of the three repeated experiments for each sample and their standard deviations are summarized in Table 4.6. Both the baseline textile and the coated textile samples showed high wettability.
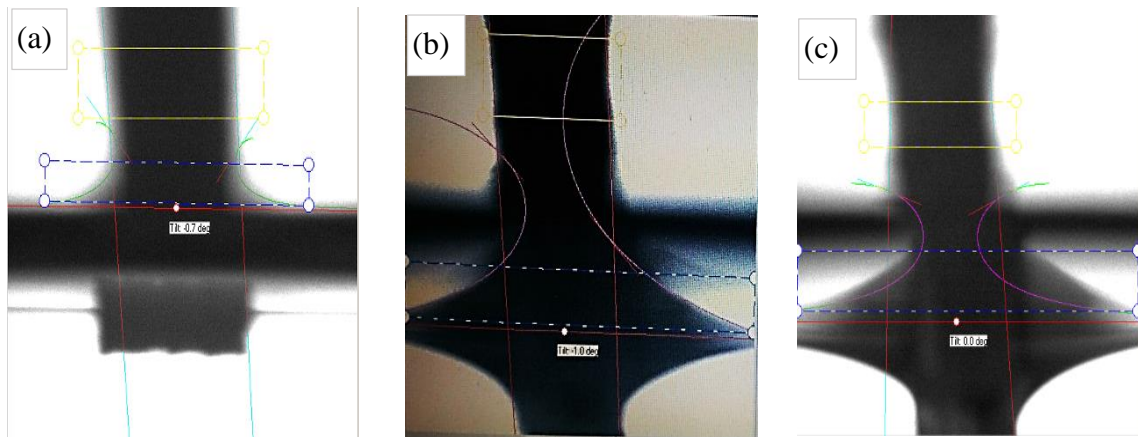
Figure 4.31. Contact angle analyses conducted on baseline textile (a) and textiles coated with 0.1wt% anatase (b) and 0.1wt% anatase presence of 0.001wt% branched silica in finishing solution (c).

Table 4.5. Contact angle values of baseline and coated textiles.

Photocatalytic particles on textiles	Contact angle (°)	Deviation
Baseline	41.23	0.05
0.1wt% Anatase	48.51	0.89
0.1wt%Anatase+0.001wt%B.silica	66.83	4.14

4.4.6. Physical testing of the self-cleaning textiles

4.4.6.1. Resistance Tests

The resistance testing of textiles is a procedure to determine the suitability of the garment in daily usage after production. The textile resistance analysis is based on BS EN ISO 13936-1, BS EN ISO 13934-1, BS 4303, DUPONT TTM 076, BS EN ISO 12945-2 standards. Table 4.7 summarizes the comparison of the physical resistance test results for the baseline and the coated textiles based on the tests conducted at the Kivanc Tekstil laboratories.

Table 4.6. Resistance tests results for coated textiles.

Physical Tests	Test Parameter	Uncovered		0.1w%Anatase		0.1w%Anatase 0.001w% Branched Silica		Test Method	Pass/ Fail
		Length	Width	Length	Width	Length	Width		
Seam Slippage (kg)	METHODII	6mm-17,3kg	6mm >25kg	6mm-16.30kg	6mm >25kg	6 mm-11.45kg	6 mm >25kg	BS EN ISO 13936-1	**Pass**
Tensile Strength (kg)		>40	>40	108.86	69.44	101.58	69.72	BS EN ISO 13934-1	**Pass**
Tear Strength (gr)		>1200	>1200	2890	7290	3030	4960	BS 4303	**Pass**
Elongation (%)		29		38		39		DUPONT TTM 076	**Pass**
Pilling Resistance (mn)	2000REVS.	1/2						BS EN ISO 12945-2	**Pass**

The coated textiles passed all the physical tests according to the conditions adopted by the textile standards. The maximum values of the textiles for daily usage are seam slippage>11kg, tensile strength>1.2kg, elongation>%25 and pilling resistance of 1/2 according to the given ISO standards. It is seen that the new coating did not affect the fabric quality negatively

4.4.6.2. Washing tests

The washing tests for the coated textile were performed in order to understand the amount of particle loss as the textiles are washed. Before and after the conducted washing cycle, the textiles were weighed and the calculated weights were averaged as listed in Figure 4.32.
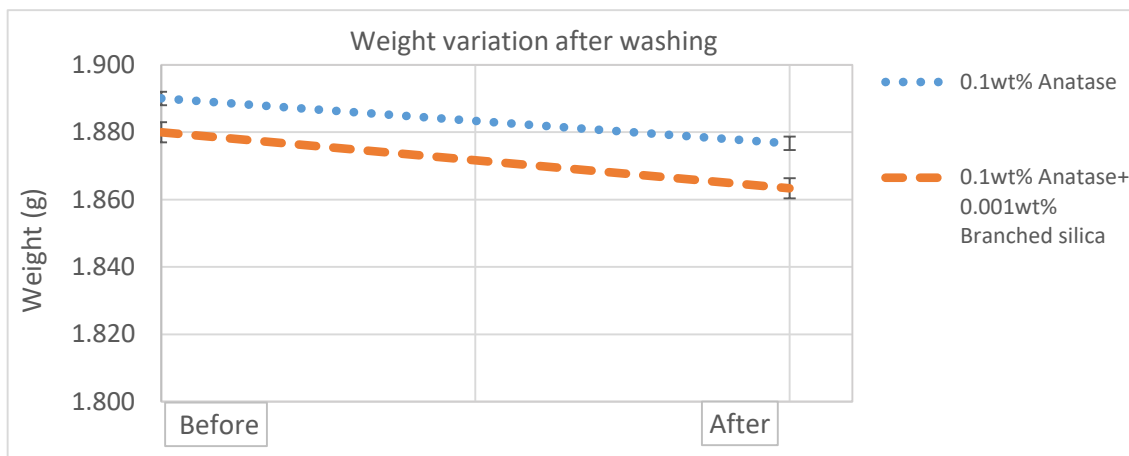
Figure 4.32. Weight variation as function of before and after washing of textiles coated with 0.1wt% anatase and 0.1wt% anatase doped with 0.001wt% branched silica in finishing solution

Table 4.7. Weight variation of coated textiles by washing tests.

Photocatalytic particles on textiles	Before washing(g)	After washing(g)	Deviation
0.1wt% Anatase	1.890	1.877	0.003
0.1wt%Anatase+0.001wt%B.silica	1.880	1.863	0.002

The washing tests showed that the amount of particle loss for each sample were a small amount which can be neglected. Thus, it can be observed that the particles were held on to the textile surface properly and they do not leave the textile surface due to simple friction.

4.4.6.3. Water transmission tests

The water vapor transmission through the textiles is another vital factor which effects the thermo-physiological comfort of human being and respiration of human skin (Ara., 2010). After coating the particles in the coating material on textile, they can cover up the porosity on the textile surface, which may limit the breathability of the garment.

The water vapor transmission analyses of the coated textiles were performed and used for determination of the rate of vapor transferred through the textile. The textiles coated with 0.1wt% anatase and 0.1wt% anatase doped with 0.001wt% branched silica in the finishing solution were exposed to the WVTR analyses for detecting water vapor transmission rate. The weight change of the full experimental set-up as a function of time are presented in Figure 4.33 and Table 4.9, respectively which demonstrates the water vapor transmission by the time. Generally, The WVTR is around %35 for each textile sample. Since WVTR follows the humidity and temperature, in winter conditions under the 22°C and 20% moisture environment, the WVTR values were lower than the values in summer (around 75%).
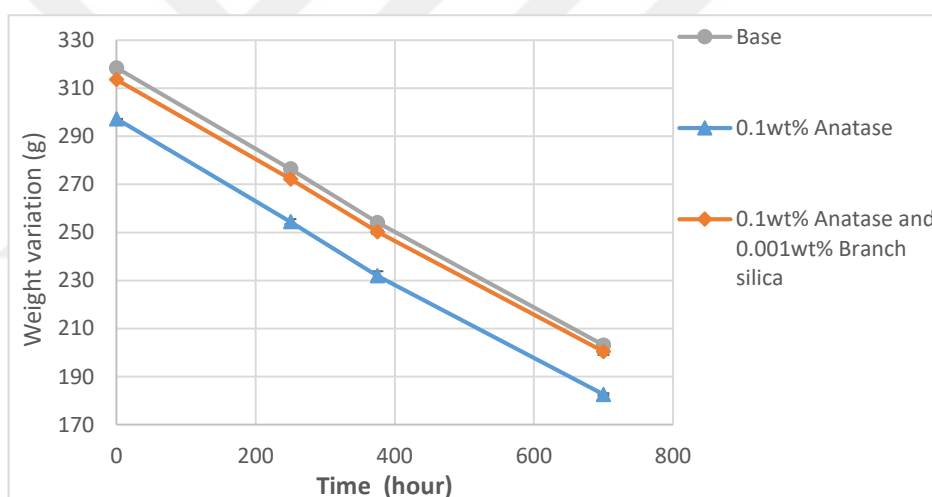
Figure 4.33. Weight variation as function of time for WVTR setup of textiles coated with 0.1wt% anatase and 0.1wt% anatase doped with 0.001wt% branched silica in finishing solution.

Table 4.8. Water vapor transmission rate for baseline and coated textiles.

Type of Textile (%20 moisture and 22°C)	WVTR (%)	Deviation
Baseline	36.55	1.87
0.1%w Anatase in finishing solution	34.61	0.48
0.1%w Anatase and 0.001%w Branched silica in F.S.	35.04	1.42

Hence, only the results of the winter test were presented here for the consistency. The humidity and temperature are central factors affecting the water vapor transmission rate (Ara., 2010). Yet, the tests conducted in both seasons pointed out that WVTR values of the coated textiles were quite close to WVTR of the baseline textile. Thus, coating process didn't affect the vapor transmission rate significantly. Consequently, the developed coating method isn't an obstacle for human skin respiration and thermos-physiological comfort of human being.

4.4.7. Post *Washing- absorbance tests*

The photocatalytic efficiency of the textiles coated with 0.1wt% anatase doped with 0.001wt% branched silica in the finishing solution was further evaluated through washing-absorbance tests. As the washing of the textiles did not cause a significant loss of the emplaced photocatalytic particles, the absorbance tests were evaluated to understand any degradation to the photocatalytic activity due to surface nature changes. The washing-absorbance tests were carried out after the treated textiles were washed once, two and three times. Results of the washing-absorbance tests are presented in figure 4.34.
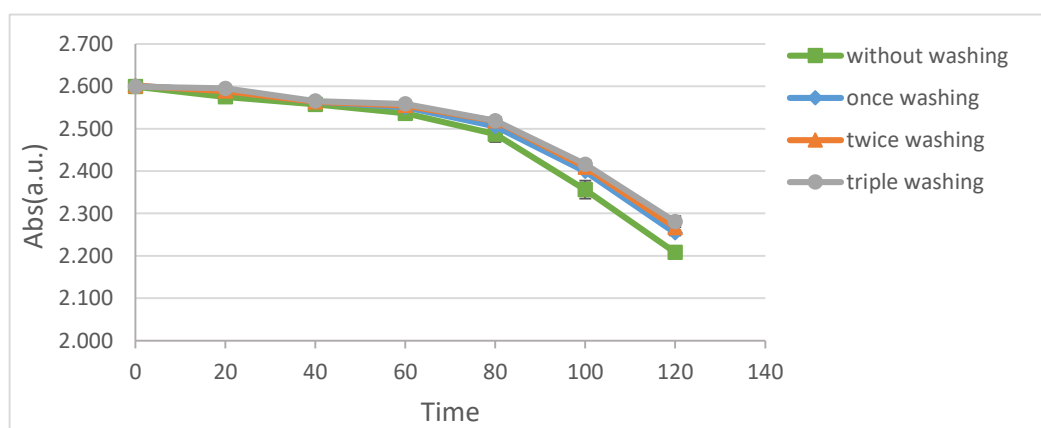
Figure 4.34. The absorbance tests conducted as function of time for the coated textiles after once, twice and treble washing.
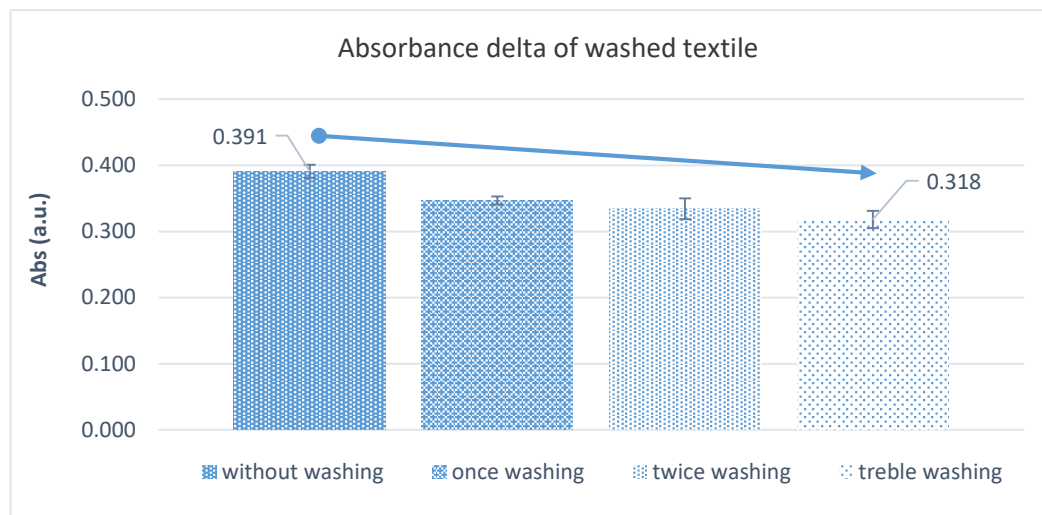
Figure 4.35. The absorbance delta variation as function of washing cycle for textiles coated 0.1wt% anatase doped with 0.001wt% branched silica in finishing.

The washing-absorbance tests performed for 0.1wt% anatase doped with 0.001wt% branched silica in the finishing solution resulted in an absorbance delta of the textiles indicating a drop in the performance as seen in Figure 4.35. However, this trend is minimal as an expected result since the particle loss after the washing tests was also minimal. The reduction of the photocatalytic activity due to the particle loss from the washing application is negligible and even if the washing process is not recommended for daily usage of self-cleaning textiles, it is not detrimental effect.

4.5. Conclusions

The branched particles of titania and silica were evaluated for photo-catalytic activity and the particles were observed to positively affect the self-cleaning efficiency. The analyses were also aimed to understand the suitability of the adopted coating method to the daily usage as garments.

The particle size measurement results were observed to be different based on the selected analysis method. This can be attributed to the nature of the branched structure being expanded when in solution and hence adding to the particle diameter for the light

scattering tests. The branched silica particles synthesized in the laboratory were determined to be spherical in shape and prone to agglomeration when dried.

Initially, various photocatalytic particle solutions were evaluated for MB^+ degradation tests to screen out the best performing combinations. The optimization tests pointed out to three types of solutions, 0.1wt% anatase, 0.1wt% anatase doped with 0.001wt% branched titania and 0.1wt% anatase doped with 0.001wt% branched silica in finishing solution to be preferable. Among these solutions, when exposed to the MB^+ degradation tests with the coated textiles, the most active solution was determined to be 0.1wt% anatase doped with 0.001wt% branched silica in the finishing solution. Moreover, this solution was also seen to be photo active in the visible light range.

The absorbance tests were also performed for the textiles coated with these active solutions. The textiles coated with 0.1wt% anatase doped with 0.001wt% branched silica in the finishing solution was determined to be the most active photocatalytic textile. The results of stain tests realized for the textiles coated with 0.1wt% anatase and 0.1wt% anatase doped with 0.001wt% branched silica in the finishing solution was indistinguishable to human eye's perception. Hence solid color spectrometer measurements were also conducted and the most discoloration of stain was observed with the textile coated with 0.1wt% anatase doped with 0.001wt% branched silica in the finishing solution as well. Therefore, the textile coated with 0.1wt% anatase doped with 0.001wt% branched silica in the finishing solution was chosen as being the most active cleaning ability on the grounds of its photocatalytic efficiency, as proven from the results of the absorbance experiments, stain tests and solid color spectroscopy measurements.

The surface characterizations were also conducted through zeta potential, isoelectric point determination, AFM scanning and wettability measurements for the optimal textile

coating. The zeta potential analyses showed that doping textile surface decreases the surface charge as a results of the interactions between the anatase and the branched silica with the water environment. Furthermore, the Walline PE, which is an anti-static cationic agent for textile surface also affected the isoelectric points post coating. In addition, AFM results demonstrated that the particles were deposited on the textiles homogeneously after the coating process and the surface roughness values were reproducible. On the other hand, the evaluation of textile surface in terms of wettability also indicated an increase in hydrophobicity in the presence of the branched silica.

The textiles resistance, water transmission rate determination, washing tests and washing-absorbance tests were also measured to determine the suitability for daily usage. Resistance tests conducted for comparison of coating effects on textiles demonstrated that the coating process and coated particles didn't reduce the textile's resistance parameters so as to affect usage. Secondly, water transmission rate determination did not limit the respiration of human skin when the coated textiles were evaluated against the baseline. Although washing tests showed a negligible loss in the amount of particles, the absorbance tests canalized after washing cycling only showed a minimal decrease in the photocatalytic efficiency. However, this reduction was in an acceptable range because the photocatalytic efficiency of textile, which was washed three times (less active than the unwashed textiles), was still more active as compared to the textiles only coated with anatase or anatase and branched titania.

CHAPTER 5

CONCLUSIONS AND RECOMMENDATIONS FOR FUTURE WORK

5.1. Summary

This study was initiated to achieve photocatalytic functionality in the visible light range by synthesizing novel dopant combinations to achieve equivalent or better results as compared to the literature. Hence, the experimental steps of the study were started from the evaluation of baseline photocatalytic materials followed by pure dopant trials and finalized by the composite novel particle systems and the assessment of contributions of these particles to advanced photocatalysis.

The baseline photocatalytic particles, anatase and degussa P25, were initially evaluated in terms of their suitability emplacement to finishing process implemented for the selected textile in our textile manufacturing. To provide stable particle suspensions, which is critical for industrial scale adaptability of the process, stability and particle size measurements were carried out for the two forms of the TiO_2 in DI-water and the finishing solution. The best stability and reduction of agglomeration was obtained by anatase in the finishing solution. The photocatalytic efficiency of these two forms of the TiO_2 were established by absorbance and stain tests as established in the literature. The detailed examinations have shown that the finishing solution composition helped improve the photocatalysis and the textile sample coated with 0.1wt% anatase in the finishing solution showed the best self-cleaning ability among these standard photocatalytic particles.

The use of pure boron was also thought as a potential breakthrough as the p=type dopants are not explored well enough in the literature as related to photocatalysis. The degradation of methylene blue solution analyses named as absorbance tests were conducted according to the experimental set-up of Design-Expert software. The most active anatase doping determined in the preliminary analysis combined with the pure boron at various dosages was evaluated for photocatalytic efficiency, yet did not show significant improvement. Furthermore, the dark color of the pure nano-boron resulted in limited applications in industrial production due to the pure boron changing the white color of fabric after the coating process. Despite the fact that the textiles coated with anatase in the presence of pure boron in DI-water indicated photocatalytic activity, its photocatalytic activity was not as pronounced as compared to the photocatalytic efficiency of the textile coated with anatase in DI-water. Thus, boron doping was not very effective as a potential for self-cleaning textile manufacturing.

In order to bring the photocatalytic activity within the visible light range, new particles were synthesized as the next step. Initially, the new particles were evaluated for their photocatalytic efficiency in the solution form to obtain the most active concentrations. It was found that 0.1wt% anatase, 0.1wt% anatase doped with 0.001wt% branched titania and 0.1wt% anatase doped with 0.001wt% branched silica in the finishing solution had the most effective photocatalytic activity. These samples were analyzed through absorbance and degradation tests in order to determine the most pronounced photo-catalytic sample, which was the textile coated with 0.1wt% anatase doped with 0.001wt% branched silica in the finishing solution based on the results of the absorbance tests. In terms of the degradation tests conducted with the cool light (580-600nm), the most active sample was also active in the visible light range. The photocatalytic activity of this most active sample was compared to the textile coated with 0.1wt% anatase in the finishing

solution by stain tests as well as the standard quality tests implemented on the textiles in manufacturing.

In summary, the textile coated with 0.1wt% anatase doped with 0.001wt% branched silica in finishing solution showed the best photocatalytic efficiency. In addition to its photocatalytic activity, the effectiveness of the coating was also tested with the washing and post wash absorbance tests. It was observed that the textiles coated with this most effective blend of dopants also preserved their photocatalytic activity even after the washing tests and the textile morphology and water vapor transmission properties have also stayed comparable. In short, the textile coated with 0.1wt% anatase doped with 0.001wt% branched silica in finishing solution passed all the physical and chemical test standards as well as the photocatalytic efficacy evaluations. This optimal textile treatment formulation is a breakthrough for photocatalysis since self-cleaning textiles irradiated with visible light can be achieved and the sample is a suitable candidate to mass manufacturing.

5.2. Recommendations for the future work

The 0.1wt% anatase doped with 0.001wt% branched silica was found to exhibit the greatest photocatalytic activity. However, alternative evaluations of self-cleaning textiles can be performed after high volume manufacturing. Furthermore, the satisfaction of people with the self-cleaning textile products should be evaluated through surveys and results of these surveys should be extended for manufacturability and sustainability.

The main materials of fibers used in the textile manufacturing may also be improved and varied with the most newly developing technologies. The search for new and more compatible materials may also be needed for the ongoing developments of the technological textiles. Moreover, the coating methods can also be improved to adopt the

developing technological improvements. This is confirmed with our pre-laboratory studies indicating that the textiles coated with Chemical Bath Deposition (CBD) tend to show hydrophobic properties. However, post CBD, the particle loss was very high after washing to be able to provide similar photocatalytic ability post wash. Yet, it may also be possible to prevent particles loss by developing new binders. Another future recommendation can be improving new synthesis methods and particles, which are able to increase photocatalytic activity for textiles including more active p-type dopants.

Considering all these recommendations, developing stronger and permanent self-cleaning textile products obviously require time, more development on the application devices as well as the development of new methods.

REFERENCES

Aida, T., E. W. Meijer, and S. I. Stupp. 2012. "Functional Supramolecular Polymers." *Science* 335 (6070): 813–17. doi:10.1126/science.1205962.

Akbar, Wazir, Mohamed Radzi Noor, Katarzyna Kowal, Tofail Syed, Tewfik Soulimane, and G. Bahar Basim. 2016. "Characterization and Antibacterial Properties of Nanoboron Powders and Nanoboron Powder Coated Textiles." *Advanced Powder Technology* 28 (2). Society of Powder Technology Japan: 596–610. doi:10.1016/j.apt.2016.11.012.

Arabuli, Svitlana, Viktoriia Vlasenko, Antonin Havelka, and Zdenek Kus. 2010. "Analysis of Modern Methods for Measuring Vapor Permeability Properties of Textiles." *7th International Conference - TEXSCI*, 1–6.

Atac Makina. 2016. "ATC-GK40C/S Padding Machine." *Www.atacmakina.com.tr*. http://www.atacmakina.com.tr/index.php?id=31&tx_ttnews%5Btt_news%5D=37&cHash=888172a056c2b032f8fda14de232ff92.

Bao, Yan, Chunhua Shi, Tong Wang, Xiaolu Li, and Jianzhong Ma. 2016. "Recent Progress in Hollow Silica: Template Synthesis, Morphologies and Applications." *Microporous and Mesoporous Materials* 227 (June). Elsevier Ltd: 121–36. doi:10.1016/j.micromeso.2016.02.040.

Beydoun, Donia, and Rose Amal. 2002. "Implications of Heat Treatment on the Properties of a Magnetic Iron Oxide-Titanium Dioxide Photocatalyst." *Materials Science and Engineering B: Solid-State Materials for Advanced Technology* 94 (1): 71–81. doi:10.1016/S0921-5107(02)00085-5.

Bozzi, A., T. Yuranova, and John Kiwi. 2005. "Self-Cleaning of Wool-Polyamide and

Polyester Textiles by TiO2-Rutile Modification under Daylight Irradiation at Ambient Temperature." *Journal of Photochemistry and Photobiology A: Chemistry* 172 (1): 27–34. doi:10.1016/j.jphotochem.2004.11.010.

Bracco, Gianangelo, and Bodil Holst. 2013. *Surface Science Techniques. Springer Series in Surface Sciences*. Vol. 51. doi:10.1007/978-3-642-34243-1.

Brinker, C. Jeffrey. 2013. "Dip Coating." In *Chemical Solution Deposition of Functional Oxide Thin Films*, 233–61. Vienna: Springer Vienna. doi:10.1007/978-3-211-99311-8_10.

Castellote, Marta, and Nicklas Bengtsson. 2011. "Principles of TiO2 Photocatalysis." In *Applications of Titanium Dioxide Photocatalysis to Construction Materials*, edited by Yoshihiko Ohama and Dionys Van Gemert, 5–10. Dordrecht: Springer Netherlands. doi:10.1007/978-94-007-1297-3_2.

Cerhan, Asena. 2015. "Growth and Characterization of SnS Thin Films From Silar Technique." Erzincan: Erzincan University.

Chawla, Krishan K. 2012. "Nonconventional Composites." In *Composite Materials*, 497–510. New York, NY: Springer New York. doi:10.1007/978-0-387-74365-3_15.

Cieśla, Paweł, Przemysław Kocot, Piotr Mytych, and Zofia Stasicka. 2004. "Homogeneous Photocatalysis by Transition Metal Complexes in the Environment." *Journal of Molecular Catalysis A: Chemical* 224 (1–2): 17–33. doi:10.1016/j.molcata.2004.08.043.

Cohen-Tannoudji, Claude, Bernard Diu, and Franck Laloë. 1977. "Quantum Mechanics Vol. I." Newyork: Wiley.

Coronado, Juan M, Fernando Fresno, María D Hernández-Alonso, and Raquel Portela. 2013. *Design of Advanced Photocatalytic Materials for Energy and Environmental Applications*. doi:10.1007/978-1-4471-5061-9.

ÇALIK, Döne. 2008. "Photocatalytic Oxidation of A Reactive Dye in Textile Effluents." Ankara University.

Devi, L. Gomathi, and R. Kavitha. 2013. "A Review on Non Metal Ion Doped Titania for the Photocatalytic Degradation of Organic Pollutants under UV/solar Light: Role of Photogenerated Charge Carrier Dynamics in Enhancing the Activity." *Applied Catalysis B: Environmental* 140–141 (August): 559–87. doi:10.1016/j.apcatb.2013.04.035.

Ding, Jianqiang, Yali Yuan, Jinsheng Xu, Jian Deng, and Jianbo Guo. 2009. "TiO2 Nanopowder Co-Doped with Iodine and Boron to Enhance Visible-Light Photocatalytic Activity." *Journal of Biomedical Nanotechnology* 5 (5): 521–27. doi:10.1166/jbn.2009.1060.

Filippo, Emanuela, Claudia Carlucci, Agostina Lina Capodilupo, Patrizia Perulli, Francesca Conciauro, Giuseppina Anna Corrente, Giuseppe Gigli, et al. 2015. "Enhanced Photocatalytic Activity of Pure Anatase Tio 2 and Pt-Tio 2 Nanoparticles Synthesized by Green Microwave Assisted Route 2 . Experimental Section." *Materials Research* 18 (3): 473–81. doi:10.1590/1516-1439.301914.

G. Fouda, Moustafa M. 2012. "Antibacterial Modification of Textiles Using Nanotechnology." In *A Search for Antibacterial Agents*. InTech. doi:10.5772/45653.

Godet, C., L. Schmirgeld, L. Zuppiroli, G. Sardin, S. Gujrathi, and K. Oxorn. 1991. "Optical Properties and Chemical Reactivity of Hydrogenated Amorphous Boron

Thin Films." *Journal of Materials Science* 26 (23): 6408–18. doi:10.1007/BF02387822.

Gomez-Merino, A. I., F. J. Rubio-Hernandez, J. F. Velazquez-Navarro, J. Aguiar, Jime, and C. Nez-Agredano. 2014. "Study of the Aggregation State of Anatase Water Nanofluids Using Rheological and DLS Methods." *Ceramics International* 40 (9 PART A). Elsevier: 14045–50. doi:10.1016/j.ceramint.2014.05.132.

Goor, Olga J. G. M., Henk M. Keizer, Anne L. Bruinen, Moniek G. J. Schmitz, Ron M. Versteegen, Henk M. Janssen, Ron M. A. Heeren, and Patricia Y. W. Dankers. 2017. "Efficient Functionalization of Additives at Supramolecular Material Surfaces." *Advanced Materials* 29 (5): 1604652. doi:10.1002/adma.201604652.

Govender, Kuveshni, David S. Boyle, Peter B. Kenway, and Paul O'Brien. 2004. "Understanding the Factors That Govern the Deposition and Morphology of Thin Films of ZnO from Aqueous Solution." *J. Mater. Chem.* 14 (16): 2575–91. doi:10.1039/B404784B.

Gumy, D., C. Morais, P. Bowen, C. Pulgarin, S. Giraldo, R. Hajdu, and J. Kiwi. 2006. "Catalytic Activity of Commercial of TiO2 Powders for the Abatement of the Bacteria (E. Coli) under Solar Simulated Light: Influence of the Isoelectric Point." *Applied Catalysis B: Environmental* 63 (1–2): 76–84. doi:10.1016/j.apcatb.2005.09.013.

Guptaa, Deepti. 2011. "Functional Clothing- Definition and Classification." *Indian Journal of Fibre and Textile Research* 36 (4): 312–26.

Haugstad, Greg. 2012. *Atomic Force Microscopy*. First edit. New Jersey: Wiley.

Hebeish, A. A., M. M. Abdelhady, and A. M. Youssef. 2013. "TiO2 Nanowire and TiO2

Nanowire Doped Ag-PVP Nanocomposite for Antimicrobial and Self-Cleaning Cotton Textile." *Carbohydrate Polymers* 91 (2). Elsevier Ltd.: 549–59. doi:10.1016/j.carbpol.2012.08.068.

Hee-Gweon Woo, Hong Li. 2011. *Advanced Functional Materials*.

Hendrix, Yuri, Alberto Lazaro, Qingliang Yu, and Jos Brouwers. 2015. "Titania-Silica Composites: A Review on the Photocatalytic Activity and Synthesis Methods." *World Journal of Nano Science and Engineering* 5 (4): 161–77. doi:10.4236/wjnse.2015.54018.

Herrmann, J. 1999. "Heterogeneous Photocatalysis: Fundamentals and Applications to the Removal of Various Types of Aqueous Pollutants." *Catalysis Today* 53 (1): 115–29. doi:10.1016/S0920-5861(99)00107-8.

Hu, J.L., and J. Lu. 2016. "Memory Polymer Coatings for Smart Textiles." In *Active Coatings for Smart Textiles*, 11–34. Elsevier. doi:10.1016/B978-0-08-100263-6.00002-2.

Hu, Jinlian. 1925. "Introduction to Active Coatings for Smart Textiles." In *Active Coatings for Smart Textiles*, 1–6. Elsevier Ltd.

Hu, Y, V Topolkaraev, A Hiltner, and E Baer. 2001. "Measurement of Water Vapor Transmission Rate in Highly Permeable Films," 1624–33.

Hudson, JR. 1981. "Physical Stability of Suspensions." *Brauindustrie* 411 (December): 393–411.

Kathalingam, a., N. Ambika, Mr Kim, J. Elanchezhiyan, Ys Chae, and Jk Rhee. 2010. "Chemical Bath Deposition and Characterization of Nanocrystalline ZnO Thin

Films." *Materials Science-Poland* 28 (2): 513–22. doi:10.3906/fiz-0905-18.

Kim, Soonhyun, Hyunwoong Park, and Wonyong Choi. 2004. "Comparative Study of Homogeneous and Heterogeneous Photocatalytic Redox Reactions: PW 12 O 40 3- vs TiO 2." *The Journal of Physical Chemistry B* 108 (20): 6402–11. doi:10.1021/jp049789g.

Kiwi, J., and S. Rtimi. 2016. "Environmentally Mild Self-Cleaning Processes on Textile Surfaces under Daylight Irradiation." In *Active Coatings for Smart Textiles*, 35–54. Elsevier. doi:10.1016/B978-0-08-100263-6.00003-4.

Kosmulski, Marek. 2001. *CHEMICAL PROPERTIES OF MATERIAL SURFACES*. 4th ed. Santa Barbara, California: MARCEL DEKKER.

López, Rosendo, and Ricardo Gómez. 2012. "Band-Gap Energy Estimation from Diffuse Reflectance Measurements on Sol–gel and Commercial TiO2: A Comparative Study." *Journal of Sol-Gel Science and Technology* 61 (1): 1–7. doi:10.1007/s10971-011-2582-9.

Meilert, K. T., D. Laub, and J. Kiwi. 2005. "Photocatalytic Self-Cleaning of Modified Cotton Textiles by TiO 2 Clusters Attached by Chemical Spacers." *Journal of Molecular Catalysis A: Chemical* 237 (1–2): 101–8. doi:10.1016/j.molcata.2005.03.040.

Mills, Andrew, Claire Hill, and Peter K J Robertson. 2012. "Overview of the Current ISO Tests for Photocatalytic Materials." *Journal of Photochemistry and Photobiology A: Chemistry* 237. Elsevier B.V.: 7–23. doi:10.1016/j.jphotochem.2012.02.024.

Mills, Andrew, and Michael McFarlane. 2007. "Current and Possible Future Methods of Assessing the Activities of Photocatalyst Films." *Catalysis Today* 129 (1–2 SPEC.

ISS.): 22–28. doi:10.1016/j.cattod.2007.06.046.

Nanayakkara, Yasith S., Sirantha Perera, Shreyas Bindiganavale, Eranda Wanigasekara, Hyejin Moon, and Daniel W. Armstrong. 2010. "The Effect of AC Frequency on the Electrowetting Behavior of Ionic Liquids." *Analytical Chemistry* 82 (8): 3146–54. doi:10.1021/ac9021852.

Ney, Paul. 1973. *Zeta-Potentiale Und Flotierbarkeit von Mineralen*. Vienna: Springer Vienna. doi:10.1007/978-3-7091-8324-3.

Nowotny, Janusz. 2012. *Oxide Semiconductors for Solar Energy Conversion: Titanium Dioxide*. Newyork: CRC Press.

Ohtani, Bunsho. 2008. "Preparing Articles on Photocatalysis—Beyond the Illusions, Misconceptions, and Speculation." *Chemistry Letters* 37 (3): 216–29. doi:10.1246/cl.2008.216.

Patra, J. K., and S. Gouda. 2013. "Application of Nanotechnology in Textile Engineering: An Overview." *Journal of Engineering and Technology Research* 5 (5): 104–11. doi:10.1016/j.jclepro.2015.03.091.

Paul, Bidyut K. and Satya P. Moulik. 2001. "Uses and Applications of Microemulsions." *SPECIAL SECTION: SOFT CONDENSED MATTERCURRENT SCIENCE* VOL. 80 (8): 990–1001.

Qian, Lei, and Gang Sun. 2005. "Durable and Regenerable Antimicrobial Textiles: Chlorine Transfer among Halamine Structures." *Industrial & Engineering Chemistry Research* 44 (4): 852–56. doi:10.1021/ie049493x.

Qiu, Xiaoqing, Masahiro Miyauchi, Kayano Sunada, Masafumi Minoshima, Min Liu,

Yue Lu, Ding Li, et al. 2012. "Hybrid Cu X O/TiO 2 Nanocomposites As Risk-Reduction Materials in Indoor Environments." *ACS Nano* 6 (2). ACS Nano 6: 1609–18. doi:10.1021/nn2045888.

Quill, Jeffery, Greg Fedor, Patrick Brennan, and Eric Everett. 2004. "Quantifying the Indoor Light Environment: Testing for Light Stability in Retail and Residential Environments." *Q-Lab, Technical Bulletin* LX-5026: 689–698. http://www.ingentaconnect.com/content/ist/nipdf/2004/00002004/00000002/art000 37.

Randazzo, Antonio, Gian Piero Spada, and Mateus Webba da Silva. 2012. *Topics in Current Chemistry*. doi:10.1007/128_2012_331.

Rui, Zebao, Shangren Wu, Chao Peng, and Hongbing Ji. 2014. "Comparison of TiO2 Degussa P25 with Anatase and Rutile Crystalline Phases for Methane Combustion." *Chemical Engineering Journal* 243 (May): 254–64. doi:10.1016/j.cej.2014.01.010.

Salopek, Branko, Dragan Krasic, and Suzana Filipovic. 1992. "Measurement and Application of Zeta-Potential." *Rudarsko-Geolosko-Naftni Zbornik* 4: 147–51.

Schiavello, Mario, ed. 1985. *Photoelectrochemistry, Photocatalysis and Photoreactors*. Dordrecht: Springer Netherlands. doi:10.1007/978-94-015-7725-0.

Schindler, W.D., and P.J. Hauser. 2004. "Chemical Finishing Processes." In *Chemical Finishing of Textiles*, 7–21. Cambridge: Elsevier. doi:10.1533/9781845690373.121.

Shim, E. 2010. "Coating and Laminating Processes and Techniques for Textiles." In *Smart Textile Coatings and Laminates*, 10–41. Elsevier. doi:10.1533/9781845697785.1.10.

Simakov, Stanislav A., and Yoed Tsur. 2007. "Surface Stabilization of Nano-Sized Titanium Dioxide: Improving the Colloidal Stability and the Sintering Morphology." *Journal of Nanoparticle Research* 9 (3): 403–17. doi:10.1007/s11051-006-9099-0.

Stöber, Werner, Arthur Fink, and Ernst Bohn. 1968. "Controlled Growth of Monodisperse Silica Spheres in the Micron Size Range." *Journal of Colloid and Interface Science* 26 (1): 62–69. doi:10.1016/0021-9797(68)90272-5.

Swanepoel, R. 1983. "Determination of the Thickness and Optical Constants of Amorphous Silicon." *Journal of Physics E: Scientific Instruments* 16 (12): 1214. http://iopscience.iop.org/article/10.1088/0022-3735/16/12/023/pdf.

Terrano, Jessie. 2017. "Scanning Electron Microscope." https://cellularphysiology.wikispaces.com/scanning+electron+microscope+(SEM).

Tesoro, Giullana C. 1968. "Textile Finishes." *Journal of the American Oil Chemists' Society* 45 (5): 351–53. doi:10.1007/BF02667109.

Tobergte, David R., and Shirley Curtis. 2013. "Application of Titanium Dioxide Photocatalysis to Construction Materials." *Journal of Chemical Information and Modeling* 53 (9): 1689–99. doi:10.1017/CBO9781107415324.004.

Turton, Richard J. 2000. "Semiconductors." In *The Physics of Solids*, 117–48. doi:10.1007/978-3-642-00710-1_2.

Uddin, M. J., F. Cesano, D. Scarano, F. Bonino, G. Agostini, G. Spoto, S. Bordiga, and A. Zecchina. 2008. "Cotton Textile Fibres Coated by Au/TiO2 Films: Synthesis, Characterization and Self Cleaning Properties." *Journal of Photochemistry and Photobiology A: Chemistry* 199 (1): 64–72. doi:10.1016/j.jphotochem.2008.05.004.

Umar, Muhammad, and Hamidi Abdul. 2013. "Photocatalytic Degradation of Organic Pollutants in Water." In *Organic Pollutants - Monitoring, Risk and Treatment*. InTech. doi:10.5772/53699.

Wubbels, Gene G. 1983. "Catalysis of Photochemical Reactions." *Accounts of Chemical Research* 16 (8): 285–92. doi:10.1021/ar00092a004.

Yin, Wan-Jian, Shiyou Chen, Ji-Hui Yang, Xin-Gao Gong, Yanfa Yan, and Su-Huai Wei. 2010. "Effective Band Gap Narrowing of Anatase TiO2 by Strain along a Soft Crystal Direction." *Applied Physics Letters* 96 (22): 221901. doi:10.1063/1.3430005.

Yuranova, T., R. Mosteo, J. Bandara, D. Laub, and J. Kiwi. 2006. "Self-Cleaning Cotton Textiles Surfaces Modified by Photoactive SiO 2/TiO2 Coating." *Journal of Molecular Catalysis A: Chemical* 244 (1–2): 160–67. doi:10.1016/j.molcata.2005.08.059.

Zimmermann, Jan, Felix A. Reifler, Giuseppino Fortunato, Lutz-Christian Gerhardt, and Stefan Seeger. 2008. "A Simple, One-Step Approach to Durable and Robust Superhydrophobic Textiles." *Advanced Functional Materials* 18 (22): 3662–69. doi:10.1002/adfm.200800755.

VITA

Asena Cerhan was born in Ardahan. She completed primary and secondary education in Balıkesir, Gönen and received her BSc degree from Ataturk University Physics Department in 2011. Then, she got accepted for a master's degree on atomic physics and gained her MSc on solid state physics by studying a national project on gas sensors and thin film growth as well as characterization at the Science Institute of Erzincan University in 2015. In the same year, she began to study on PhotoCat project for her second MSc degree (interdisciplinary studies) in Ozyegin University. Her areas of interests include; thin film growth methods, characterization, and application, interacting electrons in thin semiconductors, semiconductor lasers, and nanomaterials.